POLYCYCLIC ANGULAR THIENO, THIAZETO, THIAZOLO AND FUROBENZO[h]QUINOLINES: DESIGN, SYNTHESIS, In Vitro AND In Silico EVALUATION

ABEER AHMED ABUELMAGD AHMED

Polycyclic Angular Thieno, Thiazeto, Thiazolo and Furobenzo[*h*]quinolines: Design, Synthesis, *In Vitro* and *In Silico* Evaluation

By

Abeer Ahmed Abuelmagd Ahmed

A Thesis submitted to the School of Graduate Studies
in partial fulfillment of the requirements
for the degree of Doctor of Philosophy

School of Pharmacy
Memorial University

St. John's Newfoundland and Labrador

December, 2011

ABSTRACT

Functionalized quinolines and their benzo/hetero-fused analogs are an important class of organic molecules that have attracted the attention of synthetic and medicinal chemists, because of their presence in numerous natural products and their wide range of biological activities. The quinolines, particularly those substituted at position 4, have marked antimalarial, antibacterial, anti-inflammatory, anticancer, and antiviral activities.

The remarkable applications of these compounds have not only prompted many chemists to synthesize these types of compounds, they have also become an active research area of continuing interest.

In this work a structure-based drug design was done using Hyperchem-3^{TM} in order to develop a quinoline-originated Topoisomerase inhibitor with a potential anticancer and a better pharmacokinetic profile. The work involves the design and synthesis of many ring fused quinoline systems including thieno-, thiazeto-, thiazolo- and furobenzo[*h*] quinolines in order to clarify the structural requirements for the activity; the *in-silico* data determined in this work provides a deep understanding of the binding affinities of these types of derivatives.

The results obtained in this study showed that the synthesized quinoline derivatives have good binding affinities to Human Topoisomerase II, particulary in the ATP binding region. Also, these derivatives were not able to chelate with Mg^{2+} which helped to account for the lack of cytotoxicity exihibited by these derivatives.

ACKNOWLEDGEMENTS

All praises are for Almighty Allah, who has given me the opportunity to accomplish this work. Throughout my PhD study and research, it has been a pleasure, working with my great colleagues and mentors and this dissertation owes much to their sincere help and encouragement.

First, I am deeply indebted to my supervisor, without whom this work would not have seen daylight: Dr. Mohsen Daneshtalab for offering the sparkling ideas and innovative thinking to meet the goals of the research requirements for my PhD work.

My thanks are also extended to my supervisory committee members Dr. Sunil Pansare and Dr. Hu Liu for providing instruction, comments and suggestions to improve the overall quality of the work.

I would like to take this opportunity to convey my thanks to Dr. Jules Doré from the Division of Biomedical Sciences, Faculty of Medicine for assisting me in the biological test, Dr. Peter Warburton from the Chemistry Department for providing the computational calculations, and Dr. Louise Dawe for the X-ray data analysis.

I appreciate and acknowledge the financial support of the Egyptian Higher Education Ministry. I also thank the School of Graduate Studies and School of Pharmacy, Memorial University of Newfoundland, for their relevant support.

I would also like to extend my gratitude to my labmates for their support during the course of study.

Last, but not least, I would like to give my special and warmest thanks to my husband, Mohamed Khalifa and my beloved children, Hashem and Mennatullah, for their patience, sacrifices and support during my study.

To my Parents

Table of Contents

ABSTRACT ii

ACKNOWLEDGEMENTS iii

Table of Contents v

List of Tables ix

List of Figures x

List of Schemes xiii

List of Abbreviations xv

CHAPTER 1 1

Introduction and Overview 1

1.1 Structure-based drug design 2

1.1.1 Ligand-based drug design 2

1.1.2 Structure-based drug design (SBDD) 3

1.1.3 Structure-based drug design steps 3

1.2 Research scope 5

1.3 Thesis overview 6

References 9

CHAPTER 2 10

Literature Review: Non-Classical Biological Activities of Quinolone Derivatives 10

2.1 Introduction 12

2.2 The chemistry of 4-quinolones 13

2.3 Biological targets of antibacterial quinolones 16

2.4 Supercoiling and Topoisomerases 17

2.5 Important structural features of antibacterial quinolones 19
2.6 Dual targets mechanism of action 21
2.6.1 Differences between DNA gyrase and eukaryotic topo II 22
2.7 Quinolone-based anticancer derivatives 23
2.7.1 Historic development of cytotoxic quinolones. 24
2.7.2 Important structural features of anticancer quinolones 25
2.7.3 Quinoline/one derivatives as topoisomerase inhibitors 30
2.7.4 Signal transducers and activators of transcription (STATs) inhibition 34
2.8 Quinolone scaffold-based antiviral agents 35
2.8.1 Quinolone-based anti-HIV agents 36
2.8.2 Quinolones as anti-HCV (Hepatitis C virus) agents 45
2.9 Conclusion 48
References 49
CHAPTER 3 68
Thieno [2,3-*b*]Benzo[*h*]quinoline Derivatives: Design, Synthesis, Preliminary *In Vitro* and *In Silico* Study 68
Abstract 69
3.1 Introduction 70
3.2 *O*-Alkylated products 74
3.3 Materials and methods 82
3.3.1 *In vitro* testing 82
3.4 Molecular modeling 84
3.4.1 Methods 84

3.5 Results and discussion 89

3.5.1 Brine Shrimp Lethality bioassay results 89

3.5.2 MTT Cytotoxicity results 90

3.6 Conclusion 91

3.7 Experimental 92

References 105

CHAPTER 4 114

Synthesis of Novel 4-Oxo-1,4-Dihydro Benzo[*h*][1,3]Thiazeto[3,2-*a*]quinoline Carboxylic Acids Via Oxidative Cyclization of the Corresponding 2-Mercaptoquinoline Precursors; Proof of the Mechanism 114

Abstract 115

4.1 Introduction 115

4.2 Chemistry 119

4.3 *In vitro* testing 125

4.4 Molecular modeling 126

4.4.1 Methods 126

4.4.2 Human topoisomerase II docking 127

4.4.3 Docking experiment 128

4.5 Focused docking results 128

4.6 *In vitro* testing 130

4.6.1 Cytotoxicity assay 130

4.7 Computational methods 130

4.7.1 Computational results 131

4.8 Conclusion 139

4.9 Experimental 139

Appendix 4A: Structure Report, 4-Oxo-1,4-Dihydrobenzo[*h*][1,3]thiazeto[3,2-*a*]quinoline-1,3-Dicarboxylic Acid 147

Abstract 148

4A.1 Related literature 148

4A.2 Experimental 148

4A.2.1 Crystal data 148

4A.2.2 Data collection 149

4A.2.3 Refinement 149

4A.3 Comment 150

4A.4 Refinement 151

References 153

CHAPTER 5 160

Development of Anti-Viral Angular Furobenzo[*h*] [2,3-*b*]Quinoline Agents Using Molecular Modeling and Virtual Screening Techniques 160

Abstract 161

5.1 Introduction 162

5.2 Molecular modeling 170

5.2.1 Methods 170

5.2.2 Results 171

5.2.3 Blind docking results 172

5.2.4 Focused docking results 173

5.3 Conclusion 174

5.4 Experimental 175

References 183

CHAPTER 6 193

Conclusion and Future Research 193

6.1 Conclusion and future research 194

6.2 Originality of the thesis 202

List of Tables

Table 3-1: Docking energies of the investigated compounds at the ATP binding site..... 87

Table 3-2: Brine shrimp lethality bioassay results..... 90

Table 3-3: Results of cytotoxicity testing against HeLa and Kb cell lines..... 90

Table 4-1: Cytotoxicity results of tested derivatives. 126

Table 4-2: Calculated interactions of Compound 4b at the ATP binding site. 129

Table 4-3: Hydrogen-bond geometry (Å, °). 150

Table 4-4: Π..... Π interactions (Å, °) 150

Table 5-1: Docking energies of the investigated compounds at the ATP binding site... 173

Table 5-2: Interactions of Compound 3c with HCV helicase at the ATP binding site... 174

List of Figures

Figure 1-1: Thesis organization. 6

Figure 2-1: Mechanism of action of fluoroquinolones 16

Figure 2-2: DNA cleavage-religation mechanism of DNA Gyrase 18

Figure 2-3: General structure of the most-commonly used quinolone molecule 19

Figure 2-4: Structure of the cytotoxic quinolone Rosoxacin. 25

Figure 2-5: Anti-cancer quinolones. 26

Figure 2-6: Structures of Compounds 15 and 16. 27

Figure 2-7: Structures of 6 and or 8-difluoroquinolones. 28

Figure 2-8: Structure of Compound CP-67,804 28

Figure 2-9: Structure of Voreloxin. 30

Figure 2-10: Different overlays of the structure of Compound A (dotted line) and Compound B (solid line), and structure of Compound 6a (designed derivative). 32

Figure 2-11: Overlapping image of Compounds 6a (green color) and Kyorin/Kyowa Hakko compound (A-blue color) at the ATP binding site of 1QZR 33

Figure 2-12: Compound 6a docked at the ATP binding site of 1QZR. 33

Figure 2-13: Structures of Compounds 17 and 18. 34

Figure 2-14: Compound 19: $R^1 = R^2 = R^4 = Cl$, $R^3 = H$ and Compound 20: $R^1 = R^2 = H$, R^3-R^4 = -CH=CH=CH=CH- 35

Figure 2-15: Structure of ofloxacin (Compound 21). 36

Figure 2-16: Structure of Compound 22. 37

Figure 2-17: Structure of Compound 23. 38

Figure 2-18: Strucure of Compound GS-9137 39

Figure 2-19: Structures of Compounds 24 and 25. 40

Figure 2-20: Structures of Compounds GS-9137 and GS-9160. 42

Figure 2-21: Structures of Compounds L-870810, FZ-41, S-1360 and SQ1 43

Figure 2-22: Structures of fluoroquinolonenucleosides 26 and 27. 44

Figure 2-23: Structure of Compound A-782759 47

Figure 3-1: Different overlays of the structure of Compound A (dotted lines) and Compound B (solid lines). 72

Figure 3-2: ORTEP Representation of the linear pentacyclic derivative 9 with 50% probability ellipsoids 79

Figure 3-3: ORTEP representation of Compound 10 with 50% probability ellipsoids. ... 82

Figure 3-4: Compound 6a docked at the ATP binding site of 1QZR. 87

Figure 3-5: Overlapping image of Compounds 6a (green colour) and A (blue colour) at the ATP binding site of 1QZR. 88

Figure 4-1: Structure of Prulifloxacin (A). 116

Figure 4-2: Structure of Compounds (B) and (C). 117

Figure 4-3: Prulifloxacin synthesis schematic 118

Figure 4-4: ORTEP representations of the X-ray structures of thiazetoquinoline derivatives 4a and 4b, with 50% probability ellipsoids. 124

Figure 4-5: Docked structure of Compound 4b at the ATP binding site of 1QZR 129

Figure 4-6: Reactant complex (a), transition state (b) and product complex (c) for the carbanion formation step calculated at the B3LYP/6-311G(d) level of theory. 133

Figure 4-7: The structure of the 3a-a/bromide product complex at the HF/6-311G(d) level of theory. 134

Figure 4-8: Phenolate form of 3a-a (a), ring closing transition state (b) and 4a/iodide product complex (c) for the ring closing step at the B3LYP/6-311G(d) level of theory. 138

Figure 4-9: A view of the molecular structure of the title molecule, with displacement ellipsoids drawn at the 50% probability level. 151

Figure 4-10: A partial view of the crystal packing of the title compound. 152

Figure 5-1: Compound 3c docked to HCV helicase ATP binding site. 172

List of Schemes

Scheme 2-1: Synthesis of 4-quinolones using the Gould-Jacobs reaction. 13

Scheme 2-2: Synthesis of 4-quinolones using Grohe-Heitzer reaction. 14

Scheme 2-3: Synthesis of 4-quinolone-3-carboxylic acid derivatives by palladium-catalyzed carbonylative heterocyclization. 15

Scheme 3-1: General synthesis scheme for Compound 6a. 74

Scheme 3-2: Different O-alkylated derivatives of intermediate 3. 75

Scheme 3-3: Synthesis of 9-cyano-7-hydroxy-8-oxo-8,9-dihydrobenzo[*h*]thieno[2,3-*b*]quinoline 8. 75

Scheme 3-4: Reactions on Compound 6a. 76

Scheme 3-5: Synthesis of 7-hydroxybenzo[*h*][1,2]thiazolo[5,4-*b*]quinolin-8(9*H*)-one. .. 78

Scheme 3-6: Synthesis of 9-acetyl-9*H*-benzo[*h*]pyrazolo[3',4':4,5]thieno[2,3-*b*]quinoline-7,10-diyl diacetate. 79

Scheme 3-7: Synthesis of *1H*-3-thia-11c-azaazuleno[1,8,7,6-*cdef*]phenanthrene-1,6(*5H*)-dione 11 81

Scheme 4-1: Synthesis of 4-oxo-benzo[*h*]thiazetoquinoline carboxylic acid derivatives. 120

Scheme 4-2: Synthesis of Compound 4c. 121

Scheme 4-3: A plausible mechanism for the formation of 4a from 3a. 122

Scheme 4-4: *O*-alkylated products (5 and 6). 123

Scheme 4-5: Suggested mechanism for mono decarboxylation of Compound 4b. 125

Scheme 5-1: Synthesis of cyclized Furo[2,3-*b*]quinolines. 167

Scheme 5-2: Synthesis of Furo[2,3-*b*]quinolines derivatives. 168

Scheme 5-3: Synthesis of the hydrazone derivatives 3f and 3g..... 169

Scheme 5-4: Synthesis of the furo bioisostere. 170

List of Abbreviations

A431	Human epidermoid carcinoma
AIDS	Acquired Immune Deficiency Syndrome
ANP	Phosphoaminophosphonic acid-adenylate ester
ATP	Adenosine triphosphate
BT474	A human breast tumor cell line
CC_{50}	Half maximal control concentration
CD-4	Cluster of differentiation 4
DFQs	Desfluoroquinolines
DKA	Diketoacid
DMEM	Dulbecco's Modified Eagle Medium
DMSO	Dimethylsulfoxide
DNA	Deoxyribonucleic acid
DPC	DNA-Protein Cross-links
DSB	Double-Strand Breaks
EC_{50}	Half maximal effective concentration
EGFR	Epidermal Growth Factor Receptor
FBS	Fetal Bovine Serum
GHKL	Gyrase, Hsp90, histidine Kinase, mutL
HCl	Hydrochloric acid
HCV-NS3	Hepatitis C-Virus-Non Structural protein 3

HER-2	Human Epidermal growth factor Receptor 2
HIV	Human Immunodefficiency Virus
HTS	High Throughput Screening
HuT78	Chronically infected HIV-1 cells
IBr	Iodobromide
IFN	Interferon
IN	HIV-1 Integrase
IRC	Intrinsic Reaction Coordinate
ISC	Inter Strand Cross-links
K_2CO_3	Potassium carbonate
Ki	Inhibition constant
KI	Potassium Iodide
K-ras	Kristen-ras
LC_{50}	The lethality concentration
LGA	Lamarckian Genetic Algorithm
LoVo	Human colon tumor
M/M cells	Latently infected HIV- 1cells
MA	Monoadducts
MAPK	Mitogen Activated Protein Kinase
MDA-MB-468	Breast cancer cell lines
MDR	Multi Drug Resistant
MEK	MAP Kinase

MMO	Molecular Mechanics Optimization
MSE	Modified methionine residues
MT-4, CEM, and PBMCs	Acutely infected HIV-1 cells
NF-$_k$B	Nuclear Factor-Kb
NMR	Nuclear Magnetic Resonance
NNIs	Non-Nucleoside Inhibitors
NS5B	Non-Structural Protein 5b
PDK 1	3-Phosphoinositide-Dependent Protein Kinase-1
PI3 Kα	Phosphoinositide 3-Kinase
PIP3	Phosphatidyl Inositol 3,4,5-trisphosphate
PKB/Akt	The serine/threonine protein kinase PKB
PMA	Phorbol Myristate Acetate
QRDR	Quinolone Resistance Determining Region
RdRp	The viral RNA dependent RNA polymerase
SAR	Structure Activity Relationship
SBDD	Structure-Based Drug Design
SN	Nucleophilic Substitution
SP1	Specificity Protein-1
SQ	Styrylquinolines
Src	A nonreceptor tyrosine kinase
TB	Tuberculosis
TGF-b	Transforming Growth Factor beta

THF	Tetrahydrofuran
TK	Tyrosine Kinase
Tnp	Tn5 transposase
TOF-EI	Time of Flight-Electron Impact
WHO	World Health Organization
XRC	X-Ray Crystallography

CHAPTER 1

Introduction and Overview

1.1 Structure-based drug design

The drug design industry is now one of the major players in the bioinformatics and biotechnology industries; the field is in great need for a rapid search for small molecules which will bind to the appropriate targets. Drug design is the process of finding new medications based on the knowledge of the biological target; the success in drug design necessitates both the combined use of chemical and biological research. Computational approaches are now playing a major part in rational drug design in combination with structural information derived from macromolecular x-ray crystallography and nuclear magnetic resonance (NMR) investigations. Structure-based drug design is perhaps the most reliable approach for discovering compounds possessing high specificity and efficacy. In the last few decades, novel methods of synthesizing large libraries of potentially bioactive small molecules using combinatorial methods possessing screening strategies have led to increasingly important roles in drug discovery.

There are two major types of drug design. The first is referred to as ligand-based drug design and the second, as structure-based drug design [1].

1.1.1 Ligand-based drug design

Ligand-based drug design can be identified on the basis of the knowledge of some other molecules exhibiting binding to the biological target of interest, and figuring out the possible binding interactions which in turn will lead to the identification of a pharmacophore. A pharmacophore is the model which exhibits the minimum necessary structural characteristics needed for a molecule to bind to the target [2].

1.1.2 Structure-based drug design (SBDD)

SBDD is identified on the basis of the knowledge of the three-dimensional structure of the biological target obtained through X-ray crystallography, or, via Nuclear Magnetic Resonance (NMR) spectroscopy. SBDD involves detailed knowledge of the binding sites of targets (such as proteins) associated with the particular disease of interest. The lock and key mechanism is the most applicable design for an effective drug. This drug design method involves basic knowledge of bioinformatics, proteomics, biochemistry, and computer modeling of three-dimensional protein structures [3].

1.1.3 Structure-based drug design steps

a) Drug target identification

b) Identification of the binding site

c) Virtual screening

d) Evaluation of potential lead candidate

1.1.3.1 Drug target identification

A drug target can be identified as a key biological molecule involved in a specific metabolic or signaling pathway which is related either to a particular disease condition, or the infectivity and survival of a microbial pathogen. The target molecule usually has a well-defined binding pocket in which small molecules can compete in order to modulate the function of the target. Also, the target molecule should be unique. No other pathway should be able to provide the function of the target and overcome the presence of the

inhibitor. In order to identify the potential target for the disease, different tools such as genomics, bioinformatics and proteomics [4].

1.1.3.2 Identification of the binding site

X-ray crystallography (XRC), NMR, Homology Modeling or Comparative Modeling are the most commonly used methods to identify the binding site. XRC is the main source of information for drug design as it can give high resolution structures. Once the three-dimensional structure of a protein is determined, the co-ordinates of the atoms are used by the computer to construct the protein structure.

Homology modeling is only used when there is no exact predetermined three-dimensional structure of the target (not determined either by XRC or NMR) based on an available sequence, usually provided with an empirical structure template with at least 30% sequence identity. After the structure of the target has been determined, the binding region should be determined. The binding site is considered as a cavity which exhibits hydrogen bond donors as well as hydrophobic characteristics [5].

1.1.3.3 Virtual screening (In-silico drug design)

In silico methods can help in determining drug targets *via* bioinformatics tools. Also, they can be used to analyze different target structures for checking possible binding/active sites, docking possible ligand molecules with the target, ranking them according to their binding affinites (scoring functions), and finally optimizing the structural features of tested molecules in order to improve their binding characteristics to develop the best candidate [4].

1.1.3.4 Evaluation of potential lead candidate

In order to evaluate a lead drug, Lipinski's "Rule of 5 "should be followed. Its name implies that all of the four parameters which are listed below and which are used to judge the expected efficacy of the drug should be close to five, or a multiple of 5. Lipinski [6] states that poor absorption or permeation is more likely when:

i. There are more than five H-bond donors.
ii. The molecular weight is over 500 Da.
iii. The logP (partition coefficient) is over 5.
iv. The sums of N's and O's are over 10.

1.2 Research scope

The scope of the research presented in this thesis mainly includes:

i. Applying the above-mentioned methodology (SBDD) to the synthesis of novel quinoline derivatives possessing potential biological activities.
ii. Performing isosteric and bioisosteric replacements for the newly-synthesized derivatives in order to come up with a clear idea about their Structure-Activity Relationships (SARs), and
iii. Shedding light on the requirements for the quinoline nucleus to develop anticancer derivatives.

1.3 Thesis overview

A manuscript-based thesis has been written to describe the entire work of the developed research. It combines five manuscripts following the thesis writing guidelines approved by Memorial University. The first manuscript is a literature review; the second, third and fourth manuscripts describe the first objective of the thesis achieved; and the last manuscript describes the second and third objectives of the thesis achieved. The organizational structure of the entire thesis is shown in **Figure 1-1** and the overview of the different chapters is discussed hereafter:

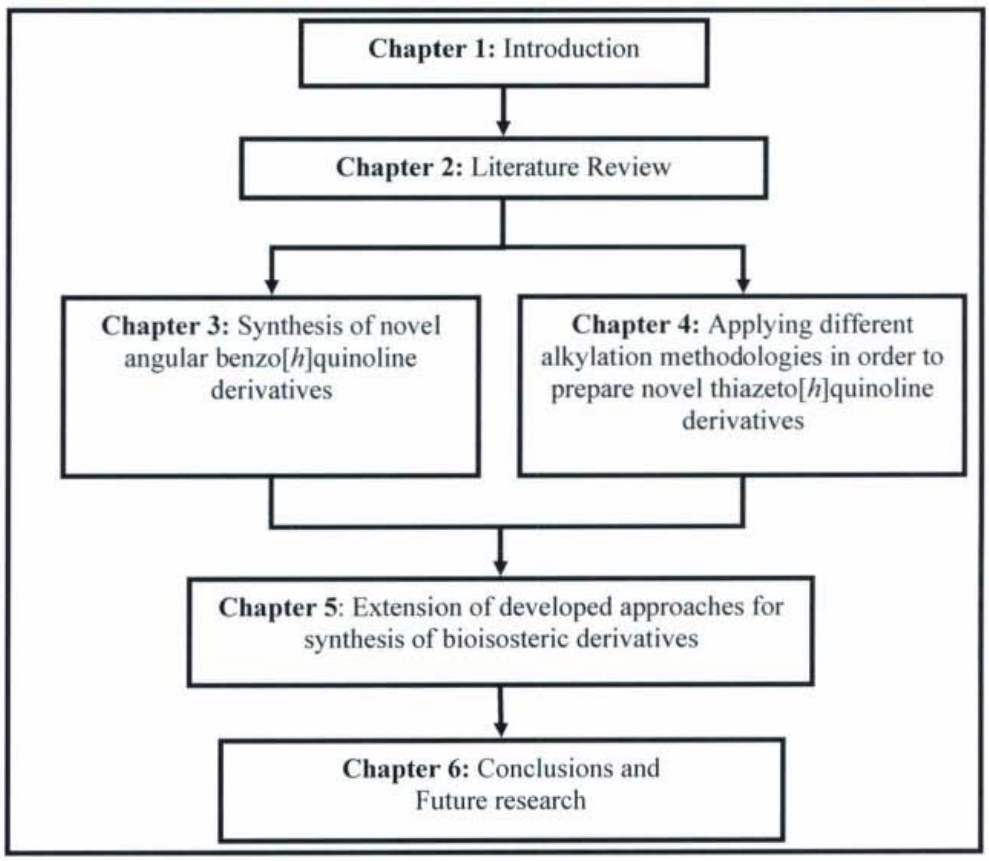

Figure 1-1: Thesis organization.

Chapter 1 introduces a broad overview of structure-based drug design, its types and the significance of each. Basic definitions and assumptions of structure-based drug design are also discussed. Finally, the research objectives are laid out.

Chapter 2 provides a discussion of the non-classical biological activities associated with the quinoline scaffold. The recent literature reviews on those activities are also discussed. This chapter comprises a manuscript which has been submitted for publication on Nov. 3rd and accepted for publication online on Dec. 9th in the Journal of pharmacy and pharmaceutical sciences under the title of Nonclassical Biological Activities of Quinolone Derivatives, 15 (1), 52-72, 2011 (available online).

Chapter 3, Chapter 4 and Chapter 5 comprise four different research papers which individually explore the frameworks, methodologies, and approaches to synthesize novel quinoline derivatives with different ring fusions.

Chapter 3: Abeer Ahmed and Mohsen Daneshtalab. Polycyclic Quinolones (Part 1) -Thieno [2,3-*b*] Benzo [*h*] Quinoline Derivatives: Design, Synthesis, Preliminary *in vitro* and *in silico* Studies, *Heterocycles*, V. 85, 2012. DOI: 10.3987/COM-11-12374 (in press, available online).

Chapter 4: Abeer Ahmed, Louise N. Dawe and Mohsen Daneshtalab. Polycyclic Quinolones (Part 2) - Synthesis Of Novel-4-Oxo-1,4-Dihydro Benzo [*h*] [1,3] Thiazeto [3,2-*a*] Quinoline Carboxylic Acids via Oxidative Cyclization Of The Corresponding Mercaptoquinoline Precursors, Heterocycles, V. 85, 2012. DOI: 10.3987/COM-11-12375 (in press, available online).

Appendix 4A: Structure of 4-Oxo-1,4-Dihydrobenzo- [*h*][1,3-Thiazeto-[3,2-*a*]Quinoline-1,3-Dicarboxylic Acid. Acta Cryst. 2011, E67, o529 (available online).

Chapter 5: Development of Anti-Viral Angular Furo[2,3-*b*]Benzo[*h*] Quinoline Agents Using Molecular Modeling and Virtual Screening Techniques (in prep).

Chapter 6 provides the summary and conclusions, and describes the originality of the research. In addition, recommendations for future research are provided.

CHAPTER 2

Literature Review: Non-Classical Biological Activities of Quinolone Derivatives

Abeer Ahmed[a] and Mohsen Daneshtalab[a]*

J Pharm Pharmaceut Sci (www.cspsCanada.org) 15(1), 52-72, 2011

Received, November 3, 2011; Accepted, December 9, 2011; Published, December 9, 2011.

[a]School of Pharmacy, Memorial University of Newfoundland, St. John's, Newfoundland and Labrador, Canada A1B 3V6. Fax: +1(709)-777-7044; E-mail: mohsen@mun.ca

Abstract

Quinolones are a family of multi-faceted drugs; their chemical synthesis is flexible and can be easily adapted to prepare new congeners with rationally devised structures. This is shown by the description of many thousands of derivatives in the scientific literature. Scientists could accurately describe their quantitative structure activity relationship (QSAR), which is essential for effective drug design. This also gave them the chance to discover new and unprecedented activities, which makes quinolones an endless source of hope and enables further development of new clinically useful drugs.

Quinolones are among the most common frameworks present in the bioactive drug molecules that have dominated the market for more than four decades. Since 1962, 4(1*H*)-quinolone-3-carboxylic acid derivatives have been widely used as antibacterial agents. Quinolones have a broad and potent spectrum of activity and are also used as second-line drugs to treat tuberculosis (TB). Recently, quinolones exihibited "non-classical" biological activities, such as antitumor, anti-HIV-1 integrase, anti-HCV-NS3 helicase and anti-NS5B-polymerase activities.

The present review focuses on the structural modifications responsible for the transformation of an antibacterial into an anticancer a gent and/or an antiviral agent. Indeed, quinolones' antimicrobial action is distinguishable among antibacterial agents, because they target different type II topoisomerase enzymes. Many derivatives of this family show high activity against bacterial topoisomerases and eukaryotic topoisomerases, and are also toxic to cultured mammalian cells and *in vivo* tumor models. Moreover, quinolones have shown antiviral activity against HIV and HCV viruses. In this

context the quinolones family of drugs seem to link three different biological activities (antibacterial, anticancer chemotherapy, and the antiviral activity) and the review will also provide an insight into the different mechanisms responsible for these activities among different species.

2.1 Introduction

Quinolones as "privileged building blocks" with simple and flexible synthetic routes, allow for the production of libraries of quinolone derivatives. Because of their diversity, drug-like properties and similarities to specific targets, they are considered a central scaffold to build chemical libraries with promising bioactivity potential.

The first quinolone discovery, as with many important discoveries, was a result of serendipity. Lesher *et al.* (1962) [1] discovered the first quinolone derivative as an impurity in the chemical manufacturing of a batch of the antimalarial agent, chloroquine. Since then, more than 10,000 quinolone derivatives have been patented or published which explains the enormous progress that has been made in understanding the molecular mechanisms of action behind the different pharmacological actions of this privileged molecule.

Quinolones as a class of antibacterial agents have been known for over 40 years. Although considerable results in the research of new antibacterial quinolones have already been achieved, they are still a matter of study because of the continuous demand of novel compounds active against resistant strains of bacteria. Research efforts are mainly focused on obtaining new compounds which are active against very resistant bacterial strains or acting on the mechanisms of resistance [1-4].

Currently, fluoroquinolones are approved as second-line drugs by the WHO to treat TB but their use in MDR-TB is increasing due to the fact that they have a broad and potent spectrum of activity and can also be administered orally. Moreover, they have favourable pharmacokinetic profiles and good absorption, including excellent penetration into host macrophages. As of today, the potential of fluoroquinolones as first-line drugs is still under investigation [5-7].

2.2 The chemistry of 4-quinolones

The original method for the preparation of 4-quinolones relies on the Gould-Jacobs reaction between aniline and a dialkyl alkoxymethylenemalonate [8].

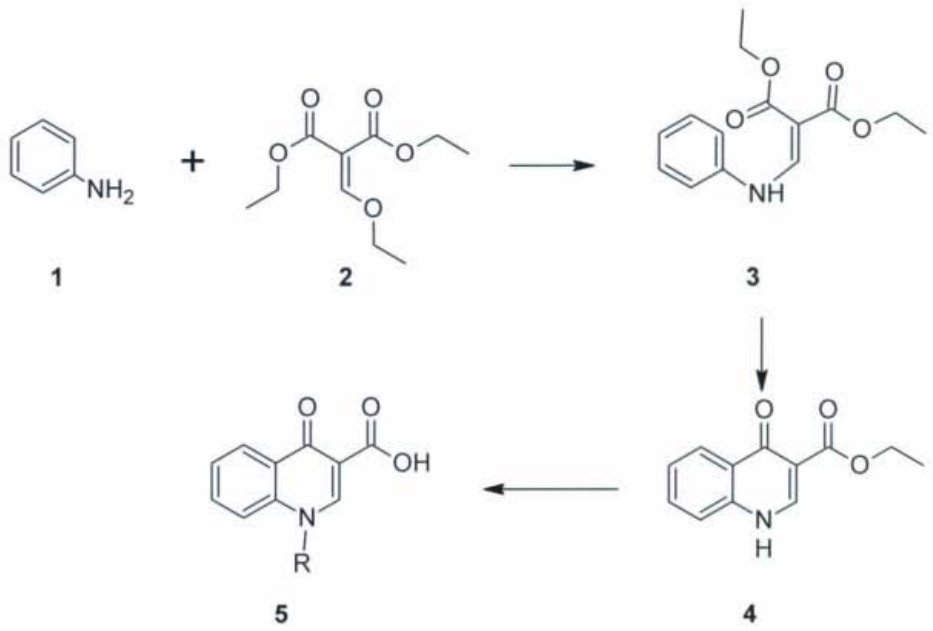

Scheme 2-1: Synthesis of 4-quinolones using the Gould-Jacobs reaction.

Lappin cyclization [9] results in cycloacylation to form **3**, on heating at a high temperature to provide the quinoline-4-one system as shown in **Scheme 2-1**. S_N2 alkylation at N-1 followed by ester hydrolysis affords the substituted 4(1*H*)- quinolone-3-carboxylic acid **5**.

The Gould-Jacobs approach allows only the introduction of primary alkyl groups, thus limiting the preparation of derivatives with more complex substituents at N-1. In this respect the Grohe-Heitzer cycloacylation expanded the synthetic possibilities of quinolones as depicted in **Scheme 2-2** [10].

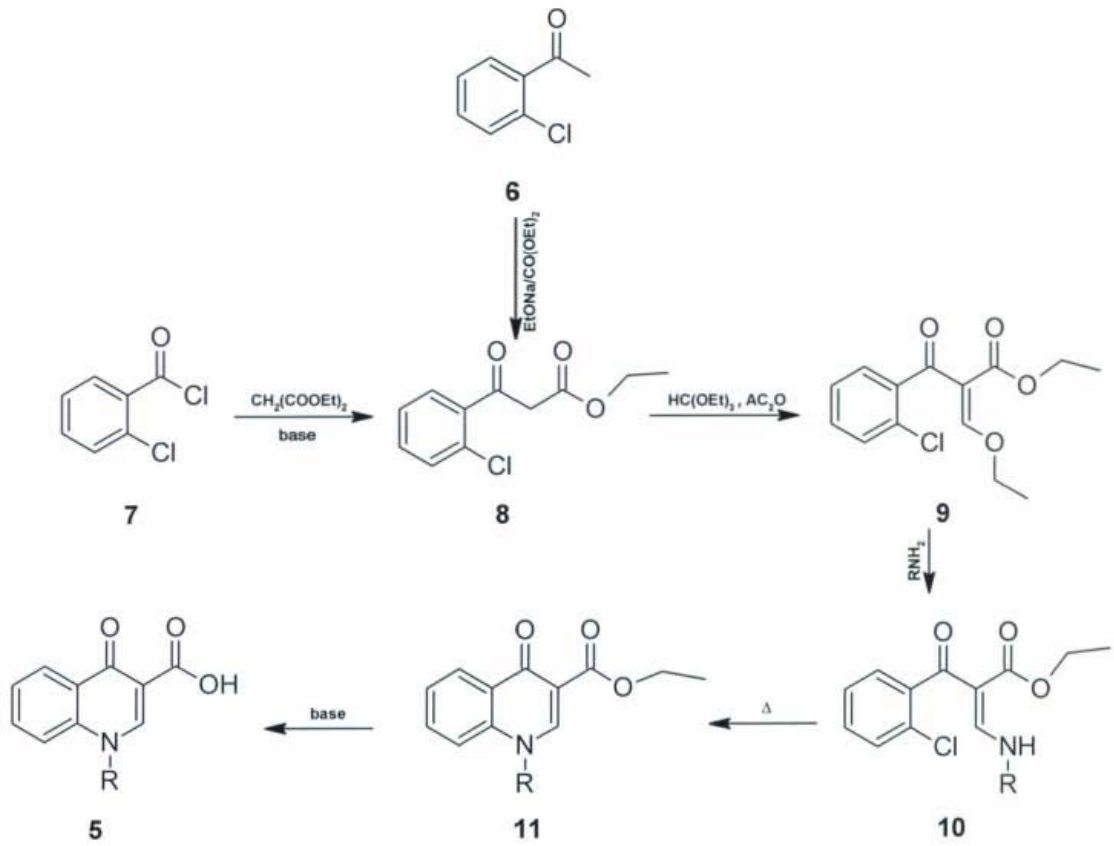

Scheme 2-2: Synthesis of 4-quinolones using Grohe-Heitzer reaction.

In the Grohe-Heitzer synthesis, the active methylene in a β-ketoester is condensed under dehydrating conditions with an orthoester, resulting in the formation of the enol ether which is further subjected to an addition-elimination reaction using an appropriate primary amine. The product obtained is cyclized through an aromatic nucleophilic displacement of a leaving group (typically Cl, F) at the *ortho* position with respect to the activating carbonyl group. Final hydrolysis of the ester function under either basic or acidic conditions gives the quinolone-3-carboxylic acid [11].

4(1*H*)-Quinolone-3-carboxylic acid derivatives containing a variety of substituents at different positions have also been prepared by palladium-catalyzed carbonylative heterocyclization [12]. Palladium cyclization enables the synthesis of several 4(1*H*)-quinolone-3-carboxylic acid derivatives in 24-82% yields. Palladium-catalyzed cyclization has the potential to accommodate substituents at position 2 which in turn offers flexibility for the design of quinolinone derivatives as depicted in **Scheme 2-3**.

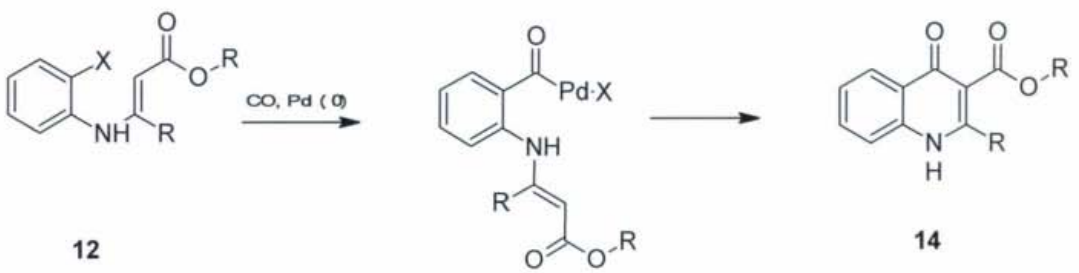

12 **13** **14**

Scheme 2-3: Synthesis of 4-quinolone-3-carboxylic acid derivatives by palladium-catalyzed carbonylative heterocyclization.

2.3 Biological targets of antibacterial quinolones

Generally, quinolones directly inhibit DNA synthesis by binding to the enzyme-DNA complex. Quinolones also stabilize DNA strand breaks created by DNA gyrase and topoisomerase IV. Ternary complexes of drug, enzyme, and DNA block progress of the replication fork. The cytotoxicity of fluoroquinolones can be explained on the basis of a 2-step process: (1) the conversion of the ternary complex (topoisomerase-quinolone-DNA) into an irreversible form; and (2) the production of a double-strand break by denaturation of the topoisomerase. The molecular basis necessary for the transition from step 1 to step 2 is still unclear [13].

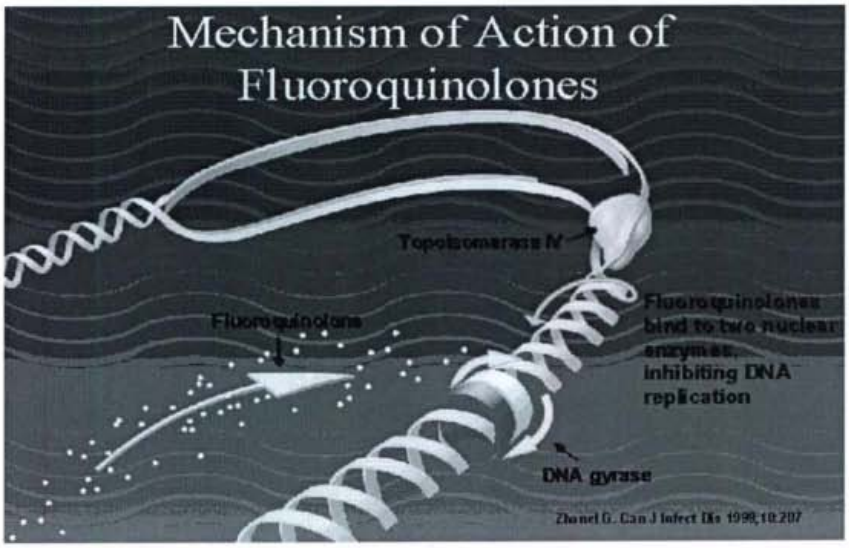

Figure 2-1: Mechanism of action of fluoroquinolones

(adopted from Zhanel *et al.*, 1999).

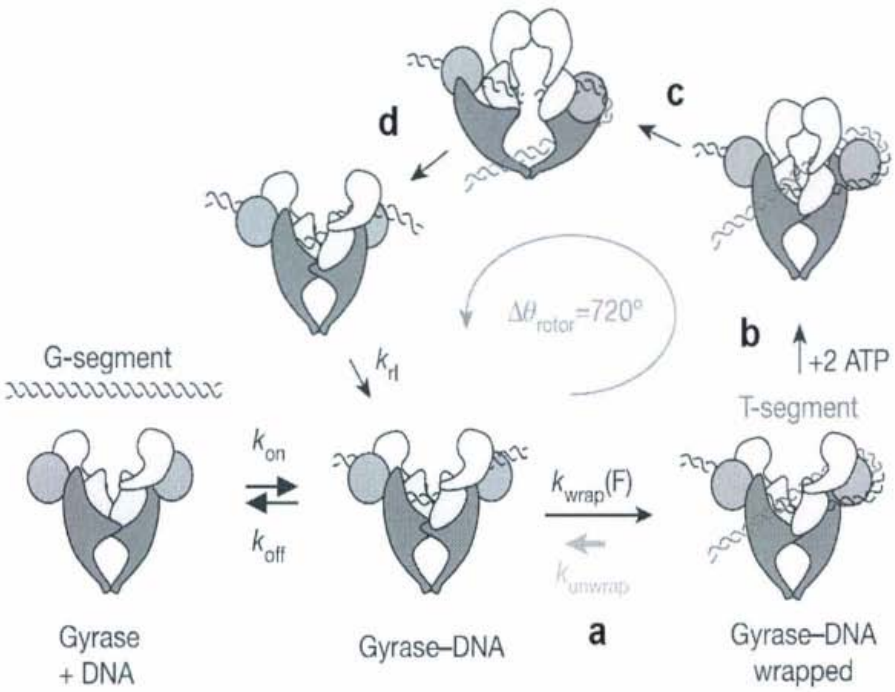

Figure 2-2: DNA cleavage-religation mechanism of DNA Gyrase

(adopted from Gore *et al.*, 2006).

(a) Gyrase binds to a DNA segment as a tetramer and wraps a DNA segment (120 – 140 bp) into a positive supercoil. **(b)** ATP binds to the GyrB subunits and a conformational change occurs. The subunits dimerise, capturing the T-segment. At the same time, a double-strand break is introduced into the G-segment. **(c)** The T-segment is transported through the G segment break, towards the central hole of the GyrA dimer. **(d)** Following the T-segment passage, the G-segment is religated and the T-segment is released through a transient opening of the primary dimer interface on the GyrA dimer. Religation of the

DNA break introduces two negative supercoils on the DNA. ATP hydrolysis promotes enzyme turnover and regenerates the starting state.

The DNA break is formed through a transesterification step which leads to the attachment of the 5′- phorphoryl group on DNA to the hydroxyl on Tyr-122 on GyrA [18]. The DNA is cut in a sequence-specific manner, creating a 4-bp staggered break on opposite strands of the DNA. In a study by Morrison *et al.,* [19] the cleavage of four double-stranded DNAs was examined. Each double-stranded DNA strand was cleaved between T and G on the one strand; however, the cleavage on the complementary strand seemed to have no sequence specificity.

2.5 Important structural features of antibacterial quinolones

It is really important to highlight the structural requirements for a quinoline pharmacophore to exihibit antibacterial activity, as presented in **Figure 2-3**.

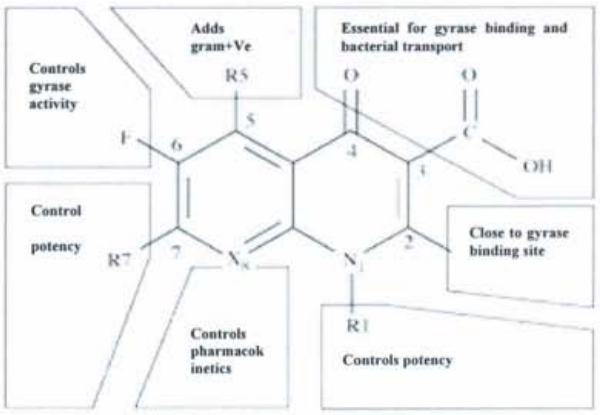

Figure 2-3: General structure of the most-commonly used quinolone molecule.

Position 1: This position is part of the enzyme-DNA binding complex, and has a hydrophobic interaction with the major grove of DNA [20]. A cyclopropyl substituent is considered the most potent substitution here; the second important substitution for the required activity is the addition of a 2,4-difluorophenyl [21].

Position 2: This location is very close to the site for the gyrase binding site (or topoisomerase IV) and it is well-known that any added bulk inhibits the transport and results in a lower level of microbiological activity [20]. Only a sulfur, incorporated into a small ring, has been able to replace hydrogen at the R-2 position [20].

Positions 3 and 4: These two positions on the quinolone nucleus are essential for gyrase binding and bacterial transport and no other useful substitutions have been reported yet. Therefore, the 3-carboxylate and 4-carbonyl groups are considered essential for antimicrobial activity [22].

Position 5: Substituents at this position of the basic quinolone nucleus appear to have the capacity to control potency. Electron-donating groups such as an amino, hydroxyl, or methyl group were found to increase *in vitro* activity against gram-positive bacteria [23].

Position 6: The substitution with a fluorine atom had markedly improved antimicrobial activity compared to the original quinolone agents, and gave rise to the now widely-used and clinically-successful fluoroquinolone compounds. As suggested by Ledoussal *et al.* [24] the 6-H is equivalent in activity to the 6-fluoro analogue even at the enzyme level.

Position 7: Five- or six-membered nitrogen heterocycles are the most commonly applied moieties at this position. This position is considered to be one that directly interacts with DNA gyrase [25].

Position 8: Of particular interest is the observation that specific changes in position 8 appear to dramatically alter the initial target in fluoroquinolones. For example, the presence of a simple hydrogen atom as in ciprofloxacin, or a fused ring (for example, ofloxacin and levofloxacin that have a benzoxazine bridge between C-8 and N-1) typically leads to high activity against topoisomerase IV, with little clinically-useful activity against DNA gyrase.

The current knowledge of structure-activity relationships has been gathered through the past development of a large number of compounds within the quinolone class and goes on to improve the antimicrobial activity and extend the useful life of such clinically-important compounds.

2.6 Dual targets mechanism of action

Quinolones act in a similar fashion against the two prokaryotic Type II enzymes. They essentially block the topoisomerase catalytic cycle when the protein is covalently linked to the cleaved DNA (cleavage complex). Stabilization of the enzyme-DNA complex has been confirmed to block the progression of the replicative machinery and to create DNA lesions that induce a bacterial SOS response [26,27]. Amino acid mutations in the Quinolone Resistance Determining Region (QRDR) greatly reduce the affinity of quinolones for the enzyme-DNA complex. The most relevant positions in *E. coli* are Ser83 and Asp87 in GyrA, and the corresponding Ser79 and Asp83 in ParC [28,29]. The structural features of the interactions between quinolone-gyrase-DNA complex were identified by the sequencing of additional mutant gyrA and gyrB genes that produce the altered quinolone susceptibility [30]. Experimental evidence suggests that quinolones, in

the presence of appropriate metal ions, bind single-stranded DNA and GyrA with moderate affinity [31,32]. However, they bind efficiently to the gyrase-DNA complex [33]. At the DNA level, cleavage is not required to stimulate drug binding: the structural distortion of the double helix, bound to the protein and stabilized by selective contacts with protein residues, appears to be sufficient to provide a favourable interaction site for quinolones [34]. Additionally, the presence of quinolones alters not only the structural features of GyrA (binding site) but also those of the overall A2B2-DNA complex [32,35] inducing modifications in the kinetic rates of different catalytic steps.

2.6.1 Differences between DNA gyrase and eukaryotic topo II

In eukaryotes, DNA gyrase and topoisomerase IV are functionally replaced by two isoenzymes: topoisomerase IIa and IIb, 170 and 180 kDa proteins respectively [3]. These proteins share a similar catalytic cycle, the main difference being in the fact that the active form of eukaryotic topoisomerase II (Topo2) is constituted by a homodimer. However, as supported by the extended sequence homology, Topo2, can be seen as the fusion of the GyrA-GyrB or ParC- ParE subunits.

Common features in the mechanism of action of antibacterial quinolones and antitumor drugs have suggested that both compounds have a similar mode of interaction with the type II DNA topoisomerase-DNA complexes. In particular, comparison between quinolones and antitumor drugs of the epipodophyllotoxin family (etoposide and teniposide) has been considered, since neither type of drug is a DNA intercalator [36]. Archaebacteria are considered as being an intermediate phylogenetic position between eukaryotes and eubacteria [37]. In these systems, comparable sensitivity to poisons of

each Type II topoisomerase was observed and the DNA cleavage patterns induced by ciprofloxacin and etoposide were found to be very similar [38,39]. These findings strongly supported a common mode of interaction with the DNA- topoisomerase II complexes for ciprofloxacin and etoposide.

2.7 Quinolone-based anticancer derivatives

Quinolone derivatives represent a large number of antiproliferative agents exhibiting cytotoxicity through DNA intercalation, causing interference in the replication process [40-42]. Actinomycin D, doxorubicin, mitoxantrone and streptonigrin are quinoline analogs possessing antibacterial or anti-cancer activity through DNA intercalation. Most of these drugs are currently used in the treatment of human malignancies targeting topoisomerase (Types II) enzymes [43-45].

An interesting point which was highlighted in many quinolones' previous reviews, is: how can small molecules discriminate efficiently between such similar enzymes? It was found that a minute change in the quinoline structure enabled the drug to act on another different target. High throughput screening revealed that there are two major types of modification that appear to drive the quinolone action from antibacterial to anticancer: i) The disruption of the zwitterionic properties of the compounds by modifying either the C7 basic substituent or the C3 carbonyl group, or both, will affect the electron density distribution and protonation equilibria; ii) The increase in the extent of aromatic/condensed rings mostly lead to increase the affinity of quinolones for double-stranded DNA, while antibacterial quinolones interact better with single-stranded DNA [46].

2.7.1 Historic development of cytotoxic quinolones.

Topoisomerase II is the primary target for several classes of antineoplastic drugs [47,48,49]. These agents are widely used for the treatment of human cancers [47,48,49] and their clinical efficacies correlate with their abilities to stabilize covalent enzyme-cleaved DNA complexes that are intermediates in the catalytic cycle of the enzyme [47-51]. While quinolone-based drugs have been developed extensively as antimicrobial agents (targeted to DNA gyrase, the prokaryotic counterpart of topoisomerase II) [52,53], these studies provided evidence that quinolones may have potential as antineoplastic drugs. When comparing the known sequences of topoisomerases from bacteria to mammals, the sequences appear to be similar around active site tyrosine, not only among type II topoisomerase but also among type I. They also share the same mechanism of cell killing which is performed by trapping topoisomerase II in an intermediary cleavable complex with DNA, termed the "cleavable complex," which is detected as DNA double strand breaks [54]. The pioneering study in this field showed that ciprofloxacin and ofloxacin interfer only slightly with the function of Calf Thymus Topo II, the prokaryotic gyrase being approximately 100-fold more sensitive to inhibition than its eukaryotic counterpart [55].

Rosoxacin, a 7-(4-pyridinyl)quinolone derivative **Figure 2-4**, showed great promise in treating gonococcal infections [56]. Morover, the 7-(4-pyridinyl) derivatives produced an unacceptable toxicity profile *in vitro*, inducing a genetic toxicity endpoint [57].

Since that time, different directions were followed to elucidate the structural activity relationships responsible for the interference of quinolones with eukaryotic topoisomerase II.

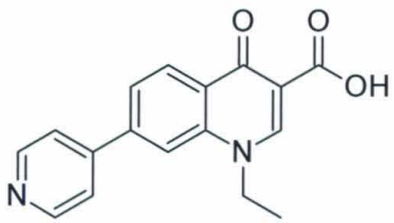

Figure 2-4: Structure of the cytotoxic quinolone Rosoxacin.

2.7.2 Important structural features of anticancer quinolones

2.7.2.1 Position 3 substituents

It is well established that, in antibacterial quinolones, the 3-carboxyl functional group or its isosteric replacement is a fundamental requirement for activity. However, this functional group can be replaced even with a hydrogen atom, and effective poisoning of Topo2 can still be maintained. It seems that, to inhibit the eukaryotic enzyme, the basic requirement is the coplanarity of the C-3 substituent with the quinoline ring. Thus, although in 3-H derivatives small substituents can be beneficial at C-2, no such residue can be introduced if the carboxyl group is present, as it will destabilize the coplanar orientation of the acidic moiety [58]. Removal of the carboxylic group opened up new synthetic opportunities. In fact, introduction of a phenyl group or a related heteroaromatic ring at C-2 enhanced Topo2 poisoning activity [59]. The distance between the two aromatic moieties is apparently crucial, as only a methylene linker allowed the

maintainance of biological activity. Further increase in cytotoxic activity was obtained upon introduction of hydroxyl- substituents into the C-2 phenyl group. In particular, the 2,6-dihydroxy benzyl derivative (**WIN 64593, Figure 2-5**) is the most active quinolone derivative. In quinolones carrying the carboxyl group, the acidic moiety can participate with the ketone at position 4 in chelating metal ions, or can be involved in hydrogen bonding with the target macromolecules.

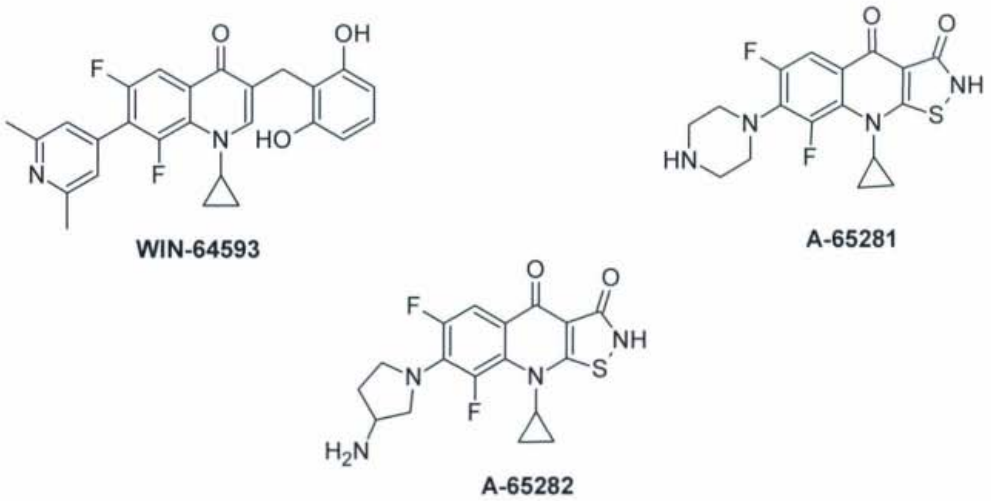

Figure 2-5: Anti-cancer quinolones.

The substitution of the nitrogen at position 1 with a sulfur atom leads to inactive derivatives [58]. However, as reported, other positions can support the introduction of this heteroatom without the loss of activity. An example is represented by the isothiazolo quinolones **A-65281** and **A-65282** [60]. These derivatives exhibit a heterocyclic moiety fused onto the quinolone system, which can be considered as a modification of the carboxylic group. It is worth noting that, in spite of the fact that these derivatives do not exhibit an aromatic substituent at position C-7, they are active against both bacterial and

eukaryotic type II topoisomerases. More recently, [61] derivatives bearing a 3-dimethylaminopropyl substituent on the quinolone nitrogen and a methoxycarbonyl group at position 9 (Compound **15)** exhibited prominent antitumor activity. Cytotoxicity was reduced when an anilido substituent was present at position 9 (Compound **16, Figure 2-6)**.

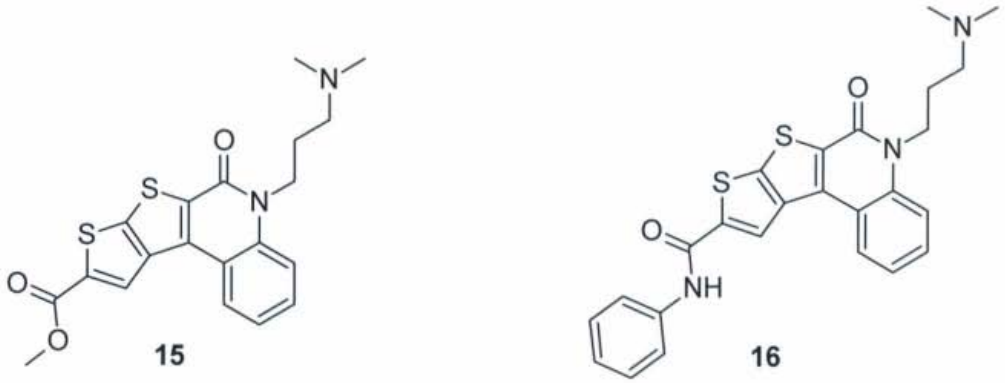

Figure 2-6: Structures of Compounds **15** and **16**.

2.7.2.2 Positions 6 and 8

A study done in 1991 [62] showed that 6,8-difluoroquinolones were potent in affecting the eukaryotic topoisomerase II. Following another study [63] showing the contribution of the C-8 fluorine to drug potency, the authors compared the effects of CP-115,955 [6-fluoro-7-(4-hydroxyphenyl)-1-cyclopropyl-4-quinolone-3-carboxylic acid] **Figure 2-7** on the enzymatic activities of *Drosophila melanogaster* topoisomerase II with those of **CP-115,953** (the 6,8-difluoro parent compound of **CP-115,955**). Results showed that removal of the C-8 fluoro substituent decreased the ability of the quinolone to enhance the enzyme-mediated DNA cleavage ~2.5-fold.

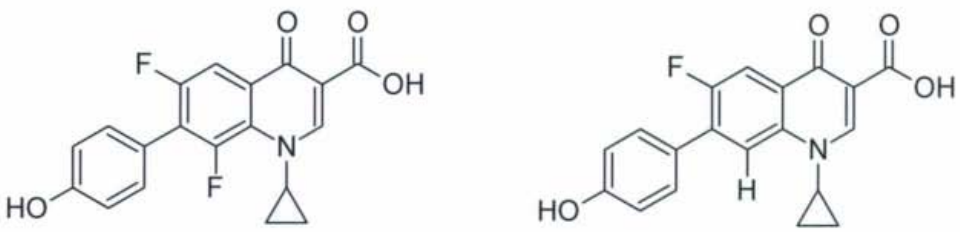

Figure 2-7: Structures of 6 and or 8-difluoroquinolones.

2.7.2.3 Ring position N-1

Considerable evidence [64] indicates that the presence of a cyclopropyl as opposed to an ethyl group at position N-1 increases quinolone potency against DNA gyrase and by comparing the DNA cleavage-enhancing activity of ciprofloxacin with that of norfloxacin or the activity of **CP-115,953** with that of **CP-67,804, Figure 2-8**, it was determined that substitution of an ethyl group at N-1 decreased quinolone potency against calf thymus topoisomerase II between -30- to -40- fold, respectively.

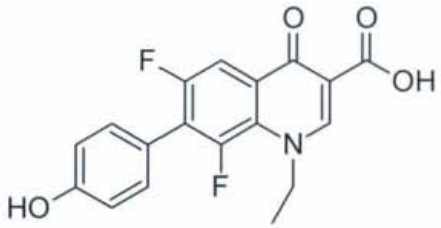

Figure 2-8: Structure of Compound **CP-67,804**.

2.7.2.4 Substitution at C-7

A variety of substitutions were also introduced at position C-7. In fact, the presence of a basic amino group in the aliphatic cyclic substituent at position C-7 is a strict

requirement for antibacterial activity. Additionally, modifications at this position were shown to play a key role in directing the drug preferentially towards Gyr or Topo 4 [65]. These results suggested a direct interaction of this portion of the quinolone with the enzyme. Conceivably, the C-7 substituent should affect the prokaryotic/eukaryotic enzyme selectively. Indeed, methyl substituents at the C-7 piperazine group influenced potency against the mammalian enzyme. In fact 3,5-dimethylpiperazinyl derivatives were active in stimulating enzyme-mediated DNA cleavage only in the *trans* configuration. This was particularly interesting because *cis*- or *trans*-methyl substitution on the piperazine had little effect on the activity against Gyr, suggesting that only in the mammalian enzyme does an asymmetric barrier exists which influences productive quinolone interaction, and favours the less bulky trans-3,5-dimethylpiperazine substituent at C-7 [66]. Parallel studies demonstrated that compounds with C-7 pyrrolidine substituents were more cytotoxic than those with piperazine substituents [67]. This is actually in line with observations made on derivatives related to the earlier cytotoxic quinolones [68]. Looking both at the stimulation of DNA cleavage and the cytotoxicity against cultured mammalian cells, it was observed that the presence of an aromatic group contributed greatly to drug activity. In particular, 4'-hydroxyphenyl substituent at the C-7 position was found to be critical for potency towards the mammalian Topo 2 [64]. From this series **CP-115953**, a 6,8-difluoro-7-(4'-hydroxyphenyl)-1-cyclopropyl-4-quinolone-3-carboxylic acid was found to be the most cytotoxic quinolone derivative [62].

2.7.3 Quinoline/one derivatives as topoisomerase inhibitors

Vosaroxin **Figure 2-9** [69] (formerly voreloxin) is an anticancer quinolone derivative that intercalates DNA and inhibits topoisomerase II, inducing site-selective double-strand breaks (DSB), G2 arrest and apoptosis. The quinolone-based scaffold differentiates vosaroxin from the anthracyclines and anthracenediones. It has been reported that vosaroxin induces a cell cycle specific pattern of DNA damage and repair that is distinct from anthracycline and doxorubicin [69].

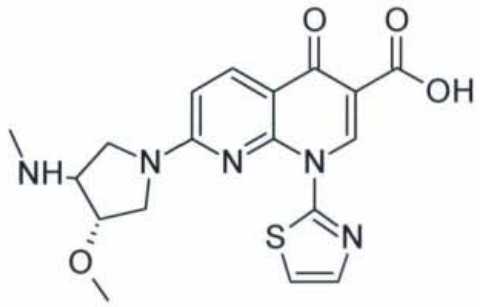

Figure 2-9: Structure of Voreloxin.

In 1989, Kyorin/Kyowa-Hakko described thiazoloquinolone carboxylic acids with an impressive anticancer profile (Compound **A**, **Figure 2-10**) [70]. The clinical candidate had exhibited favourable drug-like properties in different animal models in preclinical studies.

Compound A, like other quinolone carboxylic acid derivatives, was presumed to interact with topoisomerase II via its β-keto acid functional group by chelating with the Mg^{2+} ion to inhibit the enzyme. Considering this mode of action, [71] we hypothesized that a quinolone with a β-diketo functionality may be able to mimic the action of β-ketoester functionality, thus potentially providing the same level of complexity with the

Mg^{2+} ion at the active site of the topoisomerase II. Also, due to the absence of free carboxylic acid, the target quinolone may cause less gastric damage when used via oral administration.

The design of target compounds was based on a structure-based design program using the Hyperchem-3™ molecular modeling program. By applying Molecular Mechanics Optimization (MMO) and Molecular Dynamic Option methods we were able to identify linear tricyclic quinolones with β-diketo components that matched the angular feature of Compound A. In this respect, Compound B, 9-benzyl-7-fluoro-3-hydroxythieno [4,5-*b*]quinoline-4(9*H*)-one, at its optimized steric/energetic configuration, was found to have the best match with a perfect 3-point overlay with Compound A as depicted in **Figure 2-10**.

Compound B and its derivatives were synthesized in our group using the Gould Jacob method. This series of compounds displayed promising cytotoxic activity against several cancer cell lines [72].

Compound **6a** also was designed to act in the same manner as compounds B and A applying the most important structural features which is the coplanarity of the β-diketo functionality.

Figure 2-11: Overlapping image of Compounds **6a** (green color) and Kyorin/Kyowa Hakko compound (**A**-blue color) at the ATP binding site of 1QZR.

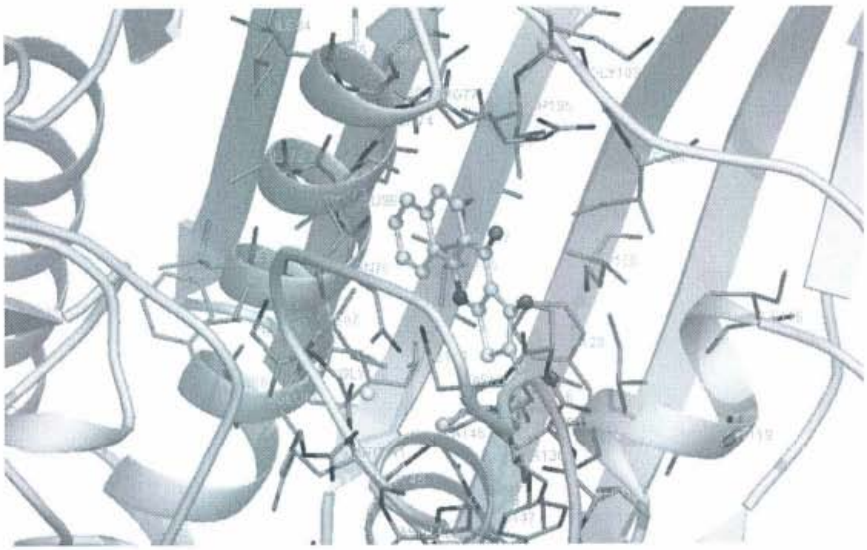

Figure 2-12: Compound **6a** docked at the ATP binding site of 1QZR.

These derivatives did not show cytotoxicity against cancer cell lines. We attributed this finding to a solubility problem and efflux pump mechanisms.

2.7.4 Signal transducers and activators of transcription (STATs) inhibition

STATs are an important family of molecules that mediate signal transduction in cells [74,75]. Accumulating evidence indicates that STAT family members play important roles in carcinogenesis and, in particular, STAT3 has emerged as a good target for cancer therapy [76-78]. Very recently, a high throughput screening approach allowed the identification of the highly

Fluorinated quinolone derivative **17** (R_1= R_2 = F), **Figure 2-13**, that inhibits the STAT3 pathway and causes cell apoptosis (EC_{50} =4.6 μM). Lead optimization with modification of the phenyl moiety led to the identification of the 4-cyanophenyl derivative **18** (R_1=CN, R_2=H) with a 30-fold increase in potency (EC_{50} = 170 nM) in which cell apoptosis induction correlates well with inhibition of steady state and cytokine induced JAK and STAT3 activation [79].

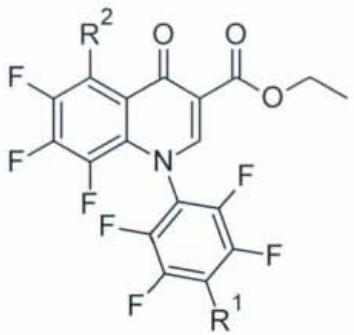

Figure 2-13: Structures of Compounds **17** and **18**.

In a receptor-based virtual screening of around 70.000 compounds, some 3-carboxy-4(1*H*)-quinolones were revealed to be human protein kinase CK2 inhibitors [80]. Protein kinase CK2 participates not only in the development of some types of cancers but also in viral infections and inflammatory failures. Thus, quinolones could be considered not only potential antitumor, but also anti-infectious and anti-inflammatory drugs. The compounds with high docking scores were selected for *in vitro* tests, and Compounds **19** and **20** displayed IC_{50} values of 0.3 and 1 μM, respectively. These findings led to investigating other derivatives of this class in order to determine the effects of certain substituents on their inhibitory activity.

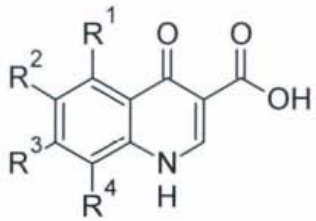

Figure 2-14: Compound **19**: $R^1 = R^2 = R^4 = Cl$, $R^3 = H$ and Compound **20**: $R^1 = R^2 = H$, R^3-R^4 = -CH=CH=CH=CH-.

2.8 Quinolone scaffold-based antiviral agents

Quinolines are not new to the field of antiviral agents. Previously reported data on their binding with bacterial chromosome had strengthened the hypothesis that these drugs could also bind to the viral nucleic acid, and prompted the investigation of their antiviral activity [81-86].

Many structures containing the basic quinolone carboxylic acid template and different lipophilic substituents were patented as antiviral agents: most of them were tested against human immunodeficiency virus-1 (HIV-1) and were claimed to be effective in the treatment or prophylaxis of Acquired Immune Deficiency Syndrome (AIDS) [87-89]. However, their mechanism of action was not reported.

2.8.1 Quinolone-based anti-HIV agents

An earlier work done by Furusawa *et al.* [90], reported that several fluoroquinolones protect cells from HIV-mediated cytotoxicity. The results showed that after ofloxacin **21** treatment, the protected cells were able to survive for an extra 3 months without any loss in cell viability. The l-isomer of ofloxacin (DR-3355) [91] was also reported to protect cells from HIV-1 mediated cytolysis in which the surviving cells were unable to produce an infective virus and also lost expression of the CD4 antigen [90].

The exact mechanism of action of antiviral quinolones is still unknown. The following classification is done according to the authors' postulations.

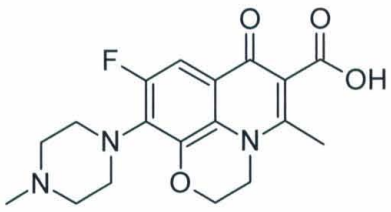

Figure 2-15: Structure of ofloxacin (Compound **21**).

2.8.1.1 Integration of proviral DNA into mRNA

Baba *et al.* [92] found that antibacterial fluoroquinolones can exhibit antiviral activity as well. Analogues, bearing a 8-difluoromethoxy-1-ethyl-6-fluoro-1,4-didehydro-7-[4-(2-methoxyphenyl)-1-piperazinyl]-4-oxoquinoline-3-carboxylic acid (**22**), exhibited EC_{50} < 50 nM in chronically-infected cells. Compound **22** suppressed tumor necrosis factor alpha (TNF-α)-induced HIV-1 expression in latently infected cells (OM-10.1) and constitutive viral production in chronically-infected cells (MOLT-4/III_B) at a concentration of 0.8 mM. It was reported that Compound **22** could also inhibit HIV-1 antigen expression in OM-10.1 and MOLT-4/III_B cells at the same concentration [92]. Inhibitors of this step, which is considered a crucial step in HIV replication, will be able to suppress HIV replication not only in acutely- but also in chronically-infected cells [93].

Figure 2-16: Structure of Compound **22**.

2.8.1.2 *Interference with a postintegrational target of the HIV-1 replication cycle*

Much of the pertinent literature [94-96] has addressed the potential of 6-aminoquinoline series to inhibit the HIV replication cycle. The prototype was Compound **23.** The synthesized derivatives showed very strong activity on HIV-1 acutely-infected MT-4, CEM, and PBMCs cells, as well as on chronically infected HuT78. A potent antiviral activity was also observed in latently HIV-1-infected M/M cells at drug concentrations as low as 40 ηg/mL. This activity was further confirmed in an *in vivo* model for HIV-1 latency, which provided encouraging evidence for the use of quinolones in the control of HIV-1 infection [97]. The studies on the mechanism of action revealed that 6-DFQs interfere with a postintegrational target of the HIV-1 replication cycle.

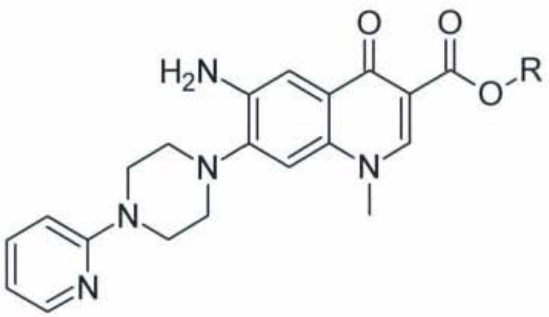

Figure 2-17: Structure of Compound **23**.

2.8.1.3 *HIV-1 integrase inhibitors*

HIV-1 integrase (IN) [98-103], along with HIV-1 reverse transcriptase and HIV-1 protease, are essential enzymes for retroviral replication and represent important targets

for interrupting the viral replication cycle. The HIV integrase catalytic cycle is illustrated in **Figure 2-8**.

IN is an attractive target because it has no counterpart in mammalian cells; therefore, most IN inhibitors should possess high selectivity and low toxicity. Quinolone derivatives, as a class of HIV-1 inhibitors, have become of great interest due to their high molecular versatility, easy synthesis at low cost and on a large scale, and well-recognized biochemical properties that make them very suitable pharmacophore structures. The first quinolone-based structure Elvitegravir (**GS-9137**) **w**ith very strong antiretroviral properties owes its anti-HIV activity exclusively to the inhibition of the viral enzyme integrase.

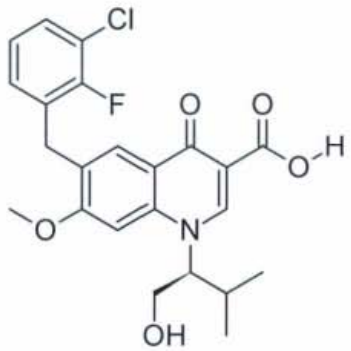

Figure 2-18: Strucure of Compound **GS-9137**.

The quinolone-based structure was also assumed to be the new pharmacophore for designing new generation HIV-1 IN inhibitors. The diketo acid moiety (γ-ketone, enolizable α-ketone, and carboxylic acid) was believed to be essential for the inhibitory activity of this series of integrase inhibitors [101] and the structures of diketotriazole [104] diketotetrazole [105] diketopyridine [106] and 7-oxo-8-hydroxy-(1,6)-

naphthyridine [107,108] were reported to be bioisosteres of the diketo acid pharmacophore. It was found that the carboxylic acid could be replaced not only with acidic bioisosteres, such as tetrazole and triazole groups, but also by a basic heterocycle bearing a lone pair donor atom, such as a pyridine ring. Also, The enolizable ketone at the α-position of diketo acids can be replaced with a phenolic hydroxyl group, indicating that the α-enol form of each diketo acid is its biologically active coplanar conformation. The 4-quinolone-3-glyoxylic acid **24** was treated as a new scaffold that maintained the coplanarity of diketo acid functional groups. Interestingly, the 4-quinolone-3-glyoxlic acid and also its precursor 4-quinolone-3-carboxylic acid **25** showed integrase inhibitory activity [101]. The 4-quinolone-3-carboxylic acid only had two functional groups, a *β*-ketone and a carboxylic acid, which were coplanar. This result showed that the coplanar monoketo acid motif in 4-quinolone-3-carboxylic acid could be an alternative to the diketo acid motif, and provided novel insight into the structural requirements and the binding mode of this type of inhibitor [108].

24

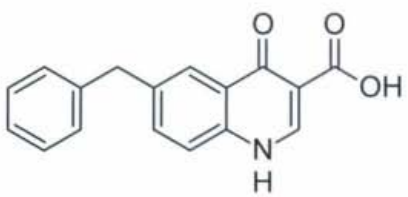

25

Figure 2-19: Structures of Compounds **24** and **25**.

The emergence of resistant mutants against available antiretroviral drugs brings out the need to develop new therapeutic targets. HIV integrase inhibitors open up a new way as a promising class of antiretroviral drugs. They act by inhibiting the action of the integrase, a viral enzyme that inserts the viral genome into the DNA of the host cell preventing formation of the provirus. The replicative life cycle of the HIV virus requires the integration of viral DNA into genomic DNA of the host cell, a process which is mediated by the viral protein integrase (IN). The development of inhibitors of IN activity constitutes a new challenge for the treatment of HIV-1 infection. Diketoacid functionality is critical for enzyme inhibition. Their derivatives as well constitute one of the most successful classes of IN inhibitors that exhibit potent strand transfer (ST) inhibition as well as good antiviral activity. Recently [109] a series of potential HIV integrase inhibitors derived from quinolone antibiotics was described. The structurally optimized and highly potent monoketo Compound **GS-9137** was identified as the most promising candidate, exhibiting potent inhibitory activity against integrase-catalyzed DNA strand transfer. **GS-9137** was shown to be well tolerated in healthy volunteers and HIV-infected patients. Moreover, monotherapy resulted in substantial antiviral activity in infected subjects. The agent is undergoing phase III clinical evaluation for the treatment of HIV-1 infection.

Another IN inhibitor [110] **GS-9160** has potent and selective antiviral activity in primary human T-lymphocytes producing an EC_{50} of ~2 nM with a selectivity index (CC_{50}/EC_{50}) of ~2000, but later on, **GS-9160** suffered from unfavorable pharmacokinetic properties.

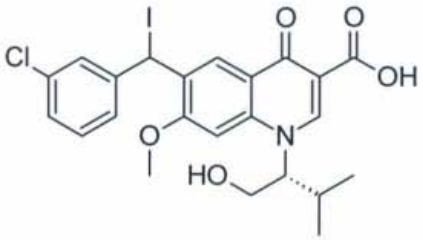

GS-9137

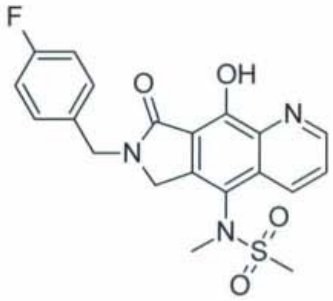

GS-9160

Figure 2-20: Structures of Compounds **GS-9137** and **GS-9160**.

Diketoacid compounds (DKA) constitute a promising class of HIV IN inhibitors with *in vivo* antiviral activity [111, 112]. Styrylquinolines (SQ) are another group that are also capable of IN inhibition [113,114]. Several compounds of both classes are under clinical trials, **S-1360** [115] or **L-870810** (DKA) [116], or earlier stages of drug development projects, **FZ-41**(SQ) [117]. Comparison of these two classes shows some similarities, but they also differ in their inhibitory activity. Compound **SQ1** which is synthesized in an attempt to mimic the DKA pharmacophore in the styrylquinoline series, showed inactive *in vitro* profile against IN [118]. On the other hand, this compound exhibited a significant antiviral activity in the *in vivo* experiment [118].

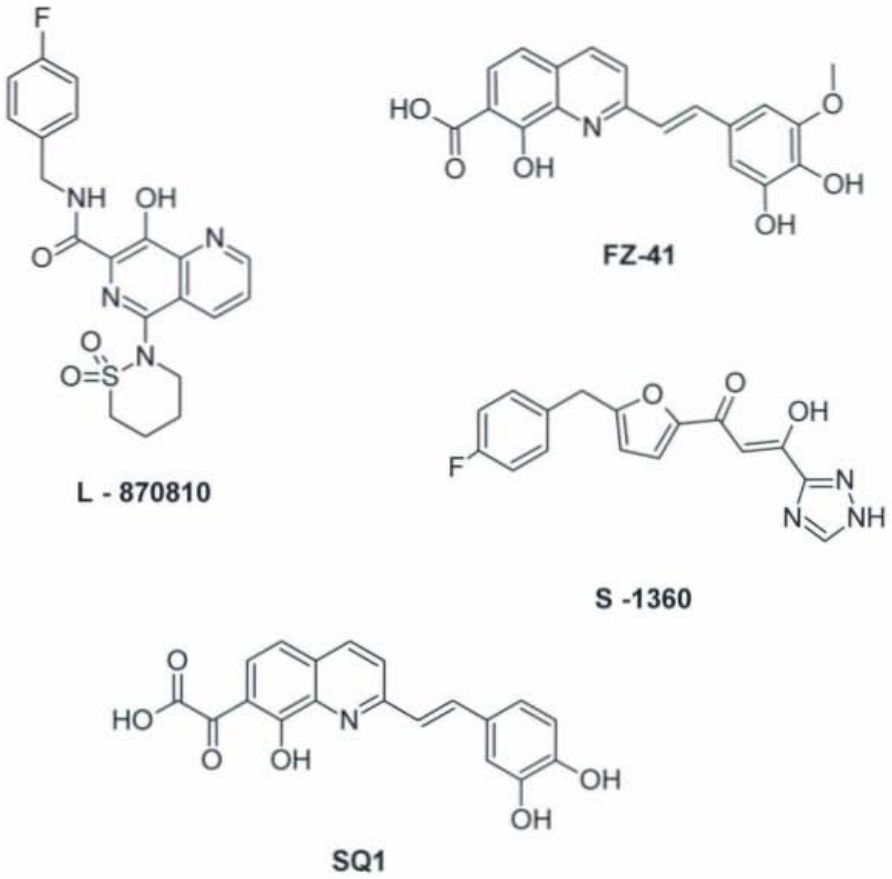

Figure 2-21: Structures of Compounds **L-870810**, **FZ-41**, **S-1360** and **SQ1**.

Moreover, Engels *et al.* [119], described the microwave-assisted synthesis of fluoroquinolonenucleosides **26, 27** and their evaluation as HIV-1 integrase inhibitors. These compounds were proved to be inactive against HIV-1 replication at subtoxic concentrations in the MT-4/MTT assay.

Accordingly, the activity of quinolones is likely due to sequestration of divalent metal ions within the IN active site in complex with viral DNA [121]. Although the crystallographic structure of IN in complex with viral DNA has not yet been resolved, it has been reported that Tn5 transposase (Tnp), which belongs to the superfamily of polynucleotidyl transferases as does IN, can be considered as an excellent surrogate model for studying the mechanism of action of ST inhibitors [121]. In this context, docking calculations on these derivatives together with **S-1360** were performed on the Tn5 Tnp-DNA complex by following the computational protocol described by Barreca *et al.* [121]. In its best docking pose (conformation with the highest fitness score and belonging to the most populated cluster), Elvitagravir presented the carboxylate group, hydrogen-bonded to H329, chelating the metal ion between E326 and D97 and the β-ketone oxygen together with the fluorine atom coordinating the other metal ion. It was found that the binding mode proposed for Elvitagravir was in accordance with its mutation profile as well as with the pharmacophoric model for quinolones recently reported [120].

2.8.2 Quinolones as anti-HCV (Hepatitis C virus) agents

Antiviral drugs can be classified into direct and indirect agents; the direct agents target the structural components or enzymes encoded by the virus while the indirect antiviral agents target the host cell components (immunomodulators etc.) [122]. Inhibitors of the NS3 protease, the NS5B polymerase, and the viral RNA are the most intensively explored antiviral agents. The actual treatment of HCV will be a combination of drugs of variable mechanisms in order to reduce the emergence of resistance [122].

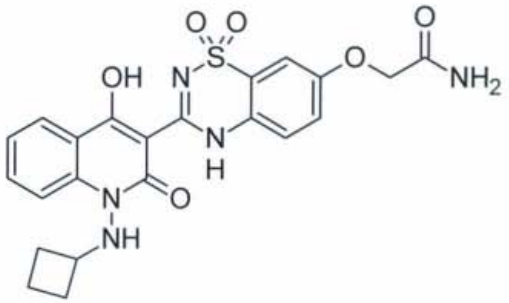

Figure 2-23: Structure of Compound **A-782759**.

A-782759, a 2-(1-aminoquinolone-3-yl) benzothiadiazine derivative, was identified as an inhibitor of HCV NS5B RdRp [128]. The combination therapy between Hepatitis C virus (HCV) polymerase **A-782759** with either Boehringer Ingelheim HCV NS3 protease inhibitor BILN-2061 or interferon (IFN) [129, 130] showed an interesting additive effect to synergistic relationships over a range of concentrations of two-drug combinations. Treatment of HCV replicon with **A-782759**, **IFN** or **BILN-2061** for about 16 days resulted in dramatic reductions in HCV RNA (5.1, 3.0 and 3.9 log RNA copies, respectively). Surprisingly, none of these compounds when tested alone showed any replicon RNA reduction. Results showed that a monotherapy with either drug alone possibly results in development of resistant mutants. However, a combination therapy lowers the likelihood of resistance development [131].

Antiviral quinolones are promising compounds in the search for new therapeutically effective agents. Diketo functionality seems to play an important role in targeting the viral enzymes.The information gained so far will be useful for future rational drug design aimed at developing new compounds with optimized antiviral activity.

2.9 Conclusion

The 4-quinolone scaffold exhibits many pharmacological profiles. Beside the antibacterial acivity there are antiischemic, anixolytic, antitumor and antiviral activities. In this review we have tried to highlight the most important pharmacological activities (antibacterial, antitumor and antiviral activities). SAR studies revealed that very fine changes in the main skeleton as well as changing the fused rings will effectively affect the pharmacophore pharmacological activity.

References

1. Letafat, B., Emami, S., Mohammadhosseini, N., Faramarzi, M. A., Samadi, N., Shafiee, A., & Foroumadi, A. (2007). Synthesis and antibacterial activity of new N-[2-(thiophen-3-yl)ethyl] piperazinyl quinolones. *Chem. Pharm. Bull.(Tokyo) , 55* (6), 894-8.
2. Srivastava, B. K., Solanki, M., Mishra, B., Soni, R., Jayadev, S., Valani, D., Jain, M., & Patel, P. R. (2007). Synthesis and antibacterial activity of 4,5,6,7-tetrahydro-thieno[3,2-c]pyridine quinolones. Bioorg. Med. Chem. Lett., 17 (7), 1924-9.
3. Wang, J. C. (1985). DNA topoisomerases. Annu. Rev. Biochem., 54 (1), 665-697.
4. Okumura, R., Hirata, T., Onodera, Y., Hoshino, K., Otani, T., & Yamamoto, T. (2008). Dual-targeting properties of the 3-aminopyrrolidyl quinolones, DC-159a and sitafloxacin, against DNA gyrase and topoisomerase IV: Contribution to reducing in vitro emergence of quinolone-resistant streptococcus pneumoniae. J. Antimicrob. Chemoth., 62 (1), 98-104.
5. O'Brien, R. J. (2003). Development of fluoroquinolones as first-line drugs for tuberculosis--at long last. Am. J. Resp. Crit. Care., 168 (11), 1266-8.
6. Janin, Y. L. (2007). Antituberculosis drugs: Ten years of research. Bioorg. Med. Chem., 15 (7), 2479-513.
7. Mdluli, K., & Ma, Z. (2007). Mycobacterium tuberculosis DNA gyrase as a target for drug discovery. Infect. Disord. Drug Targets, 7 (2), 159-68.
8. Gould, R. G., & Jacobs, W. A. (1939). J. Am. Chem. Soc., 61(10), 2890-2895.

9. Lappin, G. R. (1948). Cyclization of 2-aminopyridine derivatives. I. substituted ethyl 2-pyridylaminomethylenemalonates. J. Am. Chem. Soc., 70 (10), 3348-3350.
10. Grohe, K., & Heitzer, H. (1987). Cycloacylation of Enamines, I. – Synthesis of 4-Quinolone-3-carboxylic Acids. Liebigs Ann.Chem., 1987 (1), 29-37.
11. Cecchetti, V., Fravolini, A., Lorenzini, M. C., Tabarrini, O., Terni, P., & Xin, T. (1996). Studies on 6-aminoquinolones: Synthesis and antibacterial evaluation of 6-amino-8-methylquinolones. J. Med. Chem., 39 (2), 436-45.
12. Torii, S., Okumoto, H., & He Xu, L. (1990). A direct approach to 2-substituted 1,4-dihydro-4-oxo-quinoline-3-carboxylates by palladium-catalyzed carbonylative cyclization. Tetrahedron lett., 31(49) 7175-78.
13. Willmott, C., Critchlow, S., Eperon, I., & Maxwell, A. (1994). The complex of DNA gyrase and quinolone drugs with DNA forms a barrier to transcription by RNA polymerase. J. Mol. Biol., 242 (4), 351-363.
14. Gómez-Eichelmann, M. C., & Camacho-Carranza, R. (1995). DNA supercoiling and topoisomerases in escherichia coli . Rev. Latinoam. Microbiol., 37 (3), 291-304.
15. Zechiedrich, E. L., Khodursky, A. B., Bachellier, S., Schneider, R., Chen, D., Lilley, D. M., & Cozzarelli, N. R. (2000). Roles of topoisomerases in maintaining steady-state DNA supercoiling in escherichia coli. J. Biol. Chem., 275 (11), 8103-13
16. Couturier, M., Bahassi el-M., & Van Melderen L. (1998). Bacterial death by DNA gyrase poisoning. Trends Microbiol., 6 (7), 269-75.

17. Gore, J., Bryant, Z., Stone, M. D., Nöllmann, M., Cozzarelli, N. R., & Bustamante, C. (2006). Mechanochemical analysis of DNA gyrase using rotor bead tracking. Nature, 439 (7072), 100-4.

18. Gootz, T. D., & Brighty, K. E. (1998). In the Quinolones, (Ed. V. T. Andriole), Academic Press, San Diego, 29.

19. Morrison, A., & Cozzarelli, N. R. (1979). Site-specific cleavage of DNA by E. coli DNA gyrase. Cell, 17 (1), 175-84.

20. Llorente, B., Leclerc, F., & Cedergren, R. (1996). Using SAR and QSAR analysis to model the activity and structure of the quinolone-DNA complex. Bioorg. Med. Chem., 4, 61–71.

21. Domagala, J. M. (1994). Structure-activity and structure side-effect relationships for the quinolone antibacterials. J. Antimicrob. Chemother., 33, 685–706.

22. Tillotson, G. S. (1996). Quinolones: Structure-activity relationships and future predictions. J. Med. Microbiol.; 44, 320–4.

23. Yoshida, T., Yamamoto, Y., Orita, H., et al. (1996). Studies on quinolone antibacterials.IV. Structure-activity relationships of antibacterial activity and side effects for 5- or 8-substituted and 5,8-disubstituted-7(3- amino -1-pyrrolidinyl)-1-cyclopropyl-1,4-dihydro-4-oxoquinoline-3-carboxylic acids. Chem. Pharm. Bull. (Tokyo), 44, 1074–85.

24. Ledoussal, B., Almstead, J. K., & Flaim, C. P. (1999). Novel fluoroquinolone, structure activity, and design of new potent and safe agents. In: Program and abstracts of the 39th Interscience Conference on Antimicrobial Agents and

Chemotherapy (San Francisco). Washington, DC: American Society for Microbiology.

25. Ma, Z., Chu, D. T., Cooper, C. S., et al. (1999). Synthesis and antimicrobial activity of 4(H)-4-oxoquinolizine derivatives: consequences of structural modification at the C-8 position. J. Med. Chem., 42, 4202–13.
26. Wentzell, L., & Maxwell, A. (2000). The complex of DNA gyrase and quinolone drugs on DNA forms a barrier to the T7 DNA polymerase replication complex. J. Mol. Biol., 304 (5), 779-791.
27. Shea, M. E., & Hiasa, H. (2000). Distinct effects of the UvrD helicase on topoisomerase-quinolone-DNA ternary complexes. J. Biol. Chem., 275 (19), 14649-14658.
28. Yoshida, H., Bogaki, M., Nakamura, M., & Nakamura, S. (1990). Quinolone resistance-determining region in the DNA gyrase gyrA gene of Escherichia coli. Antimicrob. Agents Chemother., 34 (6), 1271-2.
29. Piddock, L. J. V. (1999). Mechanisms of fluoroquinolone resistance: An update 1994-1998. Drugs, 58 (Supplement 2), 11-18.
30. Heddle, J., Barnard, F., Wentzell, L., & Maxwell, A. (2000). The interaction of drugs with DNA gyrase: A model for the molecular basis of quinolone action. Nucleosides, Nucleotides Nucleic Acids, 19 (8), 1249-1264.
31. Palù, G., Valisena, S., Ciarrocchi, G., Gatto, B., & Palumbo, M. (1992). Quinolone binding to DNA is mediated by magnesium ions. Proc. Natl. Acad. Sci. U. S. A., 89 (20), 9671-9675.

32. Sissi, C., Perdonà, E., Domenici, E., Feriani, A., Howells, A., Maxwell, A., & Palumbo, M. (2001). Ciprofloxacin affects conformational equilibria of DNA gyrase A in the presence of magnesium ions. J. Mol. Biol., 311 (1), 195-203.

33. Shen, L. L., & Pernet, A. G. (1985). Mechanism of inhibition of DNA gyrase by analogues of nalidixic acid: The target of the drugs is DNA. Proc. Natl. Acad. Sci. USA, 82 (2), 307-311.

34. Critchlow, S. E., & Maxwell, A. (1996). DNA cleavage is not required for the binding of quinolone drugs to the DNA gyrase-DNA complex. Biochemistry, 35 (23), 7387-93.

35. Kampranis, S. C., & Maxwell, A. (1998). The DNA gyrase-quinolone complex. ATP hydrolysis and the mechanism of DNA cleavage. J. Biol. Chem., 273 (35), 22615-26.

36. Chen, G. L., Yang, L., Rowe, T. C., Halligan, B. D., Tewey, K. M., & Liu, L. F. (1984). Nonintercalative antitumor drugs interfere with the breakage-reunion reaction of mammalian DNA topoisomerase II. J. Biol. Chem., 259 (21), 13560-6.

37. Woese, C. R. (1987). Bacterial evolution. Microbiol. Rev., 51 (2), 221-71.

38. Forterre, P., Nadal, M., Elie, C., Mirambeau, G., Jaxel, C., & Duguet, M. Mechanisms of DNA synthesis and topoisomerisation in archaebacteria; reverse gyration in vitro and in vivo. System Appl. Microbiol., 1986, 7, 67.

39. Sioud, M. & Forterre, P. (1989). Ciprofloxacin and etoposide (VP16) produce a similar pattern of DNA cleavage in a plasmid of an archaebacterium. Biochemistry, 28 (9), 3638-41.

40. Ryckebusch, A., Garcin, D., Lansiaux, A., Goossens, J., Baldeyrou, B., Houssin, R., Bailly, C., & Hénichart, J. (2008). Synthesis, cytotoxicity, DNA interaction, and topoisomerase II inhibition properties of novel indeno[2,1-c]quinolin-7-one and indeno[1,2-c]isoquinolin-5,11-dione derivatives. J. Med. Chem., 51 (12), 3617-3629.

41. Ferlin, M. G., Chiarelotto, G., Gasparotto, V., Dalla Via, L., Pezzi, V., Barzon, L., Palù, G., & Castagliuolo, I. (2005). Synthesis and in vitro and in vivo antitumor activity of 2-phenylpyrroloquinolin-4-ones. J. Med. Chem., 48 (9), 3417-3427.

42. Gasparotto, V., Castagliuolo, I., Chiarelotto, G., Pezzi, V., Montanaro, D., Brun, P., Palù, G., Viola, G., & Ferlin, M. G. (2006). Synthesis and biological activity of 7-phenyl-6,9-dihydro-3H-pyrrolo[3,2-f]quinolin-9-ones: A new class of antimitotic agents devoid of aromatase activity. J. Med. Chem., 49 (6), 1910-1915.

43. Pommier, Y. (1993). DNA topoisomerase I and II in cancer chemotherapy: Update and perspectives. Cancer Chemother.Pharmacol., 32 (2), 103-108.

44. Bhargava, R., Lal, P., & Chen, B. (2005). HER-2/neu and topoisomerase IIa gene amplification and protein expression in invasive breast carcinomas: Chromogenic in situ hybridization and immunohistochemical analyses. Am. J. Clin. Pathol., 123 (6), 889-95.

45. Schmidt, F., Knobbe, C. B., Frank, B., Weller, M., & Wolburg, H. (2008). The topoisomerase II inhibitor, genistein, induces G2/M arrest and apoptosis in human malignant glioma cell lines. Oncol.Rep.,19 (4), 1061-1066.

46. Richter, S., Parolin, C., Palumbo, M., & Palu, G. (2004). Antiviral properties of quinolone-based drugs. Curr Drug Targets Infect. Disord., 4 (2), 111-116.

47. Lock, R. B., & Ross, W. E. (1987). DNA topoisomerases in cancer therapy. Anti-Cancer Drug Design, 2 (2), 151-64.

48. Schneider, E., Hsiang, Y. H., & Liu, L. F. (1990). DNA topoisomerases as anticancer drug targets. Advances in Pharmacology (San Diego, Calif.), 21, 149-83.

49. Zwelling, L. A. (1989). Topoisomerase II as a target of antileukemia drugs: A review of controversial areas. Hematologic Pathology, 3 (3), 101-12.

50. Kreuzer, K. N., & Cozzarelli, N. R. (1979). Escherichia coli mutants thermosensitive for deoxyribonucleic acid gyrase subunit A: Effects on deoxyribonucleic acid replication, transcription, and bacteriophage growth. J. Bacteriol., 140 (2), 424-35.

51. Osheroff, N., Zechiedrich, E. L., & Gale, K. C. (1991). Catalytic function of DNA topoisomerase II. BioEssays : News and Reviews in Molecular, Cellular and Developmental Biology, 13 (6), 269-73.

52. Drlica, K., & Franco, R. J. (1988). Inhibitors of DNA topoisomerases. Biochemistry, 27 (7), 2253-9.

53. Hooper, D. C., & Wolfson, J. S. (1991). Fluoroquinolone antimicrobial agents. N. Engl. J. Med., 324 (6), 384-94.

54. Yamashita, Y., Ashizawa, T., Morimoto, M., et al. (1992). Antitumor quinolones with mammalian topoisomerase II mediated DNA cleavage activity. Cancer Res., 52 (10), 2818-2822.

55. Hussy, P., Maass, G., Tummler, B., Grosse, F., & Schomburg, U. (1986). Effect of 4-quinolones and novobiocin on calf thymus DNA polymerase alpha primase complex,

topoisomerases I and II, and growth of mammalian lymphoblasts. Antimicrob. Agents Chemother., 29 (6), 1073-1078.

56. Dobson, R. A., O'Connor, J. R., Poulin, S. A., Kundsin, R. B., Smith, T. F., & Came, P. E. (1980). In vitro antimicrobial activity of rosoxacin against Neisseria gonorrhoeae, Chlamydia trachomatis, and Ureaplasma urealyticum. Antimicrob Agents Chemother., 18 (5): 738–740.
57. Carabateas, P.M.; Brundage, R.P.; Gellote, M.D.; Lorenz, R.R.; Opalka, C.J.; Thielking, W.H., Williams, G.L.; & Lesher, G.Y. (1984). 1-ethyl-1,4-dihydro-4-oxo-7-(pyridinyl)-3-quinoline carboxylic acids. II. Synthesis. J. Heterocycl. Chem., 21, 1857-1863.
58. Wentland, M. P., Lesher, G. Y., Reuman, M., Gruett, M. D., Singh, B., Aldous, S. C., et al. (1993). Mammalian topoisomerase II inhibitory activity of 1-cyclopropyl-6,8-difluoro-1,4-dihydro-7-(2,6-dimethyl-4-pyridinyl)-4-oxo-3-quinolinecarb oxylic acid and related derivatives. J. Med. Chem., 36 (19), 2801-9.
59. Eissenstat, M. A., Kuo, G., Weaver, J. D., & Wentland, M. P. (1995). 3-benzyl-quinolones: Novel, potent inhibitors of mammalian topoisomerase II. Bioorg. Med. Chem. Lett., 5 (9), 1021.
60. Kohlbrenner, W. E., Wideburg, N., Weigl, D., Saldivar, A., & Chu, D. T. (1992). Induction of calf thymus topoisomerase II-mediated DNA breakage by the antibacterial isothiazoloquinolones A-65281 and A-65282. Antimicrob. Agents Chemother., 36 (1), 81-6.

61. DoganKoruznjak, J., Slade, N., Zamola, B., Pavelić, K., & Karminski-Zamola, G. (2002). Synthesis, photochemical synthesis and antitumor evaluation of novel derivatives of thieno[3',2':4,5]thieno[2,3-c]quinolones. Chem. Pharm. Bull. (Tokyo), 50 (5), 656-60.

62. Robinson, M. J., Martin, B. A., & Gootz, T. D. (1991). Effects of quinolone derivatives on eukaryotic topoisomerase II. A novel mechanism for enhancement of enzyme-mediated DNA cleavage. J. Biol. Chem., 266, 14585-92.

63. Robinson, M. J., Martin, B. A., Gootz, T. D., McGuirk, P. R., & Osheroff, N. (1992). Effects of novel fluoroquinolones on the catalytic activities of eukaryotic topoisomerase II: Influence of the C-8 fluorine group. Antimicrob. Agents Chemother., 36 (4), 751-6.

64. Elsea, S. H., McGuirk, P. R., Gootz, T. D., Moynihan, M., & Osheroff, N. (1993). Drug features that contribute to the activity of quinolones against mammalian topoisomerase II and cultured cells: Correlation between enhancement of enzyme-mediated DNA cleavage in vitro and cytotoxic potential. Ibid., 37 (10), 2179-86.

65. Alovero, F. L., Pan, X. S., Morris, J. E., Manzo, R. H., & Fisher, L. M. (2000). Engineering the specificity of antibacterial fluoroquinolones: Benzenesulfonamide modifications at C-7 of ciprofloxacin change its primary target in Streptococcus pneumoniae from topoisomerase IV to gyrase. Ibid., 44 (2), 320-5.

66. Gootz, T. D., McGuirk, P. R., Moynihan, M. S., & Haskell, S. L. (1994). Placement of alkyl substituents on the C-7 piperazine ring of fluoroquinolones: Dramatic

differential effects on mammalian topoisomerase II and DNA gyrase. Ibid., 38 (1), 130.

67. Suto, M. J., Domagala, J. M., Roland, G. E., Mailloux, G. B., & Cohen, M. A. (1992). Fluoroquinolones: Relationships between structural variations, mammalian cell cytotoxicity, and antimicrobial activity. J. Med. Chem., 35 (25), 4745-50.
68. Barrett, J. F., Gootz, T. D., McGuirk, P. R., Farrell, C. A., & Sokolowski, S. A. (1989). Use of in vitro topoisomerase II assays for studying quinolone antibacterial agents. Antimicrob. Agents Chemother., 33 (10), 1697-703.
69. Advani, R. H., Hurwitz, H. I., Gordon, M. S., Ebbinghaus, S. W., Mendelson, D. S., Wakelee, H. A., et al. (2010). Voreloxin, a first-in-class anticancer quinolone derivative, in Relapsed/Refractory solid tumors: A report on two dosing schedules. Clin. Canc. Res., 16 (7), 2167-2175.
70. Hosomi, J.; Asahina, Y.; & Suzue, S. (1989). PCT Int. Appl. WO 89 12055. Preparation of thiazoloquinolonecarboxylic acid derivatives and their pharmaceutical compositions as antitumor agents (Chem.. Abstr. 1990, 113, 6328m).
71. Sissi, C., & Palumbo, M. (2003). The quinolone family: From antibacterial to anticancer agents. Curr. Med. Chem.:Anti-Cancer Agents. 3 (6), 439-50.
72. Amoozgar, Z., & Daneshtalab, M. (2007). Regioselective N1-alkylation of 4-quinoline- 3-carboxylic acid esters using modified mitsnobu reaction. 21st International Congress for Heterocyclic Chemistry (ICHC-21) Sydney, Australia, abstract # TP-21.

73. Ahmed, A., & Daneshtalab, M. (2012). Polycyclic quinolones (Part 1)-Thieno [2,3-b] benzo [h] quinoline derivatives: design, synthesis, preliminary in vitro and in silico studies. Heterocycl., 85 (1), DOI: 10.3987/COM-11-12374 (In Press.)

74. Bromberg, J., & Darnell, J. E. (2000). The role of STATs in transcriptional control and their impact on cellular function. Oncogene, 19, 2468-2473.

75. Levy, D. E., & Darnell, J. E. (2002). STATs: transcriptional control and biological impact. Nat. Rev. Mol. Cell Biol., 3, 651-662.

76. Klampfer, L. (2006). Signal transducers and activators of transcription (STATs): novel targets of chemopreventive and chemotherapeutic drugs. Curr. Cancer Drug Targets, 6, 107-121.

77. Darnell, J. E. (2005). Validating STAT3 in cancer therapy. Nat. Med., 11, 595-596.

78. Jing, N., & Tweardy, D. J. (2005). Targeting STAT3 in cancer therapy. Anti-Cancer Drugs, 16, 601-607.

79. Xu, J., Cole, D. C., Chang, C. P. B., Ayyad, R., Asselin, M., Hao, W., Gibbons, J., Jelinsky, S. A., Saraf, K. A., & Park, K. (2008). Inhibition of the signal transducer and activator of transcription-3 (STAT3) signalling pathway by 4-oxo-1-phenyl-1,4-dihydro quinoline-3-carboxylic acid esters J. Med. Chem., 51, 4115-4121.

80. Golub, A. G., Yakovenko, O. Y., Bdzhola, V. G., Sapelkin, V. M., Zien, P., & Yarmoluk, S. M. (2006). Evaluation of 3-carboxy-4(1H)- quinolones as inhibitors of human protein kinase CK2. J. Med.Chem., 49 (22), 6443-6450.

81. Palù, G., Valisena, S., Ciarrocchi, G., Gatto, B., & Palumbo, M. (1992). Quinolone binding to DNA is mediated by magnesium ions. Proc. Natl. Acad. Sci. U. S. A., 89 (20), 9671-9675.

82. Shen, L. L., & Pernet, A. G. (1985). Mechanism of inhibition of DNA gyrase by analogues of nalidixic acid: The target of the drugs is DNA. Proc. Natl. Acad. Sci. U. S. A., 82 (2), 307-311.

83. Shen, L. L., Kohlbrenner, W. E., Weigl, D., & Baranowski, J. (1989). Mechanism of quinolone inhibition of DNA gyrase appearance of unique norfloxacin binding sites in enzyme-DNA complexes. J. Biol. Chem., 264 (5), 2973-8.

84. Shen, L. L., Baranowski, J., & Pernet, A. G. (1989). Mechanism of inhibition of DNA gyrase by quinolone antibacterials: Specificity and cooperativity of drug binding to DNA. Biochemistry, 28 (9), 3879-85.

85. Shen, L. L., Mitscher, L. A., Sharma, P. N., O'Donnell, T. J., Chu, D. W., Cooper, C. S., et al. (1989). Mechanism of inhibition of DNA gyrase by quinolone antibacterials: A cooperative drug--DNA binding model. Biochemistry, 28 (9), 3886-94.

86. Palumbo, M., Gatto, B., Zagotto, G., & Palù, G. (1993). On the mechanism of action of quinolone drugs. Trends Microbiol., 1 (6), 232-5.

87. Kimura, T., and Katsube, T. (1993). Aminoquinoline derivatives as anti-HIV agents. European patent 572259.

88. Bender, W.; Roeben, W.; Paesens, A., & Bartel, S. (1996). WO9602540, Preparation of piperazinoquinolonecarboxylates as antiviral agents. Ger. Offen. DE 4425647 A1 19960125.

89. Bender, W.; Roeben W.; Paesens, A., & Bartel, S. (1996). WO9602532, Preparation of 7-piperazinyl-1,4-dihydro-4-oxo-1-[4-(1H-1,2,4-triazol-1-yl-methyl)phenyl] quinoline-3-carboxylic acids as virucides. Ger. Offen. DE 4425660 A1 19960125.

90. Nozaki-Renard, J., Iino, T., Sato, Y., Marumoto, Y., Ohta, G., & Furusawa, M. (1990). Fluoroquinolones protect the human lymphocyte CEM cell line from HIV-1-mediated cytotoxicity. Cell Structure and Function, 15 (5), 295-9.

91. Nozaki-Renard, J., Iino, T., Sato, Y., Marumoto, Y., Ohta, G., & Furusawa, M. (1990). A fluoroquinolone (DR-3355) protects human lymphocyte cell lines from HIV-1-induced cytotoxicity. AIDS (London, England), 4 (12), 1283-6.

92. Baba, M., Okamoto, M., Makino, M., Kimura, Y., Ikeuchi, T., Sakaguchi, T., et al. (1997). Potent and selective inhibition of human immunodeficiency virus type 1 transcription by piperazinyloxoquinoline derivatives. Antimicrob. Agents Chemother., 41 (6), 1250-5.

93. Daelemans, D., Vandamme, A. M., & De Clercq, E. (1999). Human immunodeficiency virus gene regulation as a target for antiviral chemotherapy. Antiviral Chem. Chemother., 10 (1), 1-14.

94. Parolin, C., Gatto, B., Del Vecchio, C., Pecere, T., Tramontano, E., Cecchetti, V., et al. (2003). New anti-human immunodeficiency virus type 1 6-aminoquinolones: Mechanism of action. Antimicrob. Agents Chemother., 47 (3), 889-96.

95. Tabarrini, O., Stevens, M., Cecchetti, V., Sabatini, S., Dell'Uomo, M., Manfroni, G., et al. (2004). Structure modifications of 6-aminoquinolones with potent anti-HIV activity. J. Med. Chem., 47 (22), 5567-78.

96. Tabarrini, O., Massari, S., Daelemans, D., Stevens, M., Manfroni, G., Sabatini, S., et al. (2008). Structure−Activity relationship study on anti-HIV 6-desfluoroquinolones. J. Med. Chem., 51 (17), 5454-5458.

97. Stevens, M., Pollicita, M., Pannecouque, C., Verbeken, E., Tabarrini, O., Cecchetti, V., et al. (2007). Novel in vivo model for the study of human immunodeficiency virus type 1 transcription inhibitors: Evaluation of new 6-desfluoroquinolone derivatives. Antimicrob. Agents Chemother., 51(4), 1407-13.

98. Pommier, Y., Johnson, A., & Marchand, C. (2005). Integrase inhibitors to treat HIV/AIDS. Nat. Rev. Drug Discovery, 4 (3), 236-248.

99. Boros, E. E., Johns, B. A., Garvey, E. P., Koble, C. S., & Miller, W. H. (2006). Synthesis and HIV-integrase strand transfer inhibition activity of 7-hydroxy[1,3]thiazolo[5,4-b]pyridin-5(4H)-ones. Bioorg. Med. Chem. Lett., 16 (21), 5668-72.

100. Cecchetti, V., Parolin, C., Moro, S., Pecere, T., Filipponi, E., Calistri, A., et al. (2000). 6-aminoquinolones as new potential anti-HIV agents. J. Med. Chem., 43 (20), 3799-802.

101. Sato, M., Motomura, T., Aramaki, H., Matsuda, T., Yamashita, M., Ito, Y., et al. (2006). Novel HIV-1 integrase inhibitors derived from quinolone antibiotics. J. Med. Chem., 49 (5), 1506-8.

102. Dayam, R., Sanchez, T., & Neamati, N. (2005). Diketo acid pharmacophore. 2. discovery of structurally diverse inhibitors of HIV-1 integrase. Ibid., 48 (25), 8009-15.

103. Dayam, R., Al-Mawsawi, L. Q., Zawahir, Z., Witvrouw, M., Debyser, Z., & Neamati, N. (2008). Quinolone 3-carboxylic acid pharmacophore: Design of second generation HIV-1 integrase inhibitors. ibid., 51 (5), 1136-1144.

104. Machouf, N., Thomas, R., Nguyen, V. K., Trottier, B., Boulassel, M. R., Wainberg, M. A., et al. (2006). Effects of drug resistance on viral load in patients failing antiretroviral therapy. J. Med. Virol., 78 (5), 608-13.

105. Cozzi-Lepri, A., Phillips, A. N., Ruiz, L., Clotet, B., Loveday, C., Kjaer, J., et al. (2007). Evolution of drug resistance in HIV-infected patients remaining on a virologically failing combination antiretroviral therapy regimen. AIDS (London, England), 21 (6), 721-32.

106. Friis-Møller, N., Reiss, P., Sabin, C. A., Weber, R., Monforte, A., El-Sadr, W., et al. (2007). Class of antiretroviral drugs and the risk of myocardial infarction. N. Engl. J. Med., 356 (17), 1723-35.

107. Potter, S. J., Lemey, P., Dyer, W. B., Sullivan, J. S., Chew, C. B., Vandamme, A. M., et al. (2006). Genetic analyses reveal structured HIV-1 populations in serially sampled T lymphocytes of patients receiving HAART. Virology, 348 (1), 35-46.

108. Fätkenheuer, G., Pozniak, A. L., Johnson, M. A., Plettenberg, A., Staszewski, S., Hoepelman, A. I., et al. (2005). Efficacy of short-term monotherapy with

maraviroc, a new CCR5 antagonist, in patients infected with HIV-1. Nat. Med., 11 (11), 1170-2.

109. Sorbera, L. A., & Serradell, N. (2006). Monographs - GS-9137 - anti-HIV agent, HIV integrase inhibitor. Drugs of the Future, 31 (4), 310.

110. Jones, G. S., Yu, F., Zeynalzadegan, A., Hesselgesser, J., Chen, X., Chen, J., et al. (2009). Preclinical evaluation of GS-9160, a novel inhibitor of human immunodeficiency virus type 1 integrase. Antimicrob. Agents Chemother., 53 (3), 1194-1203.

111. Hazuda, D. J., Felock, P., Witmer, M., Wolfe, A., Stillmock, K., Grobler, J. A., et al. (2000). Inhibitors of strand transfer that prevent integration and inhibit HIV-1 replication in cells. Science (New York, N.Y.), 287 (5453), 646-50.

112. Long, Y. Q., Jiang, X. H., Dayam, R., Sanchez, T., Shoemaker, R., Sei, S., et al. (2004). Rational design and synthesis of novel dimeric diketoacid-containing inhibitors of HIV-1 integrase: Implication for binding to two metal ions on the active site of integrase. J. Med. Chem., 47 (10), 2561-73.

113. Mekouar, K., Mouscadet, J. F., Desmaële, D., Subra, F., Leh, H., Savouré, D., et al. (1998). Styrylquinoline derivatives: A new class of potent HIV-1 integrase inhibitors that block HIV-1 replication in CEM cells. Ibid., 41 (15), 2846-57.

114. Polanski, J., Zouhiri, F., Jeanson, L., Desmaële, D., d'Angelo, J., Mouscadet, J. F., et al. (2002). Use of the kohonen neural network for rapid screening of ex vivo anti-HIV activity of styrylquinolines. Ibid., 45 (21), 4647-54.

115. Fujishita, T., Yoshinaga, T., & Sato, A. (2000). PCT Int. Appl. WO 2000039086A, Preparation of aromatic heterocycle compounds having HIV integrase inhibiting activities.

116. Hazuda, D. J., Anthony, N. J., Gomez, R. P., Jolly, S. M., Wai, J. S., Zhuang, L., et al. (2004). A naphthyridine carboxamide provides evidence for discordant resistance between mechanistically identical inhibitors of HIV-1 integrase. Proc. Natl. Acad. Sci. USA, 101 (31), 11233-8.

117. Mousnier, A., Leh, H., Mouscadet, J. F., & Dargemont, C. (2004). Nuclear import of HIV-1 integrase is inhibited in vitro by styrylquinoline derivatives. Mol. Pharmacol., 66 (4), 783-8.

118. a) Zouhiri, F., Desmaele, D., d'Angelo, J., Ourevitch, M., Mouscadet, J. F., Leh, H., et al. (2001). HIV-1 replication inhibitors of the styrylquinoline class: Incorporation of a masked diketo acid pharmacophore. Tetrahedron Lett., 42 (46), 8189-8192; b) Majerz-Maniecka K, Musiol R, Nitek W, et al. (2006). Intermolecular interactions in the crystal structures of potential HIV-1integrase inhibitors. Bioorg Med Chem Lett., 16, 1005-1009.

119. Adams, M. M., Bats, J. W., Nikolaus, N. V., Witvrouw, M., Debyser, Z., & Engels, J. W. (2006). Microwave-assisted synthesis of fluoroquinolones and their nucleosides as inhibitors of HIV integrase. Collect. Czech. Chem. Commun., 71 (7), 978-990.

120. Pasquini, S., Mugnaini, C., Tintori, C., Botta, M., Corelli, F., Trejos, A., et al. (2008). Investigations on the 4-quinolone-3-carboxylic acid motif. 1. synthesis and

structure-activity relationship of a class of human immunodeficiency virus type 1 integrase inhibitors. J. Med. Chem., 51 (16), 5125-5129.

121. Barreca, M. L., De Luca, L., Iraci, N., & Chimirri, A. (2006). Binding mode prediction of strand transfer HIV-1 integrase inhibitors using Tn5 transposase as a plausible surrogate model for HIV-1 integrase. Ibid.,49 (13), 3994-7.
122. RÖnn, R., & SandstrÖm, A. (2008). New developments in the discovery of agents to treat Hepatitis C. Curr.Top.Med.Chem., 8, 633-562.
123. Reed, K. E., & Rice, C. M. (1999). Expression and characterization of the HCV NS2 protease. Methods in Molecular Medicine, 19, 331-42.
124. Pallaoro, M., Lahm, A., Biasiol, G., Brunetti, M., Nardella, C., Orsatti, L., et al. (2001). Characterization of the hepatitis C virus NS2/3 processing reaction by using a purified precursor protein. J. Virol., 75 (20), 9939-46.
125. Kumar, D.V., Rai, R., Brameld, K. A., Somoza, J. R., Rajagopalan, R., Janc, J.W., et al. (2011). Quinolones as HCV NS5B polymerase inhibitors. Bioorg. Med. Chem. Lett., 21 (1), 82-87.
126. Kolykhalov, A. A., Mihalik, K., Feinstone, S. M., & Rice, C. M. (2000). Hepatitis C virus-encoded enzymatic activities and conserved RNA elements in the 3' nontranslated region are essential for virus replication in vivo. J. Virol., 74 (4), 2046-51.
127. Kneteman, N. M., Howe, A. Y. M., Gao, T., Lewis, J., Pevear, D., Lund, G., et al. (2009). HCV796: A selective nonstructural protein 5B polymerase inhibitor with

potent anti-hepatitis C virus activity in vitro, in mice with chimeric human livers, and in humans infected with hepatitis C virus. Hepatology, 49 (3), 745-752.

128. Pratt, J.K., Beno, D., Donner, P., Jiang,W., Kati,W., Kempf, D.J., Koev, G., Liu,D. , Liu, Y., Maring, C., Masse, S., Middleton, T., Mo, H., Molla, A., Montgomery, D., & Xie, Q., (2004). N-1-aza-4-hydroxyquinolone benzothiadiazines: inhibitors of HCV genotype 1 NS5B RNA-dependent RNA polymerase exhibiting replication potency and favorable rat pharmacokinetics. 55th Annual Meeting of AASLD. Hepatology 40 (S4), 697A (Abstract 1224a).
129. Lu, L., Pilot-Matias, T.J., et al., (2004). Mutations conferring resistance to a potent hepatitis C virus serine protease inhibitor in vitro. Antimicrob. Agents Chemother., 48 (6), 2260–2266.
130. Mo, H., Lu, L., et al., (2005). Mutations conferring resistance to a hepatitis C virus (HCV) RNA-dependent RNA polymerase inhibitor alone or in combination with an HCV serine protease inhibitor in vitro. Ibid., 49 (10), 4305–4314.
131. Koev, G., Dekhtyar, T., Han, L., Yan, P., Ng, T. I., Lin, C. T., et al. (2007). Antiviral interactions of an HCV polymerase inhibitor with an HCV protease inhibitor or interferon in vitro. Antiviral Res., 73 (1), 78-83.

CHAPTER 3

Thieno [2,3-*b*]Benzo[*h*]quinoline Derivatives: Design, Synthesis, Preliminary *In Vitro* and *In Silico* Study

Abeer Ahmed[a] and Mohsen Daneshtalab[a]*

Heterocycles, 85, 2012, DOI: 10.3987/COM-11-12374 (*in press, available on-line*)

[a]School of Pharmacy, Memorial University of Newfoundland, St. John's, Newfoundland and Labrador, Canada A1B 3V6. Fax: +1(709)-777-7044; E-mail: mohsen@mun.ca

Preface

The manuscript developed for this chapter provides a description of an extensive synthesis of a new series of ring fused angular quinoline derivatives based on a structure-based design approach. The chemistry, *in vitro* testing, docking experiments and also, structure elucidation using different instrumental analyses are described. A version of this manuscript has been published in *Heterocycles*.

Abstract

Heterocyclic systems with a quinoline nucleus represent the most spectacular example of privileged molecules in medicinal chemistry, as their biological activities are modulated by minor changes in structural features. Quinoline derivatives have been shown to display a wide spectrum of biological activities such as antibacterial, antifungal, antiparasitic, antiviral, cytotoxic and anti-inflammatory activities. In this study, several 7-hydroxy-8-oxo-8,9-dihydrobenzo[h]thieno[2,3-b]quinoline-9-carboxylic acids were designed, synthesized, and were further subjected to chemical reactions such as alkylation and annelation. The synthesized compounds were also subjected to docking studies and biological evaluation. This work was mainly designed to shed light on the requirements needed for the quinoline nucleus to act as an anticancer agent. Unexpectedly, the synthesized derivatives showed weak or no cytotoxicity against cancer cell lines and the increase in the extent of aromatic/condensed rings did not increase the affinity toward the double-stranded DNA. Our virtual screening demonstrated that the chelation with Mg^{2+} is a determining factor in the expected interaction with

Topoisomerases. Key synthetic issues, and crystallographic and docking studies are also encountered in this chapter.

Keywords: Thienoquinolines, thiazoloquinolines, Topoisomerase II, docking study, angular quinoline.

3.1 Introduction

Quinoline derivatives represent a major class of heterocycles. The quinoline ring system occurs in various natural products, especially in alkaloids. Its skeleton is often used for the design of many synthetic compounds with diverse pharmacological properties [1]. The 4(1*H*)-quinolone-3-carboxylic acid is one of the most studied quinoline-originated multivalent scaffolds that has been used in constructing a diverse series of biologically-active compounds such as antibacterial, anticancer and antiviral agents [2,3].

The benzo(*h*)quinolines can be seen as being a structural analogue to the antitumor benzo(*c*)phenanthridines, or, as heterocyclic isomers of acridines and phenanthridine-based antitumor agents [4].

In a search for novel small molecule heterocycles with potential antineoplastic activity, a joint patent by the Japanese pharmaceutical companies Kyorin/Kyowa-Hakko, describing thiazoloquinolone carboxylic acids with an impressive anticancer profile (Compound **A**, **Figure 3-1**) was of interest [5]. The clinical candidate compound had exhibited favourable drug-like properties in different animal models in preclinical studies.

Compound **A**, like other quinolone carboxylic acid derivatives, was presumed to interact with topoisomerase II via its β-keto acid functional group and chelation with the Mg^{2+} ion to inhibit the enzyme. Considering this mode of action [6], it was hypothesized that a quinolone with a β-diketo functionality may be able to mimic the action of the β-keto acid functionality in Compound **A**, thus potentially providing the same level of complexity as the Mg^{2+} ion at the active site of the topoisomerase II. Also, due to the absence of a free carboxylic acid, the target quinolone may cause less gastric damage when used via oral administration.

The target compounds were designed using the Hyperchem-3^{TM} molecular modeling program. By applying Molecular Mechanics Optimization (MMO) and Molecular Dynamic Option methods, we were able to identify linear tricyclic quinolones with β-diketo components that matched the angular feature of Compound **A**. In this respect, "Compound **B**", (9-benzyl-7-fluoro-3-hydroxythieno [4,5-*b*]quinoline-4(9*H*)-one), at its optimized steric/energetic configuration, was found to have the best match, with a perfect 3-point overlay with Compound **A**.

Compound **B** and its derivatives were synthesized in the Daneshtalab group using the Gould-Jacob method. This series of compounds displayed promising cytotoxic activity against several cancer cell lines [7a,b].

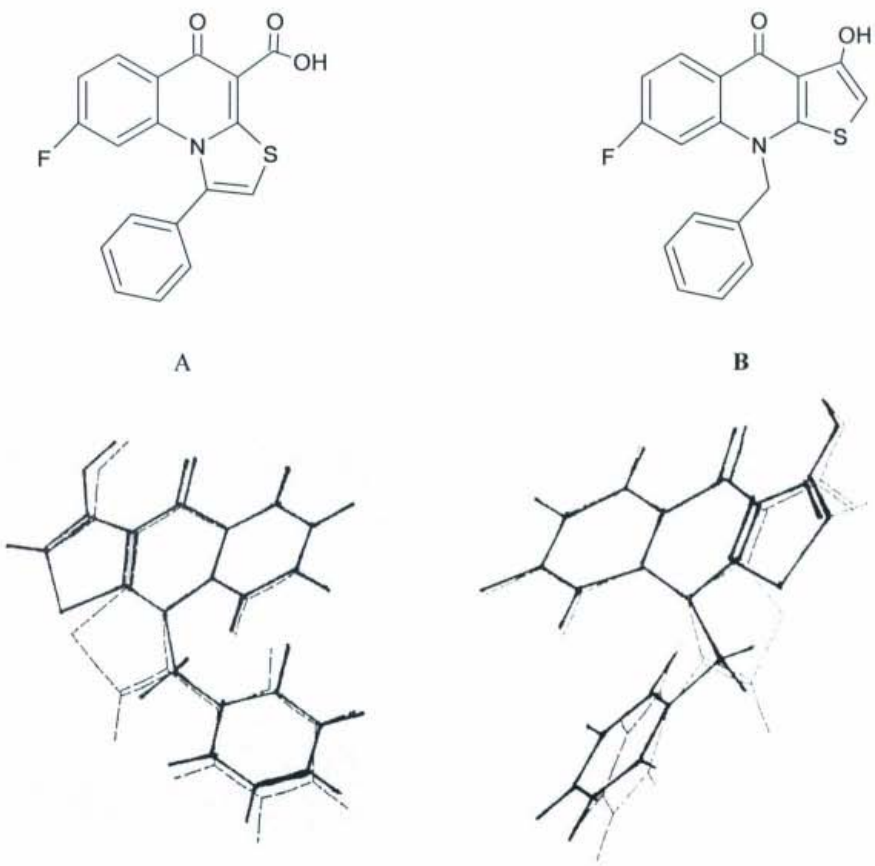

Figure 3-1: Different overlays of the structure of Compound **A** (dotted lines) and Compound **B** (solid lines).

During initial studies, we found out that the thiazoloquinolonecarboxylic acid derivatives demonstrated anti-neoplastic activity even without the presence of the required substituent at position 7 (aromatic & aliphatic amine substituents for compounds targeting euokaryotic topoisomerase II) [8-12], and also with the absence of mandatory fluorine atoms at C-6 and C-8 positions [10,12,13].

Antitumor cytotoxic agents possessing DNA-intercalative properties are characterized by the presence of a planar pharmacophore, generally a tri- or tetracyclic ring system and one or two flexible substituent groups [14].

Compounds possessing a large coplanar aromatic chromophore are likely to intercalate reversibly to the double-helical DNA. Most derivatives are not obviously related in any way except in sharing the exhibition of coplanar chromophores that favour the intercalation; for this reason they are designated as DNA intercalators. Moreover, most cytotoxic DNA-intercalating agents involve the inhibition of the enzyme DNA-topoisomerase I or II [15].

Considering the above discussion, our first target was the annelation of a thieno ring to the benzo[*h*]quinoline nucleus in an angular pattern. In this context, we attempted the syntheses of benzo[*h*]thieno[2,3-*b*]quinoline derivatives.

As a starting point, the synthesis of ethyl-7-hydroxy-8-oxo-8,9-dihydrobenzo[*h*]thieno [2,3-*b*]quinoline-9-carboxylate (**6a**) was attempted, as illustrated in **Scheme 3-1**.

1-Naphthylisothiocyanate was used as a main starting material which, by reacting with diethylmalonate and sodium hydride in acetonitrile, afforded the salt **1a**. This intermediate was allowed to react with different reagents to give rise to intermediates **2**. Thermal cyclization under vacuum enabled us to cyclize Compounds **2** in very good yields (up to 80%). Dieckman cyclization on Compound **3a** afforded Compound **6a,** saponification of which, yielded the carboxylic acid derivative **6b** as depicted in **Scheme 3-1**.

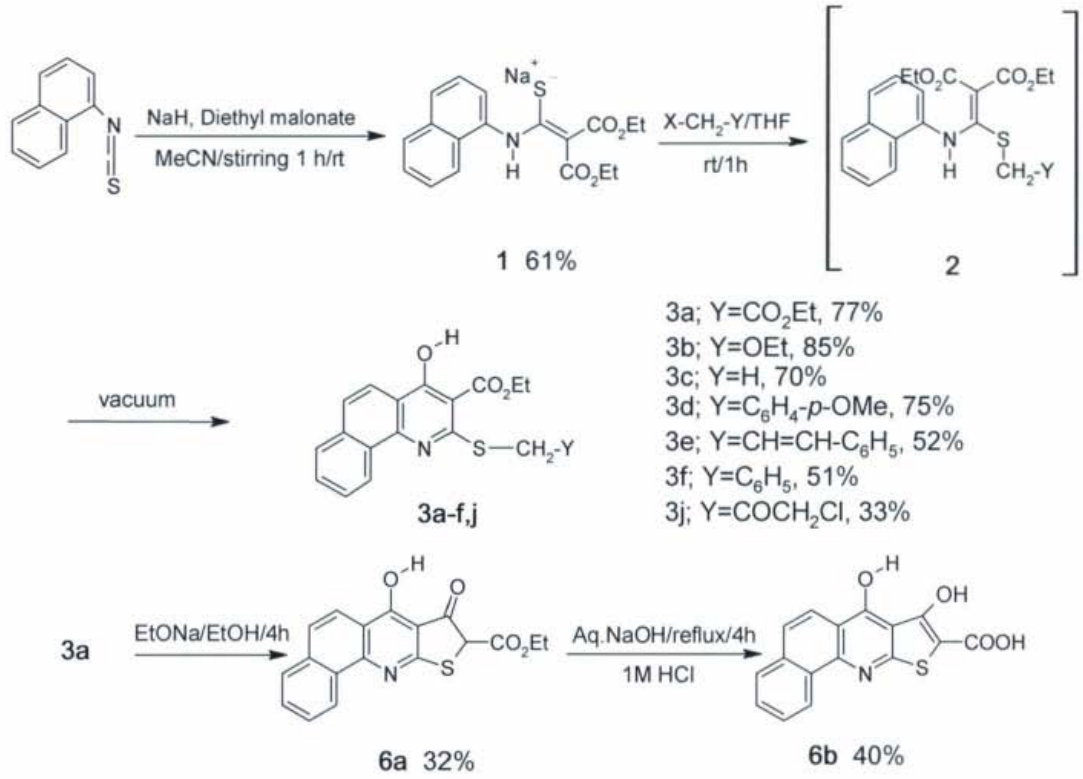

Scheme 3-1: General synthesis scheme for Compound **6a**.

3.2 *O*-Alkylated products

Alkylation reactions were attempted on derivatives **3a** using either 1,3-dibromopropane or Mitsonobu reaction conditions to obtain products **3g** and **3i**. Reaction of Compound **3b** with Diethylsulfate gave rise to the *O*-alkylated derivative **3h** as shown in **Scheme 3-2**.

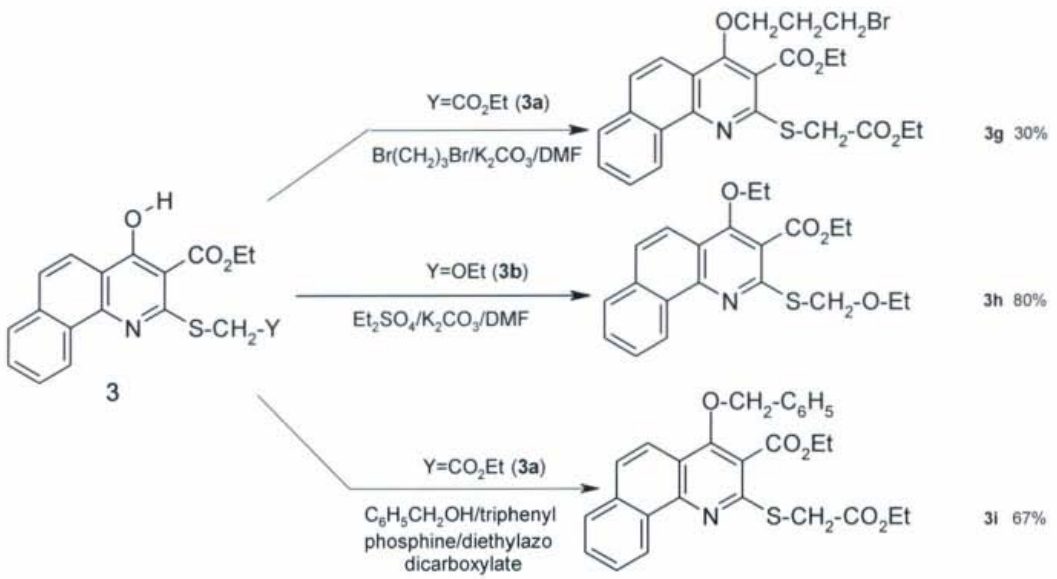

Scheme 3-2: Different O-alkylated derivatives of intermediate **3**.

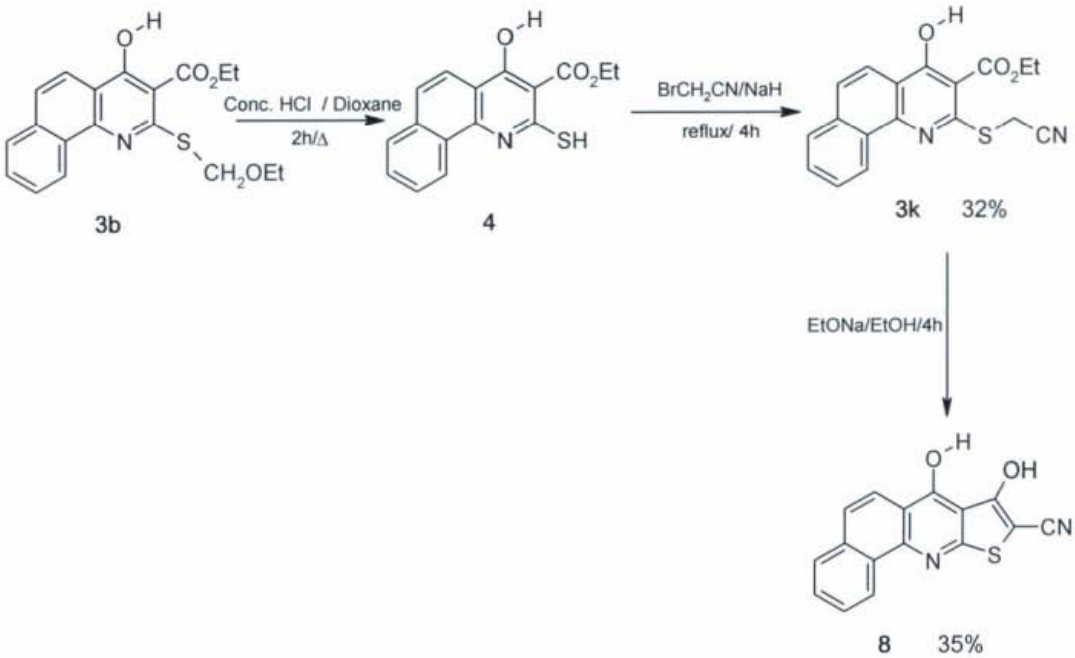

Scheme 3-3: Synthesis of 9-cyano-7-hydroxy-8-oxo-8,9-dihydrobenzo[*h*]thieno[2,3-*b*]quinoline **8**.

In order to prepare Compound **8**, deprotection of Compound **3b** was first necessary. The deprotection reaction was performed using conc. HCl in dioxane to obtain the thiol derivative **4.** Compound **4** was then subjected to alkylation using bromoacetonitrile in THF for 4 hours followed by Dieckman cyclization using sodium ethoxide in ethanol to yield Compound **8**, as shown in **Scheme 3-3.**

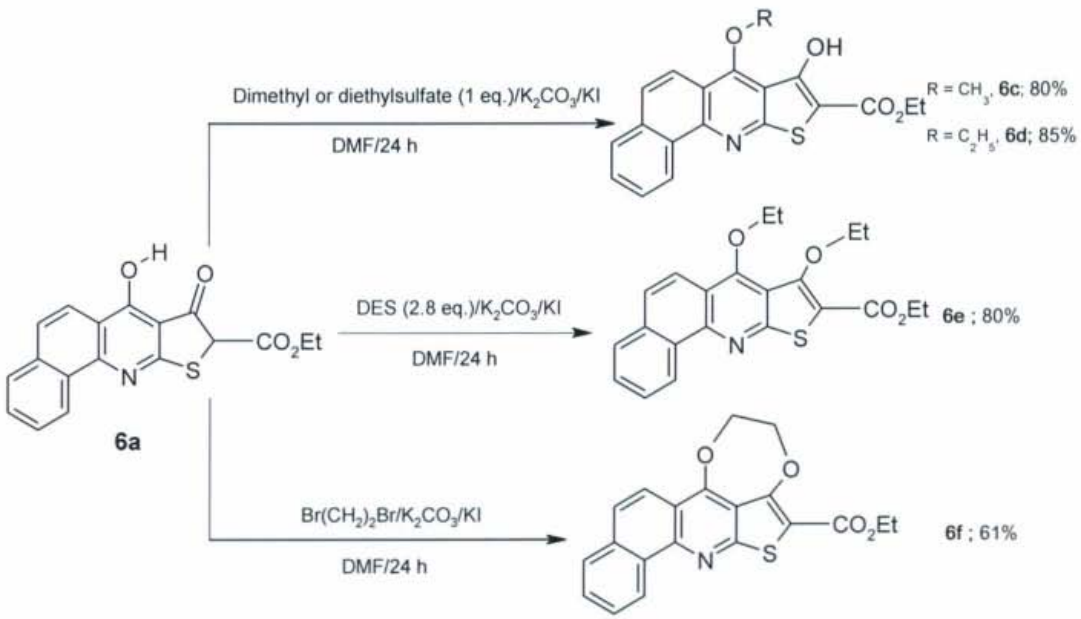

Scheme 3-4: Reactions on Compound **6a**.

N-Alkylation reactions were attempted on Compound **6a** using diethylsulfate in different proportions and dihalopropane derivatives. Interestingly, all the reactions formed the *O*-alkylated derivatives as depicted in **Scheme 3-4**.

An intensive investigation on the quinoline nucleus reveals that the 4-pyridone-3-carboxylic acid component remains a common feature of most inhibitors of DNA gyrase and topoisomerase IV. Positions C-3 and C-4 (the β-keto acid group, collectively) are

considered necessary for the binding of quinolones to DNA gyrase in the ternary complex [16].

It was found that replacement of the 3-carboxylic acid group of quinolones with isosteres such as sulfonic acid, acetic acid, hydroxamic acid, phosphoric acid and sulfonamides resulted in reduced antibacterial activity [17]. One successful strategy for the replacement of the 3-carboxylic acid group with retained (or enhanced) antibacterial activity employed a ring-fused isothiazolone group [18]. Isothiazole moiety, either in fused or isolated forms, has been frequently found to play an important role in various biological activities such as anti-inflammatory, antifungal, antibiotic, antiviral, cholesterol lowering, microbicide and the production of agrochemicals [19-25].

Our next strategy was based on annelation of the isothiazole ring onto the quinoline moiety constructed in previous steps. In this context we tried the synthesis of isothiazolobenzo[*h*]quinoline using the reported transamination of 2-sulfenamoyl-benzoates with various amines [26, 27]. We applied many reported procedures in order to synthesize the SNH_2 [28, 29]. The only successful procedure was the reaction of the thiol intermediate **4** with hydroxylamine-*O*-sulphonic acid to yield the corresponding thioamino derivative (**5**).

The use of hydroxylamine-*O*-sulfonic acid as a condensing agent in the presence of the ester group has been reported to yield an isothiazole ring [30-32]. In our case, it only yielded the thioamino derivative which further underwent cyclization to the targeted isothiazoloquinoline **7** using Dieckmann cyclization reaction conditions, as depicted in **Scheme 3-5**.

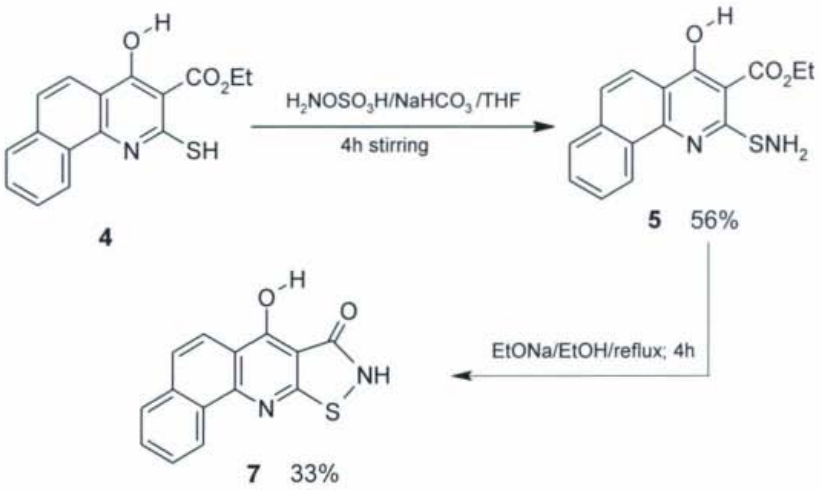

Scheme 3-5: Synthesis of 7-hydroxybenzo[*h*][1,2]thiazolo[5,4-*b*]quinolin-8(9*H*)-one.

In another attempt to increase the hydrophilicity of the quinoline system, we allowed Compound **6a** to react with hydrazine hydrate to yield the pentacyclic pyrazoloquinoline **9**. The chemistry of pyrazoloquinolines is well-established. This system has proved to be a very attractive scaffold for medicinal chemists in recent years. Pyrazoloquinolines have been extensively studied as bioactive compounds and are known to possess remarkable biological activities such as anti-cancer, anti-anxiety, anti-inflammatory, anti-asthmatic, cerebro-protective and antiviral, among others. For many of the activities, the molecular modes of actions are known [33].

The pentacyclic benzo[*h*]quinoline **9** was formed as a result of reaction of **6a** with hydrazine hydrate and cyclization in acetic anhydride solution as illustrated in **Scheme 3-6**. The structure of Compound **9** was confirmed by spectral analysis and X-ray crystallography, as shown in **Figure 3-2**.

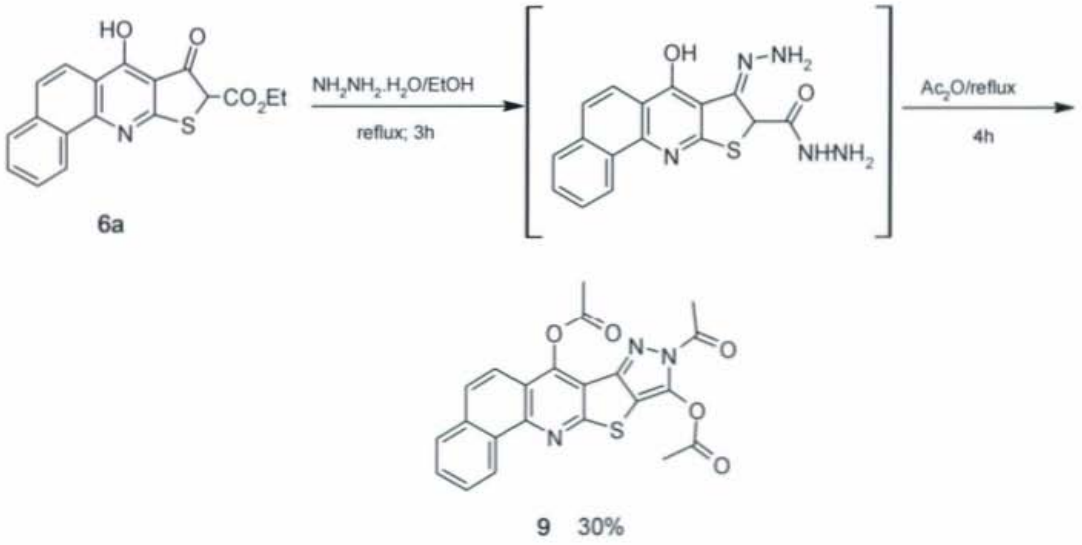

Scheme 3-6: Synthesis of 9-acetyl-9*H*-benzo[*h*]pyrazolo[3',4':4,5]thieno[2,3-*b*]quinoline-7,10-diyl diacetate.

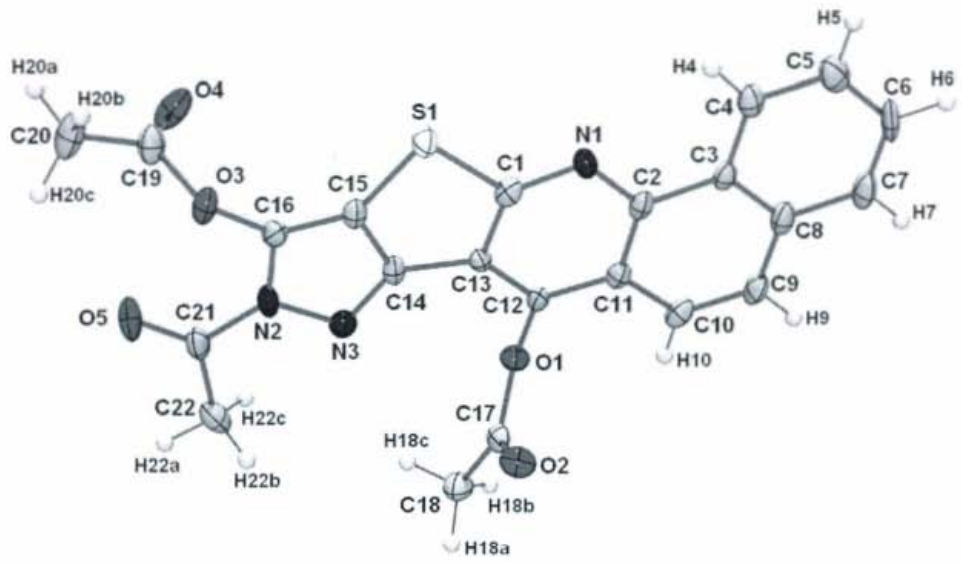

Figure 3-2: ORTEP Representation of the linear pentacyclic derivative **9** with 50% probability ellipsoids.

The synthesis of Compound **9** prompted us to further explore the effect of annelating different ring systems with quinoline-based building blocks which may possibly result in identification of novel polycyclic molecules with potential bioactivity. In this context, we attempted the synthesis of 1*H*-3-thia-11c-azaazuleno [1,8,7,6c-6f] phenanthrene-1,6(5*H*)-dione. In this structure, a thiazoloazepinone moiety is annelated to the benzoquinoline system.

Since nalidixic acid was reported by Lesher *et al.* (1962) [1], pyridone carboxylic acid antibacterials have become an important class of therapeutically useful compounds. Ofloxacin [34] (a tricyclic pyridone carboxylic acid, having an oxazine ring) is one of these agents. The oxygen atom of the oxazine ring of ofloxacin was found to give optimal antibacterial activity vs nitrogen, sulfur, or the carbon atom. Also, the tetracyclic pyridone carboxylic acids having a thiazolo-oxazine ring [35], as shown in structure **C**, have proven to improve antibacterial activity against both Gram-positive and Gram-negative bacteria.

C

In the above study, replacement of the oxygen atom of the thiazolo-oxazine ring by nitrogen, sulfur, or a carbonyl group was attempted. The antibacterial assessment of the resulting compounds revealed that the replacement of an oxygen atom of the thiazolo-oxazine ring by a nitrogen atom enhanced both *in vitro* and *in vivo* antibacterial activity.

The synthesis of Compound **11** was achieved via the reaction of **1a** with 4-chloroethylacetoacetate, followed by thermal cyclization under vacuum to afford Compound **10**. Compound **10** was subjected to cyclization using PPA, to yield the novel phenanthrene derivative **11**.

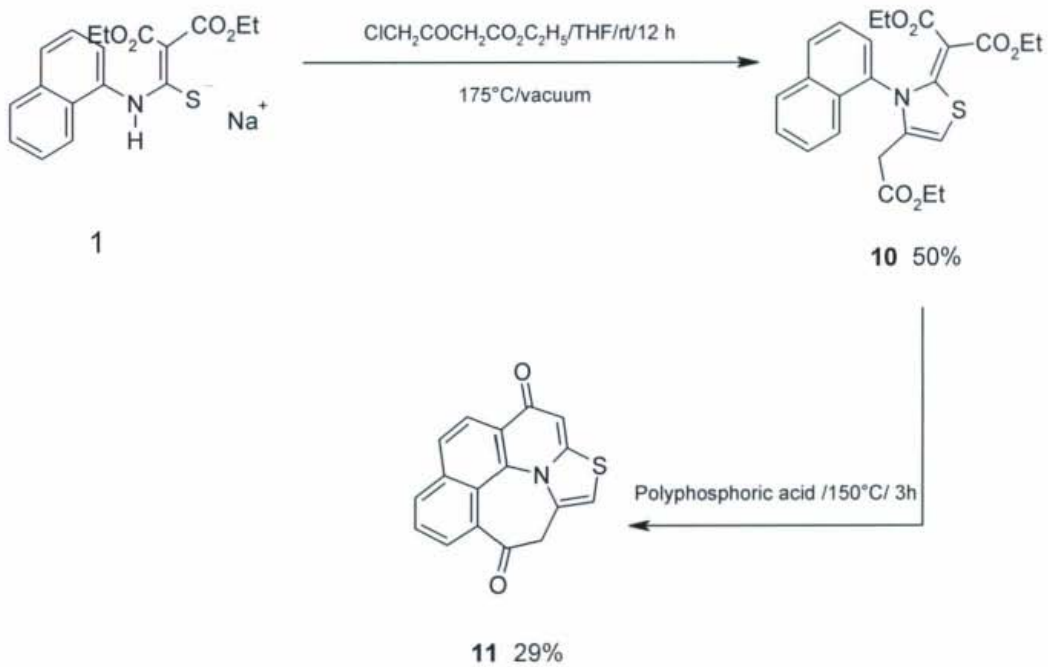

1

10 50%

11 29%

Scheme 3-7: Synthesis of *1H*-3-thia-11c-azaazuleno[1,8,7,6-*cdef*]phenanthrene-1,6(*5H*)-dione **11**.

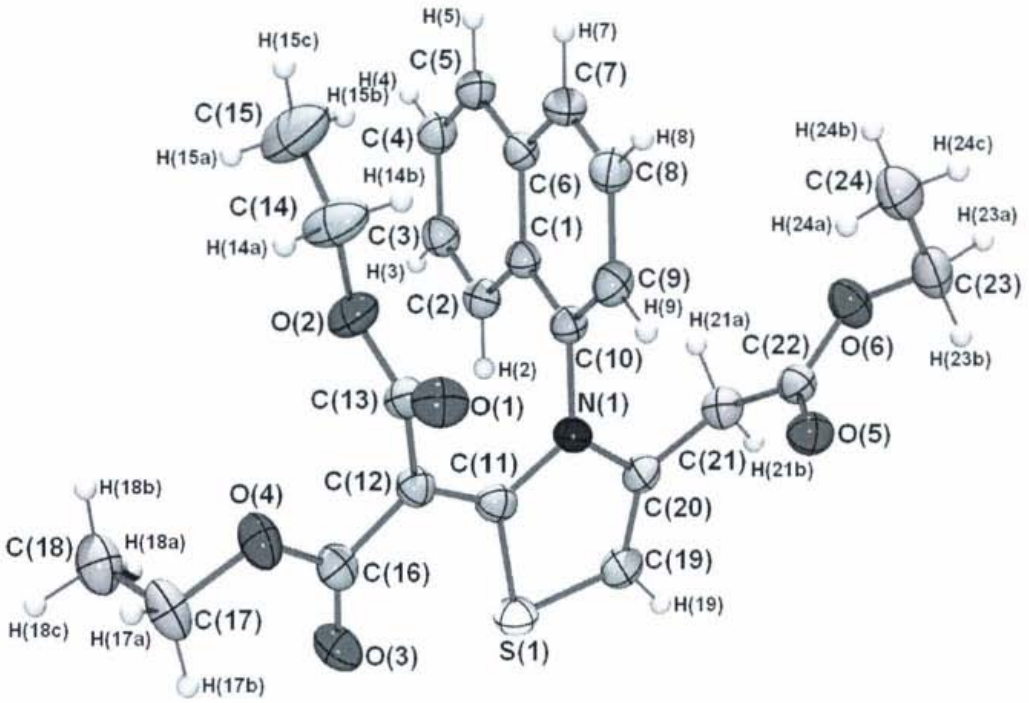

Figure 3-3: ORTEP representation of Compound **10** with 50% probability ellipsoids.

3.3 Materials and methods

3.3.1 *In vitro* testing

3.3.1.1 Brine shrimp lethality bioassay (BSL)

The determination of toxicity of the compounds against brine shrimp was conducted according to Meyer's procedure [36], with minor modifications. Toxicities of compounds were tested at 0.2, 10, 100, and 1000 μg/mL sea-water solutions with 1% DMSO (v/v). Ten one-day *nauplii* were used in each test tube and the percentage of the survivors was measured after 48 h. Three replications were used for each concentration.

3.3.1.2 MTT cytotoxicity bioassay

The general principle for the detection of cell growth or cell kill via the MTT cytotoxicity assay is the conversion of the yellow-coloured tetrazolium salt (MTT) to the purple-coloured product formazan. The concentration can be measured photometrically at 570 nm. The formation of formazan takes place via intact mitochondria.

The most cytotoxic derivatives were tested against HeLa and KB cell lines using the MTT cytotoxicity bioassay [37,38].

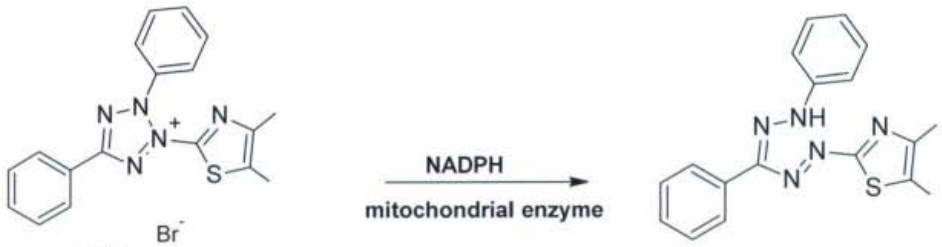

HeLa cells, human cervix adenocarcinoma, were grown in DMEM (GIBCO) with 15% FBS and antibiotics (penicillin 100 U/ml, streptomycin 100 ug/ml). Cells were maintained at 37℃ in a humidified 5% CO_2 atmosphere.

Cells were trypsinized and seeded into 96-well cell culture plates as 180ul/well (about 5000 cells/well). After 16 h incubation, the cells were treated for 48 h by the compound at final concentrations of 100, 10, 1, 0.1 μg /ml. The compounds were prepared in DMSO (stock solution of 10 μg/ml) and further diluted with culture medium to obtain the desired concentrations. All tests included controls with equivalent concentrations of media DMSO corresponding to the relevant dilutions of the test compound. The 3-(4,5-dimethylthiazol-2-yl)-2,5-diphenyl tetrazolium bromide (MTT)

was added in the final concentration of 1 mg/ml, and 30 µl/well. After 4 h incubation the MTT-formazan product was solubilized using DMSO (150 µl/well) with shaking for 10 min. The absorbance measurements were carried out using a microplate reader at 570 nm.

The weak cytotoxicity on HeLa and KB cell lines by the most cytotoxic derivatives in the BSL bioassay prompted us to explore the possibility of these derivatives to act as topoisomerase inhibitors theoretically.

3.4 Molecular modeling

3.4.1 Methods

Docking calculations were carried out according to the DockingServer methodology [39]. The MMFF94 force field [40] was used for energy minimization of the ligand molecules using DockingServer. PM6 semi-empirical charges calculated by MOPAC2009 (J. P. Stewart, Computer code MOPAC2009, Stewart Computational Chemistry, 2009) were added to the ligand atoms. Non-polar hydrogen atoms and rotatable bonds were defined.

Docking calculations were carried out on the topoisomerase II structure with the pdb code 1QZR. Essential hydrogen atoms, Kollman united atom type charges, and solvation parameters were added with the aid of AutoDock tools [41]. Affinity (grid) maps with 25×25 ×25 Å grid points and 0.375 Å spacing were generated using the Autogrid program. AutoDock parameter set- and distance-dependent dielectric functions were used in the calculation of the van der Waals and the electrostatic terms, respectively.

Docking simulations were performed using the Lamarckian genetic algorithm (LGA) and the Solis & Wets local search method [42]. Initial position, orientation, and torsions of the ligand molecules were set randomly. Each docking experiment was derived from 100 different runs that were set to terminate after a maximum of 2,500,000 energy evaluations. The population size was set to 150. During the search, a translational step of 0.2 Å, and quaternion and torsion steps of 5 were applied.

3.4.1.1 Human topoisomerase II docking

Topoisomerase II is an ATPase belonging to the GHKL (Gyrase, Hsp90, histidine Kinase, mutL) family. The mechanism of function of human toposiomerase II is to simultaneously cut both strands of the DNA helix using the energy derived from ATP hydrolysis. The inhibition of human topoisomerase II is one of the targets of current oncology research. There are several ways to inhibit the enzyme's action [43]:

1-While exerting its function, the enzyme creates a transient covalent DNA-enzyme complex. Topoisomerase II poisons exert their effect by stabilizing this transient complex, thus causing DNA damage. Since these compounds are very toxic to normal cells, alternative ways of topoisomerase II inhibition are subjects of interest in drug research.

2-An alternative way of inhibition is to block the enzyme before the DNA cleavage step or in the last step of its catalytic cycle. The competition for the ATP binding site as well as stabilization of a transient dimer interface between two ATPase monomers have been described [42,44]. Nevertheless, these ways of inhibition take place at the ATPase region of the protein. Among the available structures of the human topoisomerase II

protein, 1PVG and 1QZR carry the ATPase region. Additionally, 1PVG contains modified methionine residues (MSE), while 1QZR contains phosphoaminophosphonic acid-adenylate ester (ANP) at the ATP binding site and an inhibitor ICRF-187 at the interface of the homodimer. All our docking calculations were done using 1QZR.

3.4.1.2 Docking experiment

In order to define possible binding sites in the protein, the known human topoisomerase II inhibitor, Compound A, was docked into the crystal structure. First, a blind docking procedure was applied. The docking result showed no cluster possessing significantly higher frequency or lower energy as compared to the other clusters. Thus, blind docking in this case was not able to clearly define the possible binding site. Therefore, biochemical knowledge was used for binding site identification. The cluster possessing the highest interaction surface between the docked ligand and the protein indicating strong binding was located at the ATP binding site. None of the results were found at the inhibitor's (ICRF-187) binding site. Thus, focused docking calculations were carried out at the ATP binding site of the protein.

3.4.1.3 Focused docking results

Compound A was subjected to focused docking calculations at the ATP binding site of the protein with docking energy equal to -7.39 kcal/mol.

All compounds were calculated to bind at the ATP binding site with reasonable affinity, with **6a** possessing the lowest docking energy. It is noted that in the X-ray

structure Mg^{+2} is coordinated by 3 oxygen atoms coming from ANP. Compound A is also able to donate non-bonding electrons to the Mg^{2+} ion.

Table 3-1: Docking energies of the investigated compounds at the ATP binding site.

Compound	Docking energy (kcal/mol)
6a	-9.21
9	-9.19
6b	-9.00
6c	-8.64
6d	-8.29
11	-8.24
6f	-8.04
7	-7.94
8	-7.88
6e	-7.76
10	-7.76

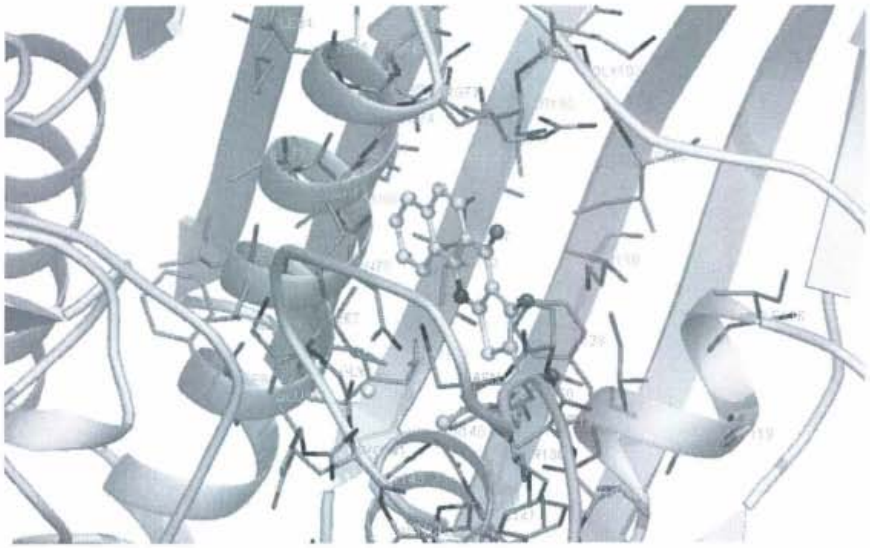

Figure 3-4: Compound **6a** docked at the ATP binding site of 1QZR.

Table 3.1 shows the calculated interaction energies at the ATP binding site. The estimated binding energies can be used to rank the ligands according to their binding affinity.

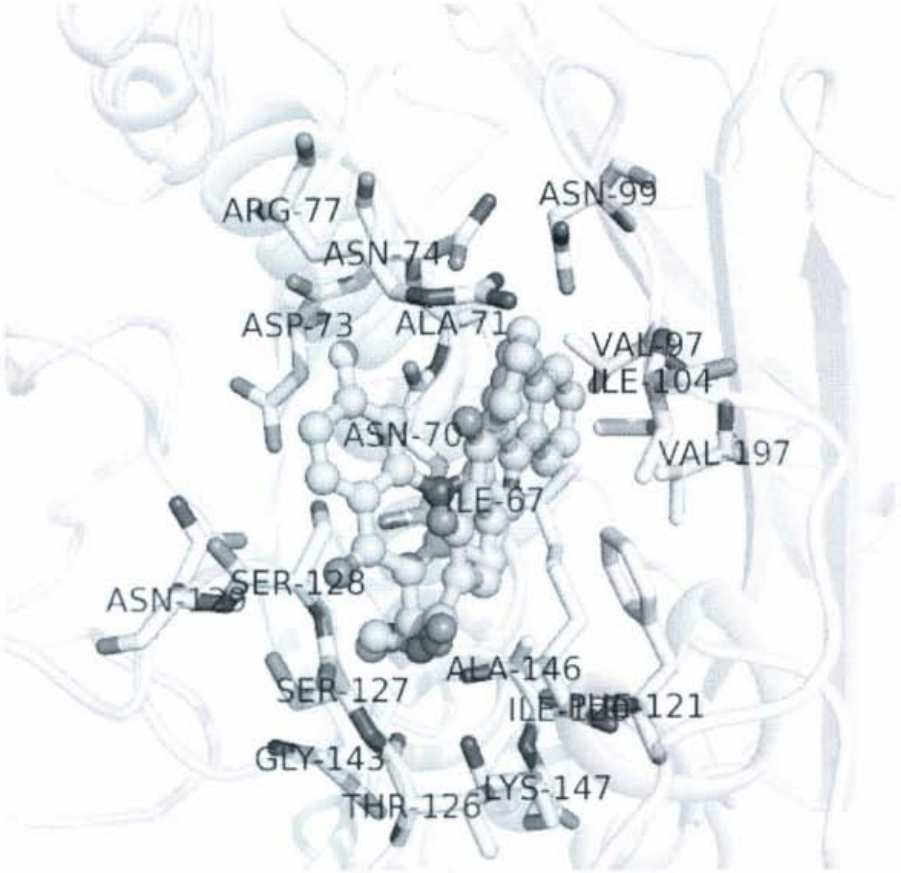

Figure 3-5: Overlapping image of Compounds **6a** (green colour) and **A** (blue colour) at the ATP binding site of 1QZR.

Compound **6a** indicates a hydrogen bonding interaction with ASN70 and LYS147. Namely, the amino group of ASN70 hydrogen-bonds to the aromatic nitrogen and the protonated nitrogen of LYS147 hydrogen-bonds to the ester carbonyl of **6a**. The aromatic planar ring system of **6a** is stabilized by a number of hydrophobic interactions with

surrounding hydrophobic amino acid residues at the binding site: ILE67, ILE120, ALA71, VAL197 and with the aromatic side chain of PHE121. It is important to note that none of the compounds used in the docking studies were involved in interactions with Mg^{2+}, in contrast to Compound **A**.

Focused docking calculations at the ATP binding site revealed that the investigated compounds are able to bind to human topoisomerase II with a reasonable binding affinity. The main difference between compound **A** and the investigated compounds is in its ability to coordinate with the Mg^{2+} ion and that explains the potent cytotoxic and topoisomerase II inhibitory effect of compound **A**, compared to the weak cytotoxic effects demonstrated by the compounds synthesized in our study.

3.5 Results and discussion

3.5.1 Brine Shrimp Lethality bioassay results

The number of shrimps surviving after 48 h exposure to compounds were counted, and based on that, the percentage inhibition was evaluated. The 50% lethal concentration (LC_{50}) was calculated, which is presented in **Table 3-2** using taxol as a reference standard. The percentage mortality at each vial and control was determined using the equation:

% mortality = (no. of dead nauplii/ initial no. of live nauplli) x 100

Probit analysis by Finney (1971) was used to determine thec oncentration at which lethality to brine shrimp represents 50% (LC_{50}).

The results showed that only three of the synthesized derivatives (**6a, 7, 8**) were considered as cytotoxic (less than 100 µg/mL). The Brine Shrimp Lethality bioassay

represents a rapid, inexpensive and simple bioassay method which in most cases correlates reasonably well with cytotoxic and antitumor properties.

Table 3-2: Brine shrimp lethality bioassay results.

Structure no.	LC_{50} (µg/mL)
6a	50
6b	500
6c	>1000
6d	>1000
6e	850
6f	920
7	70
8	95
9	950
10	>1000
Taxol	0.2

3.5.2 MTT Cytotoxicity results

The viability was calculated with regard to the untreated cell control, which was set to 100% viability. A lysis control where the cells were treated with Doxorubicin was set to 0% viability, and was found to be sufficient to induce 100% cell death.

Table 3-3: Results of cytotoxicity testing against HeLa and Kb cell lines.

Structure no.	HeLa-IC_{50}(uM)	Kb-IC_{50}(uM)
6a	17.7	20.67
7	>30	27.29
8	22	24.4

Cytotoxicity assessments were performed at Taiho and Naeja pharmaceuticals.

3.6 Conclusion

The quinoline system i s considered an attractive scaffold upon which to build chemical libraries with promising bioactivity potentials. Its unique structural feature has prompted scientists to design, synthesize, and evaluate different quinoline-based structures which exhibit diverse biological activities.

In this study, novel polycyclic quinoline-based molecules were designed having a structural relationship to a molecule that is currently under clinical investigation as an antineoplastic agent. The structure-based molecular modeling approach led us to ethyl-7-hydroxy-8-oxo-8,9-dihydrobenzo[*h*]thieno [2,3-*b*]quinoline-9-carboxylate (**6a**). A series of **6a** analogues was synthesized and tested for cyctotoxicity against different cancer cell lines. The test results revealed a lack of cytotoxic potency for these compounds. In order to rationalize the non-toxic profile of these compounds, docking experiments with the topisomerase II protein structure were evaluated using "Compound **A**", as a standard-reference topoisomerase II inhibitor. The docking experiments revealed that while the synthesized compounds interact with the protein carrying the ATP binding region, they do not coordinate with Mg^{2+} ion. However, while Compound A forms a stable coordination complex with the Mg^{2+} ion, this could possibly explain the weak cytotoxicity demonstrated by the synthesized compounds. Further bioassays of these compounds to find other potential bioactivities are ongoing in the Daneshtalab group.

3.7 Experimental

Solvents and reagents were obtained from commercial suppliers and were used without further purification. Melting points were not optimized. ^{1}H and ^{13}C NMR spectra, HSQC, and COSY spectra were recorded on a Bruker AVANCE-500 MHz NMR spectrometer using TMS as an internal standard. Mass spectra were obtained on an Agilent 1100 series LC/MSD chromatographic system. High-resolution mass spectra (EI or ESI) were obtained on Waters GCT Premier Micromass Spectrometer. X-ray structures were measured with a Rigaku Saturn 70 instrument, equipped with a CCD area detector and a SHINE optic, using Mo Kα radiation. Silicycle Ultrapure silica gel (0-20 μm) G and F-254 were used for the thin-layer chromatography (TLC), and Silicycle Silia-P Ultrapure Flash silica gel (40-63 μm) was used for flash column chromatography. TLC was conducted on Polygram SIL G/UV254 precoated plastic sheets. The reaction yields are included in corresponding schemes.

Sodium 3-ethoxy-2-(ethoxycarbonyl)-1-(naphthalen-1-ylamino)-3-oxoprop-1-ene-1-thiolate (1a):

To a suspension of sodium hydride (0.60 g, 25 mmol) in MeCN (50.00 mL) at 5-10 °C was added dropwise diethyl malonate (4.00 mL, 26.34 mmol) over a period of 15 min. The mixture was stirred at 5-10 °C for 30 min., then 1-naphthylisothiocyanate (5.00 g, 26.99 mmol) was added portionwise at the same temperature, and stirring was continued for extra 30 min. Evaporation of MeCN yielded a yellowish solid which was washed with Et_2O; mp 118-120 °C; ^{1}H-NMR: (500 MHz, DMSO-d_6): δ = 12.33 (s, NH), 8.57 (d, J = 7.1 Hz, 1H), 8.16 (t, J = 7.7 Hz, 1H), 7.91-7.86 (m,1H), 7.52 (ddd, J = 4.7, 11.1, 8.8 Hz,

3H), 7.46-7.38 (m, 1H), 4.02 (q, 2 X $O\underline{CH_2}CH_3$, J = 7.0 Hz, 4H), 1.16 (t, 2 X $OCH_2\underline{CH_3}$, J = 7.0 Hz, 6H);^{13}C NMR (175 MHz, DMSO-d_6): δ = 181.6, 166.4, 136.1, 132.5, 127.0, 126.6, 124.3, 124.2, 123.9, 121.2, 120.6, 119.4, 116.8, 95.2, 56.8 ($2CH_2$), 13.3 ($2CH_3$); APCI-MS: 368.40 **(M^++1, 100).**

Ethyl 2-[(ethoxymethyl)thio]-4-hydroxybenzo[*h*]quinoline-3-carboxylate (3a):

To the above yellow solid (**1a**, 2.00 g, 5.44 mmol) in THF (50 mL) was added $BrCH_2CO_2Et$ (0.60 mL, 5.44 mmol) dropwise at 0 °C and stirring was continued for an extra hour at room temperature, evaporated the solvent , extracted with $CHCl_3$ and dried over Na_2SO_4. The organic layer was evaporated by rotary evaporator to give yellow oil (**2a**). The obtained oil was heated at 170-180 °C in an oil bath under vacuum for 10 min. The resulting oil was solidified, then washed with ether resulting in (**3a**) as colourless needles; mp 136-138 °C; ^{1}H-NMR: (500 MHz, $CDCl_3$): δ = 13.11 (s, 1H, OH), 9.22-9.15 (m, 1H), 8.10 (d, J = 8.9 Hz, 1H), 7.89 (dd, J = 3.1, 6.0 Hz, 1H), 7.76-7.68 (m, 3H), 4.61 (q, J = 7.0, 6.9 Hz, 2H), 4.22 (q, J = 7.0, 6.9 Hz, 2H), 4.13 (s, 2H), 1.60 (t, J = 7.0 Hz, 3H), 1.29 (t, J = 7.0 Hz, 3H); ^{13}C NMR (175 MHz, $CDCl_3$): δ = 170.9, 170.4, 168.2, 158.1, 147.6, 135.8, 130.6, 129.4, 128.1, 127.1, 126.2, 125.9, 119.9, 115.1, 104.0, 63.2, 61.9, 34.6, 14.6, 14.6; HR-MS (TOFEI) calcd for $C_{20}H_{19}NO_5S$ (385.0984); found (385.0991).

Ethyl 2-[(ethoxymethyl)thio]-4-hydroxybenzo[*h*]quinoline-3-carboxylate (3b):

This compound was prepared according to the same procedure as that applied for **3a** using chloromethyl ethyl ether; yellow crystals; mp 120-122 °C; ^{1}H-NMR: (500 MHz, $CDCl_3$): δ = 13.11 (s, 1H), 9.26-9.19 (m, 1H), 8.13 (d, J = 9.0 Hz, 1H), 7.91 (d, J = 3.3

Hz, 1H), 7.75 (d, J = 9.0 Hz, 1H), 7.72 (dd, J = 3.2, 6.1 Hz, 2H), 5.76 (s, 2H), 4.60 (q, J = 7.1 Hz, 2H), 3.76 (q, J = 7.0 Hz, 2H), 1.59 (t, J = 7.0 Hz, 3H), 1.25 (t, J = 7.0 Hz, 3H);^{13}C NMR (175 MHz, $CDCl_3$): δ = 171.1, 168.3, 158.2, 147.4, 135.8, 129.4, 128.2, 127.3, 126.2, 125.7, 120.0, 115.1, 104.3, 71.4, 65.7, 63.1, 31.2, 15.4, 14.6; HR-MS (TOFEI): calcd for $C_{19}H_{19}NO_4S$ (357.1035); found (357.1031).

Ethyl 4-hydroxy-2-(methylthio)benzo[*h*]quinoline-3-carboxylate(3c):

Prepared according to the method applied for **3b**, using 1equivalent MeI; yellow powder; mp 158-160 °C; ^{1}H-NMR: (500 MHz, $CDCl_3$): δ = 13.09 (s, 1H, OH), 9.22-9.16 (m, 1H), 8.10 (d, J = 8.9 Hz, 1H), 7.87 (dd, J = 2.8, 6.0 Hz, 1H), 7.71 (d, J = 8.8 Hz, 1H), 7.69-7.65 (m, 2H), 4.57 (q, J = 7.2 Hz, 2H), 2.81 (s, 3H), 1.57 (t, J = 7.25 Hz, 3H); ^{13}C NMR (175 MHz, $CDCl_3$): δ = 170.9, 167.7, 160.1, 147.0, 135.4, 130.4, 128.9, 127.8, 126.7, 125.4, 125.3, 119.6, 114.2, 103.7, 62.6, 15.1, 14.2; HR-MS (TOFEI) calcd for $C_{17}H_{15}NO_3S$ (313.0773); found (313.0779).

Ethyl 4-hydroxy-2-[(4-methoxybenzyl)thio]benzo [*h*] quinoline-3-carboxylate (3d):

Prepared according to the method applied for **3b**, using 1 equivalent *P*-MeOBnCl; colourless crystals; mp 135-136 °C; ^{1}H-NMR: (500 MHz, $CDCl_3$): δ = 13.14 (s, 1H, OH), 9.16 (dd, J = 8.2, 5.9 Hz, 1H), 8.10 (d, J = 9.0 Hz, 1H), 7.88 (dd, J = 6.7, 2.4 Hz, 1H), 7.75-7.69 (m, 1H), 7.66 (dt, J = 7.0, 3.9 Hz, 2H), 7.43 (t, J = 5.8 Hz, 2H), 7.25 (s, 1H), 6.85 (dd, J = 9.2, 2.5 Hz, 2H), 4.70 (s, 2H), 4.53 (q, J = 7.1 Hz, 2H), 3.83 (s, 3H), 1.50 (t, J = 7.2 Hz, 3H); ^{13}C NMR (175 MHz, $CDCl_3$) : δ = 170.8, 167.8, 159.7, 158.7, 147.0, 135.5, 130.4, 130.3, 129.7, 129.0, 127.8, 126.8, 125.5, 125.3, 123.1, 121.2, 119.7,

114.5, 114.0, 103.5, 62.7, 55.2, 35.4, 14.3; H R-MS (TOFEI) calcd for $C_{24}H_{21}NO_4S$ (419.1191); found (419.1191).

Ethyl 4-hydroxy-2-{[(2Z)-3-phenylprop-2-en-1-yl] thio} benzo[*h*] quinoline-3-carboxylate (3e):

Prepared according to the method applied for **3b**, using 1 equivalent $ClCH_2C_6H_5CH{=}CH$; white powder; mp 157-159 °C; ^{1}H-NMR: (500 MHz, $CDCl_3$): δ = 13.13 (s, 1H, OH), 9.21 (m, 1H), 8.12 (d, *J* = 8.8 Hz, 1H), 7.91 (m, 1H), 7.74 (d, *J* = 9.1 Hz, 1H), 7.71 (2H, m), 7.35 (d, *J* = 7.2 Hz, 2H), 7.26 (m, 3H), 7.20 (d, *J* = 7.2 Hz, 1H) 6.76 (d, *J* = 7.5 Hz, 1H), , 4.58 (q, *J* = 7.1, 7.0 Hz, 2H), 4.28 (d, *J* = 5.6 Hz 2H), 1.56 (t, *J* = 5.8 Hz, 3H); ^{13}C NMR (175 MHz, $CDCl_3$): δ = 165.6, 162.6, 153.8, 141.8, 131.8, 130.2, 127.6, 125.2, 123.8, 123.2, 122.6, 122.2, 121.6, 121.1, 120.5, 120.3, 120.0, 119.1, 114.4, 109.2, 98.4, 57.5, 28.7, 15.0, 9.0; HR-MS (TOFEI) calcd for $C_{25}H_{21}NO_3S$ (415.1242); found (415.1246).

Ethyl 2-(benzylthio)-4-hydroxybenzo[*h*]quinoline-3-carboxylate (3f):

Prepared according to the method applied for **3b**, using 1 equivalent BnCl; white crystalline product; mp 130-132 °C; ^{1}H-NMR: (500 MHz, $CDCl_3$): δ = 13.07 (s,1H, OH), 9.10 (dd, *J* = 8.3, 6.6 Hz, 1H), 8.09-8.04 (m, 1H), 7.88-7.82 (m, 1H), 7.68 (d, *J* = 8.9 Hz, 2H), 7.66-7.59 (m, 1H), 7.52 (d, *J* = 7.1 Hz, 2H), 7.36-7.29 (m, 2H) 7.28-7.22 (m, 1H), 4.73 (s, 2H), 4.52 (q, *J* = 7.1 Hz, 2H), 1.49 (t, *J* = 7.0 Hz, 3H); ^{13}C NMR (175 MHz, $CDCl_3$): δ = 170.8, 167.8, 159.4, 147.0, 138.0, 135.5, 130.3, 129.2, 129.0, 128.5, 127.8, 127.0, 126.8, 125.6, 125.3, 123.2, 121.1, 119.7, 114.5, 103.5, 62.7, 35.9, 14.3; HR-MS (TOFEI) calcd for $C_{23}H_{19}NO_3S$ (389.1086); found (389.1093).

Ethyl 4-(3-bromopropoxy)-2-((2-ethoxy-2-oxoethyl)thio)benzo[*h*]quinoline-3-carboxylate (3g):

To a mixture of the quinoline derivative **3a** (0.385 g, 1.00 mmol) and K_2CO_3 (0.386 g, 2.800 mmol) in dry DMF (25 mL) under nitrogen atmosphere, 1,3-dibromopropane (0.565 g, 2.80 mmol) and KI (catalytic amount) were added. The reaction mixture was heated at 70°C for 24 h, then poured into ice-H_2O, the resulting product was collected by filtration and recrystalized from hexane:$CHCl_3$ (1:3) resulting in a white powder; mp 162-164 °C; ^{1}H-NMR: (500 MHz, $CDCl_3$): δ = 9.21-9.14 (m, 1H), 7.95 (d, *J* = 8.9 Hz, 1H), 7.91-7.85 (m, 1H), 7.76 (d, *J* = 8.9 Hz, 1H), 7.70 (m, 2H), 4.53 (q, *J* = 7.1 Hz, 2H), 4.35 (t, *J* = 5.8 Hz, 2H), 4.22 (q, *J* = 7.1 Hz, 2H), 4.15 (s, 2H), 3.70 (t, *J* = 6.4 Hz, 2H), 2.42 (q, *J* = 6.1 Hz, 2H), 1.49 (t, *J* = 7.1 Hz, 3H), 1.27 (t, *J* = 7.1 Hz, 3H); ^{13}C NMR (175 MHz, $CDCl_3$): δ = 162.1, 160.6, 160.2, 153.7, 148.0, 134.2, 130.2, 129.0, 127.6, 127.0, 125.9, 125.4, 119.9, 115.8, 113.8, 70.9, 70.0, 61.2, 33.8, 29.8, 25.0, 14.4, 14.3; APCI-MS: 506.40 (M^++1, 100).

Ethyl 4-ethoxy-2-[(ethoxymethyl)thio]benzo[*h*]quinoline-3-carboxylate (3h):

Utilizing the same alkylation procedure as applied for preparation of **3g** using diethylsulfate starting from **3b**; white crystals; mp 80-82 °C; ^{1}H-NMR: (500 MHz, $CDCl_3$): δ = 9.17 (m, 1H), 8.07 (m, 1H), 7.98 (dd, *J* = 9.0, 22.2 Hz, 2H), 7.81 (m, 2H), 5.76 (s, 2H), 4.46 (q, *J* = 7.0 Hz, 2H), 4.29 (q, *J* = 6.9 Hz, 2H), 3.61 (q, *J* = 7.0, 2H), 1.45 (t, *J* = 6.9 Hz, 3H), 1.39 (t, *J* = 7.1 Hz, 3H), 1.11 (t, *J* = 7.0 Hz, 3H); ^{13}C NMR (175MHz, $CDCl_3$): δ = 166.2, 163.2, 160.7, 154.9, 147.3, 134.9, 132.9, 131.9, 129.1, 128.9, 127.0,

125.2, 120.1, 119.5, 118.8, 72.1, 65.3, 62.9, 16.3, 15.6, 14.8; HR-MS (TOFEI) calcd for $C_{21}H_{23}NSO_4$ (385.1426); found (385.1441).

Ethyl 4-(benzyloxy)-2-[(2-ethoxy-2-oxoethyl)thio]benzo[*h*]quinoline-3-carboxylate (3i):

A 250 mL round bottom flask was charged with triphenylphosphine (2.70 g, 10.30 mmol) to which was added 70 mL THF. The resulting clear solution was cooled to -78°C and DEAD (1.63 mL, 10.30 mmol) was added over 5 min. The yellow reaction mixture was stirred for extra 5 min after which benzyl alcohol (1.169 mL, 11.30 mmol) was added and stirred for 5 min. Neopentyl alcohol (0.50 g, 5.70 mmol) and **3a** (3.96 g, 10.30 mmol) were added sequentially to the reaction mixture as solids. The resulting suspension was allowed to remain at -78°C for 5 min during which most of the starting material dissolved. The cooling bath was then removed and the reaction was stirred overnight at room temperature, TLC indicated complete consumption of the reactant. The clear solution was concentrated to approximately ¼ of the original volume under vaccum then applied to a silica gel column and eluted with 5:1 hexane/EtOAc resulting in a white crystalline product; mp 105-107 °C; ^{1}H-NMR: (500 MHz, $CDCl_3$): δ = 9.08 (m, 1H), 8.05 (m, 1H), 7.94 (m, 2H,), 7.81 (m, 2H), 7.79 (m, 2H), 7.41 (m, 3H), 5.26 (s, 2H), 4.44 (q, *J* = 5.3 Hz, 2H), 4.25 (s, 2H), 4.12 (q, *J* = 5.1 Hz, 2H), 1.35 (t, *J* = 6.8 Hz, 3H), 1.21 (t, *J* = 7.5 Hz, 3H); ^{13}C NMR (175 MHz, $CDCl_3$): δ = 166.2, 160.6, 154.9, 147.4, 134.3, 130.6, 128.7, 127.8, 127.1, 126.6, 124.9, 119.4, 118.5(8 carbons), 71.9, 71.2, 65.1, 62.1, 15.7, 14.9, 14.1; HR-MS (TOFEI) calcd for $C_{27}H_{25}NO_5S$ (475.1453); found (475.1458).

Ethyl 2-[(3-chloro-2-oxopropyl)thio]-4-hydroxybenzo[*h*]quinoline-3-carboxylate (3j):

Utilizing the same alkylation procedure as applied for preparation of **3b** using 1,3 - dichloroacetone; yellowish brown powder; mp 98-100 °C; ^{1}H-NMR: (500 MHz, $CDCl_3$): δ = 13.09 (s, OH), 8.93 (d, *J* = 8.5 Hz, 1H), 8.10 (d, *J* = 8.9 Hz, 1H), 7.89 (d, *J* = 7.3 Hz, 1H), 7.79-7.69 (m, 3H), 4.61 (q, *J* = 7.16, 7.17 Hz, 2H), 4.40 (s, 2H,), 4.32 (s, 2H), 1.58 (t, *J* = 7.1 Hz, 3H); ^{13}C NMR (175 MHz, $CDCl_3$): δ = 169.3, 168.0, 164.3, 157.4, 146.21, 134.6, 129.3, 129.2, 127.8, 126.9, 125.8, 124.6, 119.1, 114.3, 105.4, 35.6, 33.3, 14.0, 13.9; HR-MS (TOFEI) calcd for $C_{19}H_{16}ClNO_4S$ (389.0489); found: (389.0495).

Ethyl 2-[(cyanomethyl)thio]-4-hydroxybenzo[*h*]quinoline-3-carboxylate (3k):

To a stirring solution of **4** (0.80 g, 2.67 mmol) in THF (10 mL) and H_2O (40 mL) was added $NaHCO_3$ (1.0 g, 7.23 mmol), and stirred for 15 min., then bromoacetonitrile (0.50 g, 4.16 mmol) was added to the resulting solution and stirred for 4 h at room temperature. After completion of the reaction, the solution was acidified by acetic acid, extracted with chloroform, dried over Na_2SO_4, filtered to give **3k** as a white powder; mp 208-210 °C; ^{1}H-NMR: (500 MHz, DMSO-d_6): δ = 12.42 (s, 1H, OH), 9.26-9.21 (m, 1H), 8.12 (d, *J* = 8.8 Hz, 1H), 8.10-8.07 (m, 1H), 7.97 (d , *J* = 9.1 Hz, 1H), 7.82 (m, 2H), 4.53 (q, *J* = 7.0 Hz, 2H), 4.43 (s, 2H), 1.45 (t, *J* = 7.1 Hz, 3H); ^{13}C NMR (175 MHz, DMSO-d_6): δ = 169.9, 168.0, 155.0, 147.2, 135.5, 130.1, 129.4, 127.9, 127.4, 126.6, 125.3, 119.3, 117.4, 115.0, 103.4, 63.1, 17.2, 14.2; HR-MS (TOFEI) calcd. for $C_{18}H_{14}N_2O_3S$ (338.0725); found (338.0722).

Ethyl 2-(aminothio)-4-hydroxybenzo[*h*]quinoline-3-carboxylate (5):

To a stirring solution of **4** (0.8 g, 2.67 mmol) in THF (10 mL) and H_2O (40 mL) was added $NaHCO_3$ (1.0 g, 7.23 mmol), and stirred for 15 min., then hydroxylamine-*O*-sulfonic acid (0.50 g, 4.42 mmol) was added to the resulting solution and stirred for 4 h at room temperature. After completion of the reaction, the solution was acidified by acetic acid, extracted with $CHCl_3$, dried over Na_2SO_4, filtered to give **5** as a white fluffy powder; mp 175-177 °C; ^{1}H-NMR: (500 MHz, DMSO-d_6): δ = 8.54 (s, 1H, OH), 8.12 (t, *J* = 7.7 Hz, 2H), 7.86 (d, *J* = 8.7 Hz, 1H), 7.84-7.82 (m, 2H), 4.31 (q, *J* = 7.0 Hz, 2H), 1.33 (t, *J* = 7.0 Hz, 3H); ^{13}C NMR (175 MHz, DMSO-d_6): δ = 166.9, 162.5, 134.5, 128.9, 128.7, 127.9, 127.8, 127.5, 124.5, 121.5, 121.3, 105.4, 64.2, 61.6, 60.3, 14.3; HR-MS (TOFEI) calcd for $C_{16}H_{14}N_2O_3S$: (314.0725); found (314.0736).

Ethyl 7-hydroxy-8-oxo-8,9-dihydrobenzo[*h*]thieno[2,3-*b*]quinoline-9-carboxylate (6a):

Sodium ethoxide (0.29 g, 4.3 mmol) was added to the solution of **3a** (1.49g, 3.89 mmol) in EtOH (50 mL) and refluxed for 4 h. After completion of the reaction, EtOH was removed, added H_2O (50 mL), and acidified by AcOH, separated solid was collected and dried as a yellowish powder; mp >250 °C; ^{1}H-NMR: (500 MHz, DMSO-d_6): δ = 13.37 (s, 1H, OH), 8.74 – 8.69 (m, 1H), 8.16 (d, *J* = 8.8 Hz, 1H), 8.11 (dd, *J* = 6.8, 2.3 Hz, 1H), 7.87 – 7.83 (m, 2H), 7.84 – 7.79 (m, 1H), 4.29 (q, *J* = 7.0 Hz, 2H), 3.34 (s, 1H), 1.07 (t, *J* = 7.0 Hz, 3H).^{13}C NMR (175 MHz, DMSO-d_6): δ = 175.3, 161.8, 157.0, 156.9, 150.5, 138.4, 134.9, 129.3, 128.8, 127.2, 123.8, 122.8, 120.5, 118.4, 114.3, 95.3, 60.2, 14.4; HR-MS (TOFEI) calcd. for $C_{18}H_{13}NO_4S$ (339.0565); found (339.0560).

7-hydroxybenzo[*h*][1,2]thiazolo[5,4-*b*]quinolin-8(9*H*)-one (7):

Sodium ethoxide (0.20 g, 3.0 mmol) was added to the solution of **5** (0.84 g, 2.7 mmol) in EtOH (50 mL) and refluxed for 4 h. After completion of the reaction, EtOH was removed, added H_2O (50 mL), and acidified by AcOH, separated solid was collected and dried as a light brown powder; mp>250 °C; ^{1}H-NMR: (500 MHz, DMSO-d_6): δ = 13.13 (s, 1H, OH), 8.61 (d, J = 7.8 Hz, 1H), 8.21 (d, J = 8.73 Hz, 1H), 8.14-8.11 (m, 1H), 7.85-7.79 (m, 3H); ^{13}C NMR (175 MHz, DMSO-d_6): δ = 172.9, 165.0, 162.2, 137.7, 134.9, 129.0, 128.6, 127.1, 125.2, 123.5, 123.0, 121.4, 120.2, 107.4; HR-MS (TOFEI) calcd. for $C_{14}H_8N_2O_2S$ (268.0306); found (268.0310).

7-hydroxy-8-oxo-8,9-dihydrobenzo[*h*]thieno[2,3-*b*]quinoline-9-carboxylic acid (6b):

A mixture of ester (**6a**) (0.339 g, 1.0 mmol) and NaOH (0.088 g, 2.2 mmol) in H_2O (20 mL) was stirred at 100 °C for 4 h. After being cooled, the reaction mixture was neutralized with 1 M HCl, extracted with CH_2Cl_2 and dried. Evaporation followed by crystallization from EtOH afforded the acid as an orange red powder; mp>250 °C; ^{1}H-NMR: (500 MHz, DMSO-d_6): δ = 13.10 (s,1H, OH), 12.95 (s, 1H, OH), 12.09 (s, 1H, OH), 8.91 (d, J = 8.4Hz, 1H), 8.05 (d, J = 7.9 Hz, 1H), 7.96 (d, J = 8.8 Hz, 1H), 7.80 (t, J = 7.4 Hz, 1H), 7.76-7.68 (m, 2H); ^{13}C NMR (175 MHz, DMSO-d_6): δ = 166.2, 159.8, 158.2, 156.3, 149.4, 140.4, 133.9, 128.2, 127.3, 127.2, 123.5, 122.3, 120.4, 119.2, 115.3, 98.2; TOF-MS EI: calcd. for $C_{16}H_9NO_4S$ (311.16); found (311.16).

Ethyl 7-methoxy-8-oxo-8,9-dihydrobenzo[*h*]thieno[2,3-*b*]quinoline-9-carboxylate (6c):

To a mixture of **6a** (0.339 g,1 mmol) and K_2CO_3 (0.386 g, 2.8 mmol) in dry DMF (25 mL) under nitrogen atmosphere was added dimethyl sulfate (0.126 g, 1 mmol) along with

KI (catalytic amount). The reaction mixture was heated at 70 °C for 24 h, and then poured into ice-H_2O. The resulting alkylated derivative was collected by filtration and recrystalized from hexane: $CHCl_3$ (1:3) to afford a yellowish powder; mp charring ≥ 280 °C; ^{1}H-NMR: (500 MHz, DMSO-d_6): δ = 9.15-9.07 (m, 1H), 8.11 (d, J = 9.0 Hz, 1H), 7.98 (dd, J = 2.7, 6.2 Hz, 1H), 7.75 (d, J = 9.1 Hz, 1H), 7.74-7.69 (m, 2H), 4.35 (s, 3H), 4.10 (q, J = 7.0 Hz, 2H), 1.25 (t, J = 7.0 Hz, 3H); ^{13}C NMR (175 MHz, DMSO-d_6): δ = 176.3, 160.8, 158.0, 155.9, 150.5, 139.4, 131.9, 128.3, 128.8, 125.2, 123.8, 122.8, 120.5, 118.4, 117.3, 95.3, 60.2, 47.2, 14.3; HR-MS (TOFEI) calcd for $C_{19}H_{15}NO_4S$ (353.0722); found (353.0731).

Ethyl 7-ethoxy-8-oxo-8,9-dihydrobenzo[*h*]thieno[2,3-*b*]quinoline-9-carboxylate (6d):

Utilizing the same alkylation procedure as applied for preparation of **6c** using diethyl sulfate (0.154 g, 1mmol); yellow powder; mp 170-172 °C; ^{1}H-NMR: (500 MHz, $CDCl_3$): δ = 10.94 (s, 1H, OH), 9.35-9.28 (m, 1H), 8.16 (d, J = 9.1 Hz, 1H), 7.88 (dt, J = 3.2 Hz, 1H), 7.77-7.69 (m, 3H), 4.50 (q, J = 7.0 Hz, 2H), 4.46 (q, J = 7.1 Hz, 2H), 1.58 (t, J = 7.0 Hz, 3H), 1.45 (t, J = 7.1 Hz, 3H); ^{13}C NMR (175 MHz, $CDCl_3$): δ = 168.1, 161.1, 160.5, 157.9, 150.4, 134.8, 130.9, 129.6, 128.1, 127.5, 126.9, 125.8, 120.2, 119.1, 116.4, 100.4, 74.2, 62.1, 16.1, 14.7; HR-MS (TOFEI): calcd for $C_{20}H_{17}NO_4S$ (367.0871); found (367.0872).

Ethyl 7,8-diethoxybenzo[*h*]thieno[2,3-*b*]quinoline-9-carboxylate (6e):

Utilizing the same alkylation procedure as applied for preparation of **6d** using diethyl sulfate (0.431 g, 2.8 mmol) orange powder; m p 120-122 °C; ^{1} H-NMR: (500 MHz, $CDCl_3$): δ = 9.41-9.29 (m, 1H), 8.13 (d, J = 9.1 Hz, 1H), 7.94-7.87 (m, 1H), 7.80-7.69

(m, 3H), 4.44 (q, J = 7.0 Hz, 4H), 4.39 (q, J = 7.0 Hz, 2H), 1.56 (t, J = 6.6 Hz, 6H), 1.45 (t, J = 7.1 Hz, 3H); ^{13}C NMR (175 MHz, $CDCl_3$): δ = 162.2, 160.2, 159.9, 153.3, 149.8, 134.5, 130.5, 129.0, 128.1, 128.0, 127.5, 125.2, 119.4, 119.2, 118.8, 116.6, 73.6, 72.2, 61.3, 15.5, 15.3, 14.2; HR-MS (TOFEI) calcd for $C_{22}H_{21}NO_4S$ (395.1191); found (395.1195).

Ethyl 8,9-dihydro-7,10-dioxa-12-thia-13-azaazuleno[8,1-*ab*]phenanthrene-11-carboxylate (6f):

This compound was prepared using the same procedure as that used for the synthesis of **6e** using 1,2-dibromoethane to afford a yellow crystalline product; mp 250-252 °C; ^{1}H-NMR: (500 MHz, $CDCl_3$): δ = 9.35-9.28 (m, 1H), 8.14 (d, J = 9.1 Hz, 1H), 7.93-7.87 (m, 1H), 7.74 (dt, J = 5.9, 9.7 Hz, 3H), 4.96-4.92 (m, 2H), 4.84-4.79 (m, 2H), 4.42 (q, J = 7.1 Hz, 2H), 1.43 (t, J = 7.1 Hz, 3H); ^{13}C NMR (175 MHz, $CDCl_3$): δ = 162.1, 159.5, 158.2, 152.8, 148.3, 134.3, 130.1, 129.1, 127.6, 127.0, 125.8, 125.4, 119.4, 113.8, 111.4, 104.8, 73.6, 72.2, 61.1, 14.4; HR-MS (TOFEI) calcd for $C_{20}H_{15}NO_4S$ (365.0722); found (365.0727).

9-Cyano-7-hydroxy-8-oxo-8,9-dihydrobenzo[*h*]thieno[2,3-*b*]quinoline (8):

Sodium ethoxide (0.20 g, 3 mmol) was added to the solution of **3k** (0.91 g, 2.7 mmol) in EtOH (50 mL) and refluxed for 4 h. After completion of the reaction, EtOH was removed, added H_2O (50 mL), and acidified by AcOH; the separated solid was collected and dried as a brown powder; mp>250 °C; ^{1}H-NMR: (500 MHz, DMSO-d_6): δ = 13.39 (s, OH), 8.66 (s, 1H), 8.16 (d, J = 8.7 Hz, 1H), 8.10 (d, J = 9.1Hz, 1H), 7.83 (dd, J = 6.8, 14.0 Hz, 4H); ^{13}C NMR (175 MHz, DMSO-d_6): δ = 173.4, 165.2, 167.0, 162.5, 140.0,

138.7, 135.2, 130.0, 129.4, 127.4, 125.1, 124.5, 122.0, 121.3, 120.1, 105.3; HR-MS (TOFEI) calcd. for $C_{16}H_8N_2O_2S$ (292.3019); found (292.3017).

9-Acetyl-9H-benzo[*h*]pyrazolo[*3',4':4,5*]thieno[2,3-*b*]quinoline-7,10-diyl diacetate (9):

Compound **6a** (0.50 g, 1.5 mmol) was allowed to react with hydrazine hydrate (10.1 g, 201 mmol) by refluxing in EtOH for 3 h, then cooling. After evaporation of the solvent, the remaining mixture was refluxed with Ac_2O (5 mL) for 4 h. The reaction mixture was then cooled and was diluted with water (30 mL) and stirred for 30 min. The precipitate was collected, dried and recrystalized from THF to yield compound **9** as yellow crystals; mp ≥250 °C; ^{1}H-NMR: (500 MHz, $CDCl_3$): δ = 9.32 (dd, *J* = 9.7 , 16.2 Hz, 1H), 7.94 (dd, *J* = 4.2, 8.8 Hz, 2H), 7.86 (d, *J* = 9.0 Hz, 1H), 7.81-7.70 (m, 2H), 2.77 (s, 3H), 2.64 (s, 3H), 2.64 (s, 3H); ^{13}C NMR: (175 MHz, $CDCl_3$): δ = 169.6, 167.4, 166.9, 166.8, 150.5, 149.4, 149.1, 139.7, 134.1, 130.4, 129.3, 127.9, 127.9, 127.6, 125.3, 118.2, 117.9, 113.1, 108.8, 23.4, 20.8, 20.6; HR-MS (TOFEI): calcd for $C_{20}H_{13}N_3O_4S$ (391.0627); found (391.0638) (-$COCH_3$).

Diethyl [4-(2-ethoxy-2-oxoethyl)-3-(naphthalen-1-yl)-1,3-thiazol-2(*3H*)-ylidene]propanedioate (10):

To a stirred solution of compound **1a** (0.367 g, 1 mmol) in THF (50 mL) was added chloroethylacetoacetate (0.164 g, 1 mmol) dropwise at 0 °C and stirring was continued for an extra 12 h at room temperature. The solvent was evaporated, and the resulting oil was extracted with $CHCl_3$ and dried over Na_2SO_4. The organic layer was evaporated by rotary evaporator to give yellow oil. The obtained oil was heated at 170-180 °C in an oil

bath under vacuo for 10 min. The resulting oil was solidified then washed with ether affording compound **10** as yellow crystals; mp 140-142 °C; ^{1}H-NMR: (500 MHz, $CDCl_3$): δ = 7.95 (dt, *J* = 1.14, 1.14, 8.02 Hz, 1H), 7.92-7.89 (m, 1H), 7.55 (m, 2H), 7.51 (d, *J* = 7.85 Hz, 1H), 7.49 (d, *J* = 1.54 Hz, 1H), 7.43 (m, 1H), 6.59 (d, *J* = 0.97 Hz, 1H), 3.81 (m, 2H), 3.71-3.60 (m, 2H), 3.38 (m, 2H), 3.12 (dd, *J* = 0.91, 17.24 Hz, 1H), 2.9 (d, *J* = 1.05, 17.28 Hz, 1H), 1.02 (t, *J* = 7.16 Hz, 3H), 0.89 (t, *J* = 7.15 Hz, 6H); ^{13}C NMR: (175 MHz, $CDCl_3$): δ = 168.1, 166.2, 163.1, 134.3, 134.1, 132.5, 130.6, 129.1, 128.4, 128.1, 127.0, 125.1, 122.4, 106.7, 90.0, 61.3, 60.6, 60.0, 38.1, 34.0, 30.9, 14.5, 13.8, 13.8; HR-MS (TOFEI) calcd for $C_{24}H_{25}NO_6S$ (455.1403); found (455.1398).

1*H*-3-thia-11c-azaazuleno[*1,8,7,6-cdef*]phenanthrene-1,6(*5H*)-dione(11):

The appropriate ester (**10**) (0.455 g, 1 mmol) was added to PPA (2.27 g, 5 parts by weight) preheated to 150 °C, and the mixture was stirred for 3 h before being cooled to room temperature, H_2O was added, the solution was made basic with conc. NH_4OH, and extracted several times with CH_2Cl_2. The combined extracts were dried ($MgSO_4$), filtered and evaporated *in vacuo* to yield essentially pure brownish black crystals; mp 200-202 °C; ^{1}H-NMR: (500 MHz, CDCl3): δ = 8.80 (d, *J* = 8.7 Hz, 1H), 8.28 (dd, *J* = 6.9, 5.4 Hz, 2H), 8.09 (d, *J* = 8.7 Hz, 1H), 7.79-7.72 (m, 1H), 6.93 (s, 1H), 6.79 (s, 1H), 4.09 (d, *J* = 14.8 Hz, 2H). ^{13}C NMR: (175 MHz, $CDCl_3$): δ = 172.6, 157.0, 136.3, 135.9, 135.7, 133.0, 132.1, 130.4, 128.3, 127.4, 126.6, 124.8, 122.5, 115.6, 106.1, 105.6, 44.8; HR-MS (TOFEI) calcd for $C_{17}H_9NO_2S$ (291.0354); found (291.0349).

References

1. Lesher, G. Y, Froelich, E. J., Gruett, M. D., Balley, J. H., & Brundage, R. P. (1962). 1,8-Naphthyridine derivatives. A new class of chemotherapeutic agents. *J. Med. Pharm. Chem., 91*, 1063-5.
2. Mugnaini, C., Pasquini, S., & Corelli, F. (2009). The 4-quinolone-3-carboxylic acid motif as a multivalent scaffold in medicinal chemistry. *Curr. Med. Chem., 16* (14), 1746-1767.
3. Srivastava, S. K., Jha, A., Agarwal, S. K., Mukherjee, R., & Burman, A. C. (2007). Synthesis and structure-activity relationships of potent antitumor active quinoline and naphthyridine derivatives. *Anticancer Agents Med. Chem., 7* (6), 685-709.
4. Kerry, M. A., Boyd, G. W., Mackay, S. P., Meth-Cohn, O., & Platt, L. (1999). The synthesis of benzo[*h*]quinolines as topoisomerase inhibitors. *J. Chem. Soc., Perkin Trans.1.* (16), 2315-2321.
5. Hosomi, J., Asahina, Y., & Suzue, S. (1989). *PCT Int. Appl. WO 89 12055.* Preparation of thiazoloquinolonecarboxylic acid derivatives and their pharmaceutical compositions as antitumor agents (*Chem.. Abstr.* 1990, 113, 6328m).
6. Sissi, C., & Palumbo, M. (2003). The quinolone family: From antibacterial to anticancer agents. *Curr. Med. Chem. Anti-Canc Agents, 3* (6), 439-450.

7. **a**) Amoozgar, Z., & Daneshtalab, M. (2007). Regioselective N_1-alkylation of 4-quinoline- 3-carboxylic acid esters using modified Mitsnobu reaction. *21st International Congress for Heterocyclic Chemistry (ICHC-21)* Sydney, Australia; **b**) R .Garlapati and M. Daneshtalab. Design, Synthesis and Biological Evaluation of Thieno[2,3-b]quinolones as Topoisomerase Poisons. 22nd *International Congress For Heterocyclic Chemistry (ICHC-21),* August 2-7th. Abstract no. PO-43.
8. Chipa, K., Yamamoto, K., Miyamoto, K., Nakano, J., Matsumoto, J., Nakamura, S., Nakada, K., (Dainippon Pharmaceutical Co., Ltd., Japan). Jpn. Kokai. Tokkyo Koho 1991, 11pp. CODEN: JKXXAF *JP 03223289 A.*
9. Robinson, M. J., Martin, B. A., & Gootz, T. D. (1991). Effects of quinolone derivatives on eukaryotic topoisomerase II. A novel mechanism for enhancement of enzyme-mediated DNA cleavage. *J. Biol. Chem., 266*, 14585-92.
10. Robinson, M. J., Martin, B. A., Gootz, T. D., McGuirk, P. R., & Osheroff, N. (1992). Effects of novel fluoroquinolones on the catalytic activities of eukaryotic topoisomerase II: Influence of the C-8 fluorine group. *Antimicrob. Agents Chemother., 36* (4), 751-6.

11. Froelich-Ammon, S. J., McGuirk, P. R., Gootz, T. D., & Jefson, M. R. (1993). Novel 1-8-bridged chiral quinolones with activity against topoisomerase II: Stereospecificity of the eukaryotic enzyme. *Ibid., 37* (4), 646.

12. Elsea, S. H., McGuirk, P. R., Gootz, T. D., Moynihan, M., & Osheroff, N. (1993). Drug features that contribute to the activity of quinolones against mammalian topoisomerase II and cultured cells: Correlation between enhancement of enzyme-mediated DNA cleavage *in vitro* and cytotoxic potential. *Ibid., 37* (10), 2179-86.

13. Kohlbrenner, W. E., Wideburg, N., Weigl, D., Saldivar, A., & Chu, D. T. (1992). Induction of calf thymus topoisomerase II-mediated DNA breakage by the antibacterial isothiazoloquinolones A-65281 and A-65282. *Ibid., 36* (1), 81-6.

14. Kennard, O., & Hunter, W. N., (1991). Single-crystal X-ray diffraction studies of oligonucleotides and oligonucleotide-drug complexes. *Angew. Chem. Int. Ed. Engl.*, 30 (10), 1254-1277.

15. Sánchez, I., Reches, R., Caignard, D. H., Renard, P., & Pujol, M. D. (2006). Synthesis and biological evaluation of modified acridines: The effect of N- and O- substituent in the nitrogenated ring on antitumor activity. *Eur. J. Med. Chem., 41* (3), 340-52.

16. Shen, L. L., Mitscher, L. A., Sharma, P. N., O'Donnell, T. J., Chu, D. W., Cooper CS, et al. (1989). Mechanism of inhibition of DNA gyrase by quinolone antibacterials: A cooperative drug--DNA binding model. *Biochemistry, 28* (9), 3886-94.

17. Chu, D. T., & Fernandes, P. B. (1989). Structure-activity relationships of the fluoroquinolones. *Antimicrob. Agents Chemother., 33* (2), 131-5.

18. Chu, D. T., Fernandes, P. B., Claiborne, A. K., Shen, L., & Pernet, A. G. (1988). Structure-activity relationships in quinolone antibacterials: Design, synthesis and biological activities of novel isothiazoloquinolones. *Drugs Exp. Clin. Res., 14* (6), 379-83.

19. Komoriya, K., Nagata, I., Osada,Y., Kondo, S., *JP 90-183990*, 1992; *(Chem. Abstr*. 1992, **117**, 104253).

20. Romeo, G., Bousquet, E., Pappalardo, M. S., Ronsisvalle, G., Oliveri, S., & Cammarata, E. (1988). Synthesis and antifungal activity of new derivatives of 5-(4-halobenzoyl)-4-amino-3-(2-dialkylaminoethylthio)thieno [2,3-c] and [3,2-d] isothiazole. Farmaco. [Sci.] 43 (5), 457-67.

21. Nagano, N., Nakano, K., Shibanuma, T., Murakami, Y., & Hara, R. (1987). Studies on beta-lactam antibiotics. I. synthesis and in vitro anti-pseudomonal activity of 3-isothiazole-cephalosporin derivatives. J. Antibiot. (Tokyo), 40 (2), 173-81.

22. a) Cutrì, C. C., Garozzo, A., Siracusa, M. A., Castro, A., Tempera, G., Sarvà, M. C., et al. (2002). Synthesis of new 3-methylthio-5-aryl-4-isothiazolecarbonitriles with broad antiviral spectrum. Antiviral Res., 55 (2), 357-68; b) Inglot, A.D.; Machon, Z.; Wolna, E.; Wilimowski, M. & Prandota, J. (1973). New isothiazole derivatives. II. Cytotoxicity and antiviral activity in tissue cultures. Arch. Immunol. Ther. Exp., 21, 891.

23. Aebi, J.; Ackermann, J.; Dehmlow, H.; Maerki, H.P., & Morand, O. (2002). PCT Int. Appl. WO 036584, Preparation of cholesterol lowering benzo[b]thiophenyl and benzo[d]isothiazolyl alkylamines. (Chem. Abstr., 136, 369719r)

24. a) Kitagawa, Y.; Ishikawa, K.; Sawada, H.; Araki, Y.; Shigyo, T. & Aszmann, L. (2001). PCT Int. Appl. WO 077090. Preparation of isothiazole derivatives as microbicides (Chem. Abstr., 2001, 135, 318501).; b) Chemla, P.; Maetzke, T. & Ertl, P. (1999) PCT Int. Appl. WO 9932464. Preparation of thiazole, isothiazole, and thiadiazole derivatives having microbicidal and plant immunizing activities. (Chem. Abstr., **1**999, **1**31, 58832).

25. a) Heil, M.; Bretschneider, T.; Kleefeld, G.; Erdelen, C.; Turberg, A. & Mencke, N. (1999) Ger. Offen. DE 19736545. Acylated 5-aminoisothiazoles as insecticides, acaricides and fungicides. (Chem. Abstr., 1999, 130, 182458). b) Cetusic, J. & Rieder, B. J. (2002) PCT Int. Appl. WO 0224691. Preparation of

thiazole derivatives of 2-methoxyimino-2-(pyridinyloxymethyl)-phenyl-acetamides useful as fungicides (Chem. Abstr., 2002, 136, 279447).; (c) Assmann, L., Kitagawa, Y., Ishikawa, K., Sawada, H., Araki, Y., & Shigyo T. (2001) PCT Int. Appl, WO 0129014. Preparation of isothiazole-5-carboxylic esters as agrochemical microbicides. (Chem. Abstr., 2001, 134, 311204); (d) Andersch, W., & Wachendorff-Neumann, U. (2000) PCT Int. Appl. WO 035286. Synergistic mixtures with insecticidal and fungicidal properties. (Chem. Abstr., 2000, 133, 39470).

26. Shimizu, M., Kikumoto, H., Konakahara, T., Gama, Y., & Shibuya, I. (1999). A facile synthesis of 1,2-benzisothiazolin-3-ones from thiosalicylates. Heterocycles, 51 (12), 3005-12.
27. Shimizu, M., Takeda, A., Fukazawa, H., Abe, Y., & Shibuya, I. (2003). Synthesis of 1,2-benzisothiazolin-3-one by transamination of sulfenamides. Ibid., 60 (8), 1855-64.
28. Chiyoda, T., Iida, K., Takatori, K., & Kajiwara, M. (2000). Convenient synthesis of 1,2-benzisothiazol-3(2H)-ones by cyclization reaction of acyl azide. Synlett., (10), 1427-8.
29. Choi, J. H., Choi, E. B., & Pak, C. S. (2003). Isothiazole ring formation with substituted 2-alkylthio-3-acyl-4-quinolinone using O-(mesitylenesulfonyl) hydroxylamine (MSH). Synlett., 14 (2), 166-172.

30. Cecchetti, V., Fravolini, A., Fringuelli, R., & Schiaffella, F. (1993). 4H-1-benzothiopyran-4-one-3-carboxylic acids and 3,4-dihydro-2H-isothiazolo[5,4-b]benzothiopyran-3,4-diones as quinolone antibacterial analogs. J. Heterocycl. Chem., 30 (4), 1143-8.

31. a) Dieter, R. K., & Chang, H. J. (1989). Synthesis of isoxazoles and isothiazoles from .alpha.-oxo ketene dithioacetals. J. Org. Chem., 54 (5), 1088-1092; b) Laaman, S. M., Meth-Cohn, O., & Rees, C. W. (1999). The ready conversion of 2,5-disubstituted furans into isothiazoles. Synthesis, (5), 757-9.

32. Rahman, L. K. A., & Scrowston, R. M. (1983). 7-substituted benzo[b]thiophenes and 1,2-benzisothiazoles. part 1. hydroxy- or methoxy-derivatives. J. Chem. Soc., Perkin Trans.1, 2973-77.

33. Gaurav, A., Gautam, V., & Singh, R. (2010). An overview on synthetic methodologies and biological activities of pyrazoloquinolines. Mini Rev. Med.Chem., 10 (13), 1194-210.

34. a) Hayakawa, I., Hiramitsu, T., & Tanaka, Y. (1984). Synthesis and antibacterial activities of substituted 7-oxo-2,3-dihydro-7H-pyrido[1,2,3-de][1,4]benzoxazine-6-carboxyl ic acids. Chem. Pharm. Bull., 32(12), 4907-13.; b) Sato, K., Matsuura, Y., Inoue, M., Une, T., Osada, Y., Ogawa, H., et al. (1982). In vitro and in vivo activity of DL-8280, a new oxazine derivative. Antimicrob. Agents Chemother., 22 (4), 548-53.

35. a) Taguchi, M., Kondo, H., Inoue, Y., Kawahata, Y., Jinbo, Y., Sakamoto, F., et al. (1992). Synthesis and antibacterial activity of new tetracyclic quinolone antibacterials. J. Med. Chem., 35 (1), 94-9; b) Kotera, Y., & Mitsuhashi, S. (1989). In vitro and in vivo antibacterial activities of KB-5246, a new tetracyclic quinolone. Antimicrob. Agents Chemother., 33 (11), 1896-900.

36. Meyer, B. N., Ferrigni, N. R., Putnam, J. E., Jacobsen, L. B., Nichols, D. E., & McLaughlin, J. L. (1982). Brine shrimp: A convenient general bioassay for active plant constituents. Planta Medica, 45 (1), 31-4.

37. Mosmann, T. (1983). Rapid colorimetric assay for cellular growth and survival: Application to proliferation and cytotoxicity assays. J. Immunol. Methods, 65 (1-2), 1-2.

38. Dua, P., & Gude, R. (2006). Antiproliferative and antiproteolytic activity of pentoxifylline in cultures of B16F10 melanoma cells. Cancer Chemother. Pharmacol., 58 (2), 195-202.

39. Bikadi, Z., & Eszter Hazai, E. (2009). Application of the PM6 semi-empirical method to modeling proteins enhances docking accuracy of AutoDock. J. Chem. Inf., 1 (1), 15, doi:10.1186/1758-2946-1-15.

40. Halgren, T. A. (1996). Merck molecular force field. I. basis, form, scope, parameterization, and performance of MMFF94. J. Comput. Chem., 17 (5/6), 490-519.

41. Morris, G. M., Goodsell, D. S., Halliday, R. S., Huey, R., Hart, W. E., Belew, R. K., et al. (1998). Automated docking using a Lamarckian genetic algorithm and an empirical binding free energy function. Ibid., 19 (14), 1639-1662.

42. Solis, F. J., & Wets, R. J. (1981). Minimization by random search techniques. Math. Oper. Res., 6 (1), 19-30.

43. Classen, S., Olland, S., & Berger, J. M. (2003). Structure of the topoisomerase II ATPase region and its mechanism of inhibition by the chemotherapeutic agent ICRF-187. Proc. Nat. Acad. Sci. USA, 100 (19), 16.

44. Furet, P., Schoepfer, J., Radimerski, T., & Chene, P. (2009). Discovery of a new class of catalytic topoisomerase II inhibitors targeting the ATP-binding site by structure based design. part I. Bioorg. Med. Chem. Lett., 19 (15), 4014-4017.

CHAPTER 4

Synthesis of Novel 4-Oxo-1,4-Dihydro Benzo[*h*][1,3]Thiazeto[3,2-*a*]quinoline Carboxylic Acids Via Oxidative Cyclization of the Corresponding 2-Mercaptoquinoline Precursors; Proof of the Mechanism

Abeer Ahmed[a], Louise N. Dawe[b], Peter Warburton[b] and Mohsen Daneshtalab[a]*

Heterocycles, 85, 2012, DOI: 10.3987/COM-11-12375 (*in press, available on-line)*

[a]School of Pharmacy, Memorial University of Newfoundland, St. John's, Newfoundland and Labrador, Canada A1B 3V6. Fax: +1(709)-777-7044; E-mail: mohsen@mun.ca

[b]Department of Chemistry, Memorial University of Newfoundland, St. John's, Newfoundland and Labrador, Canada A1B 3X7.

Preface

The developed manuscript for this chapter provides a detailed synthesis of the novel benzo[*h*]thiazeto quinoline system via the oxidative cyclization mechanism. A version of this manuscript has been published in the *Heterocycles*.

Abstract

The first synthesis of a series of 4-oxo-1,4-dihydro benzo[*h*][1,3]thiazeto[3,2-*a*]quinoline carboxylic acids and their esters *via* oxidative cyclization of ethyl 2-((2-ethoxy-2-oxoethyl)thio)-4-hydroxybenzo[*h*]quinoline-3-carboxylate in the presence of a vicinal dihalolakane, KI, and K_2CO_3 is described. Structures of the synthesized compounds were characterized by spectrometric and X-ray crystallographic analyses.

Keywords: Thiazetoquinolines, *vic*-dihaloalkanes, X-ray crystallography, pseudohalide (IBr).

4.1 Introduction

4-Oxo-1,4-dihydroquinoline-3-carboxylic acid derivatives (quinolones) have dominated the antibacterial market for decades. Quinolones have a unique mechanism of action: they inhibit DNA synthesis by promoting cleavage of bacterial DNA in the DNA-enzyme complexes of DNA gyrase (the main target in Gram-negative bacteria) and type IV topoisomerase (the main target in Gram-positive bacteria), resulting in rapid bacterial death [1-3].

Inhibitory activity of quinolones against human topoisomerase-2 has been reported by Kyorin-Kyowa-Hakko researchers *via* introduction of a series of tricyclic thiazoloquinolones that exhibited impressive anticancer activity [4].

In continuation of our ongoing research towards the discovery of novel polycyclic quinoline-based antineoplastic agents using conventional synthetic procedures, we were able to isolate and identify, unexpectedly, a 4-oxo-benzo[*h*]thiazetoquinoline derivative (**4a**). The structure of this novel molecule was elucidated by ^{1}H-NMR, ^{13}C-NMR, HR-MS, and X-ray crystallography. Despite the availability of several published works on the syntheses and bioactivity of angular 4-oxo-thiazolo[3,2-*a*]quinoline-3-carboxylic acid derivatives,[4-9] there are limited reports on the synthesis of 4-oxo-thiazeto[3,2-*a*]quinolines and there is no reported synthesis of 4-oxo-benzo[*h*]thiazeto[3,2-*a*]quinoline derivatives.

Prulifloxacin [10] **Figure 4-1** (**A**) is a representative of 4-oxo-thiazetoquinoline antibiotics. It is a prodrug which is metabolized in the body to the active compound ulifloxacin [11]. It was developed over two decades ago by Nippon Shinyaku Co. and was patented in Japan in 1987 and in the United States in 1989 [12-14].

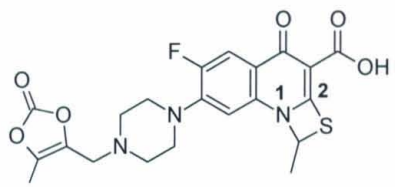

A

Figure 4-1: Structure of Prulifloxacin (**A**).

In the same context, Ito *et al.* [15] succeeded in the synthesis of 4-oxo-1,4-dihydro-[1,3]thiazeto[3,2-*a*]quinoline-3-carboxylic acid derivative (**B**) as an antibacterial, antitumor, and anti–AIDS agent.

In 1999, Matsuoka *et al.*, reported the synthesis of 6-fluoro-1-methyl-4-oxo-7-(1-piperazinyl)-4*H*-[1,3]thiazeto[3,2-*a*]quinoline-3-carboxylic acid (**C**, NM394) which showed excellent *in vitro* antibacterial activity [16a].

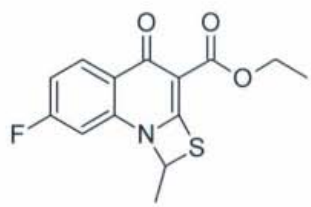

B

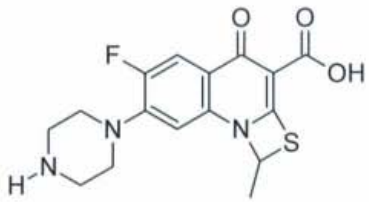

C

Figure 4-2: Structure of Compounds (**B**) and (**C**).

The rationale behind the prulifloxacin synthesis was to connect the quinoline N-1 and C-2 positions *via* a bridge in order to minimize the steric hindrance of the C-2 substituent toward the C-3 carboxyl group, and which can lead to active antibacterial agents [16b].

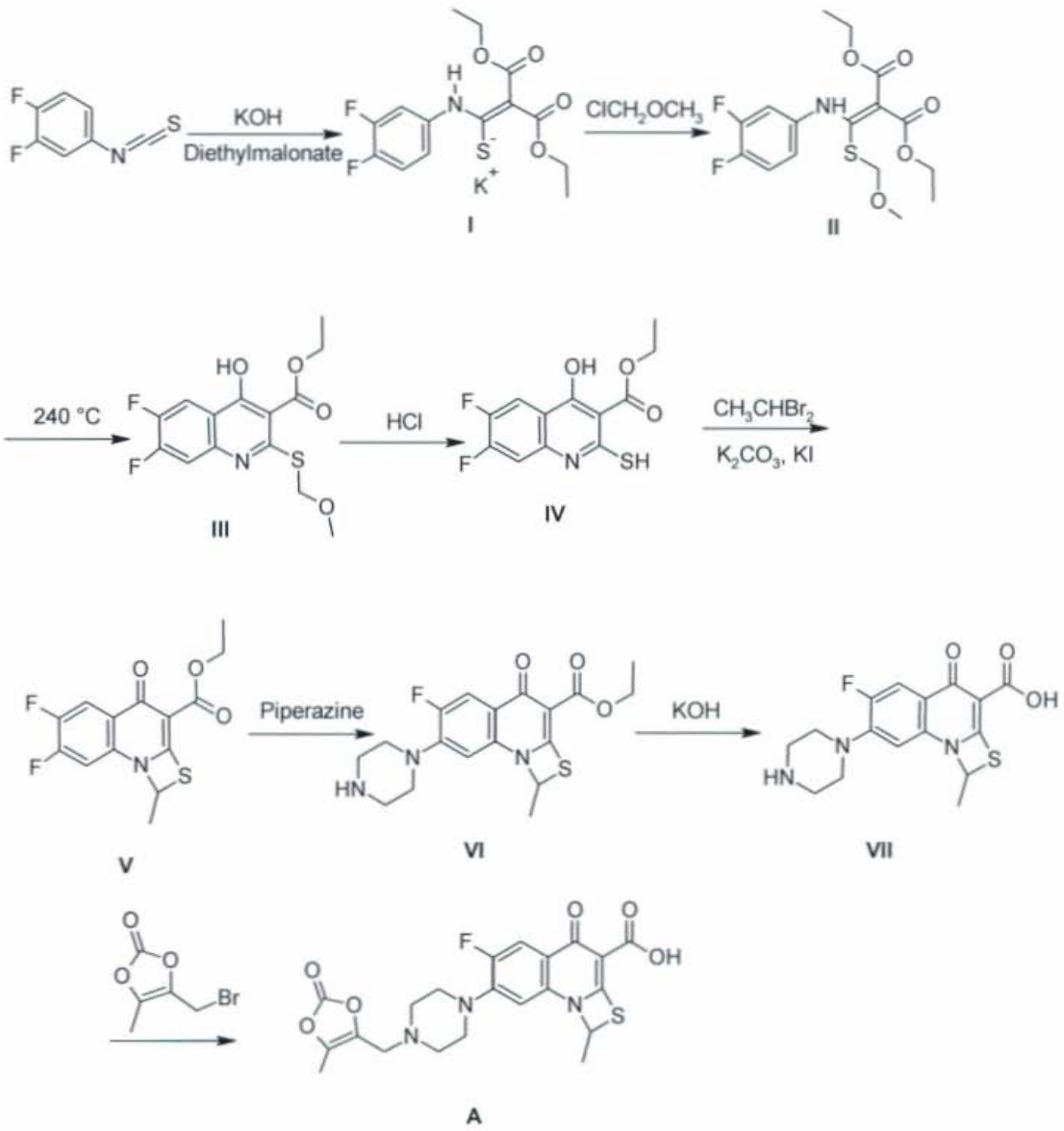

Figure 4-3: Prulifloxacin synthesis schematic

(adopted from *J. Med. Chem.* 1992, 35, 4727).

In order to achieve this goal, the authors used appropriately-substituted phenylisothiocyanate which, upon reaction with diethylmalonate and chloromethylethyl

ether, followed by thermal cyclization and deprotection of the sulfide, afforded the corresponding ethyl 2-mercapto-4 (1*H*)-oxo-quinoline-3-carboxylic acid (IV). Reaction of this compound with an alkyl- or arylsubstititued *gem*-dibromomethane derivative in the presence of K_2CO_3 and KI gave rise to the alkyl/aryl substituted 4-oxo-thiazeto[3,2-*a*]quinoline-3-carboxylic acid as depicted in **Figure 4-1**. The disadvantage of using this methodology is the limitation in the nature of substituents on the carbon connecting –S– and –N– atoms in the thiazeto ring, which originates from the corresponding *gem*-dibromomethane precursors.

In the synthesis described in this chapter (**Scheme 4-1**), the 4-oxo-thiazetoquinoline nucleus is formed *via* reaction of the carbanion at the alkylsulfide group of the C-2 position of the quinoline ring with a pseudohalogen (IBr), formed *via* reaction of iodide anion with the *vic*-dihaloalkane, or a halogen (I_2), followed by nucleophilic attack of the N-1 on halogenated carbon and the departure of halogen. The role of the vicinal dihaloalkane in this process is the provision of a pseudohalogen (such as IBr) without direct interaction with the quinoline system. This synthetic procedure produced diverse 4-oxo-thiazetoquinoline-3-carboxylic acid derivatives possessing electron-withdrawing groups at the C-1 position.

4.2 Chemistry

The synthesis of 4-oxo-benzo[*h*]thiazetoquinoline carboxylic acid derivatives is outlined in **Scheme 4-1**.

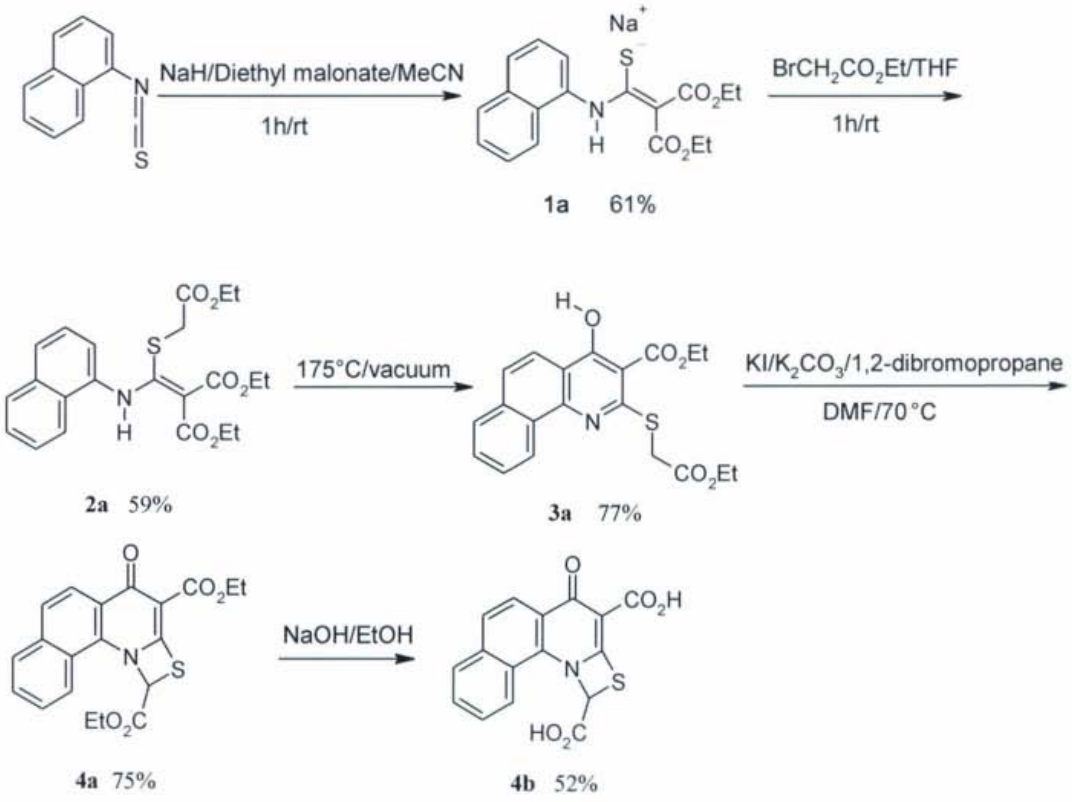

Scheme 4-1: Synthesis of 4-oxo-benzo[*h*]thiazetoquinoline carboxylic acid derivatives.

Naphthylisothiocyanate was allowed to react with diethylmalonate in the presence of sodium hydride to yield the salt **1a** which was further reacted with ethyl bromoacetate to afford **2a**. Thermal cyclization of **2a**, under vacuum, yielded Compound **3a**. This compound was later reacted with 1,2-dibromopropane in the presence of KI and K_2CO_3 to obtain **4a**, which was further saponified to afford **4b**.

Synthesis of Compound **4c** was then carried out in an analogous manner to **4a** using KI and K_2CO_3 in the presence of 1,2-dibromopropane, starting from **3c**, as depicted in **Scheme 4-2**.

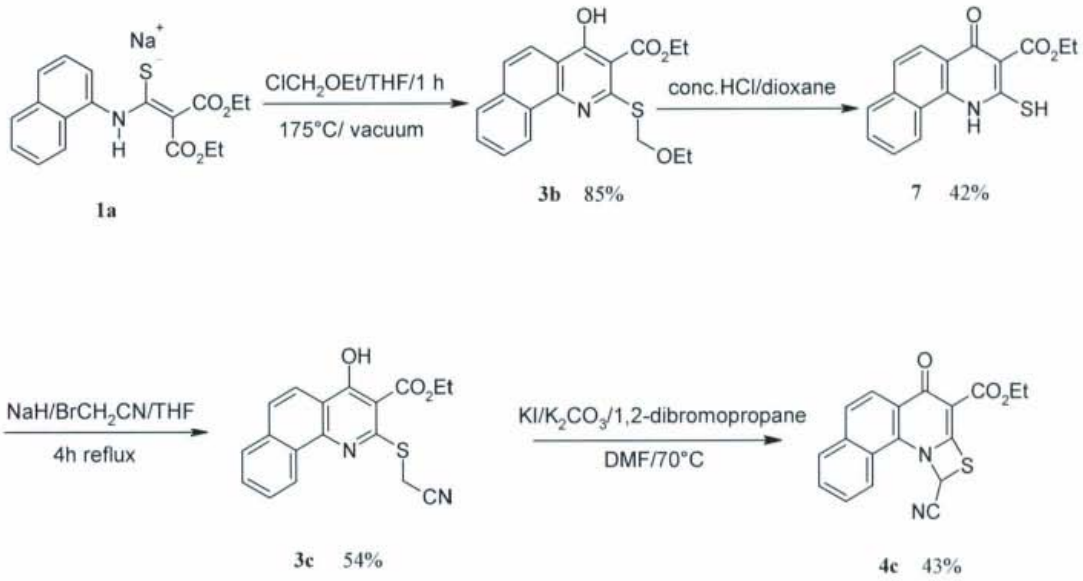

1a **3b** 85% **7** 42%

3c 54% **4c** 43%

Scheme 4-2: Synthesis of Compound **4c**.

The most interesting step in the schemes was the cyclization using a vicinal dihaloalkane instead of germinal ones, which were used in all previously reported syntheses. Also, the vicinal dihaloalkane did not appear in the final structure, which confirms the role of the vicinal dihaloalkane as a controlled source of the halogenating reagent which allows for cyclization to occur after it halogenates the carbon α to the thiol.

In order to investigate the details of the cyclization process, the following reactions were attempted:

- **3a** + KI + 1,2-dibromopropane;
- **3a** + K_2CO_3 + 1,2-dibromopropane;
- **3a** + KI + K_2CO_3;
- **3a** + KI + K_2CO_3 + 1, 2-dibromopropane.

No cyclised product was separated in the first 3 experiments and only the 4th procedure yielded the title Compound **4a**.

Based on the above information, the following pathway is suggested as a plausible mechanism for the formation of **4a** from **3a**. Nucleophilic reaction of iodide anion with 1,2-dibromoprapane would result in the formation of propene, bromide ion, and iodobromide (pseudohalide). Nucleophilic attack of the carbanion form of **3a** on iodobromide would afford the iodo intermediate **3a-a**, which upon nucleophilic cyclization yields **4a**, as depicted in **Scheme 4-3**.

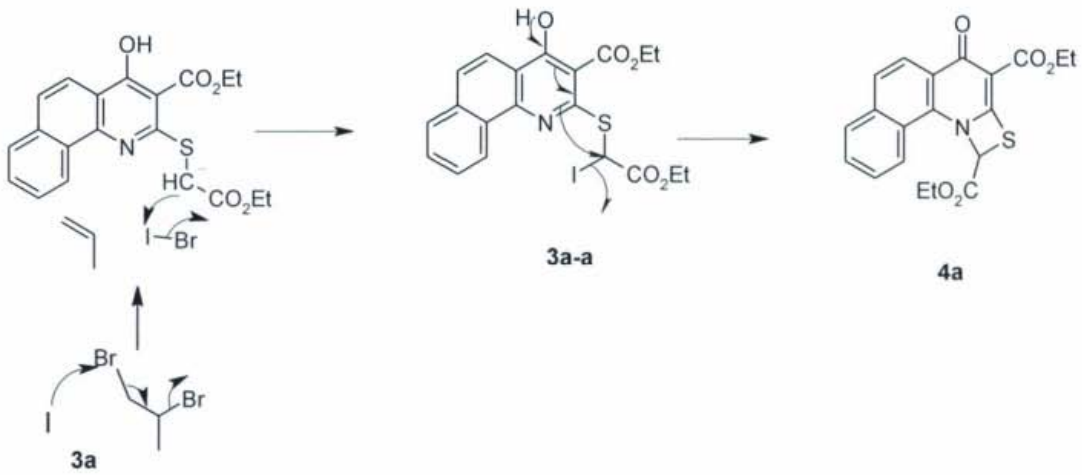

Scheme 4-3: A plausible mechanism for the formation of **4a** from **3a**.

In order to prove the critical role of 1,2-dihaloalkanes in the formation of the above 4-oxo-thiazetoquinolines, we attempted the same reaction using 1,2-dibromobutane and 1,2-dibromohexane instead of 1,2-dibromopropane. In all trials, Compound **4a** was obtained in a very good yield. On the other hand, when Compound **3a** was allowed to

react with 1,3-dibromopropane and 1,2-dibromoethane, the corresponding *O*-alkylated products (**5** and **6**) were obtained as shown in **Scheme 4-4**.

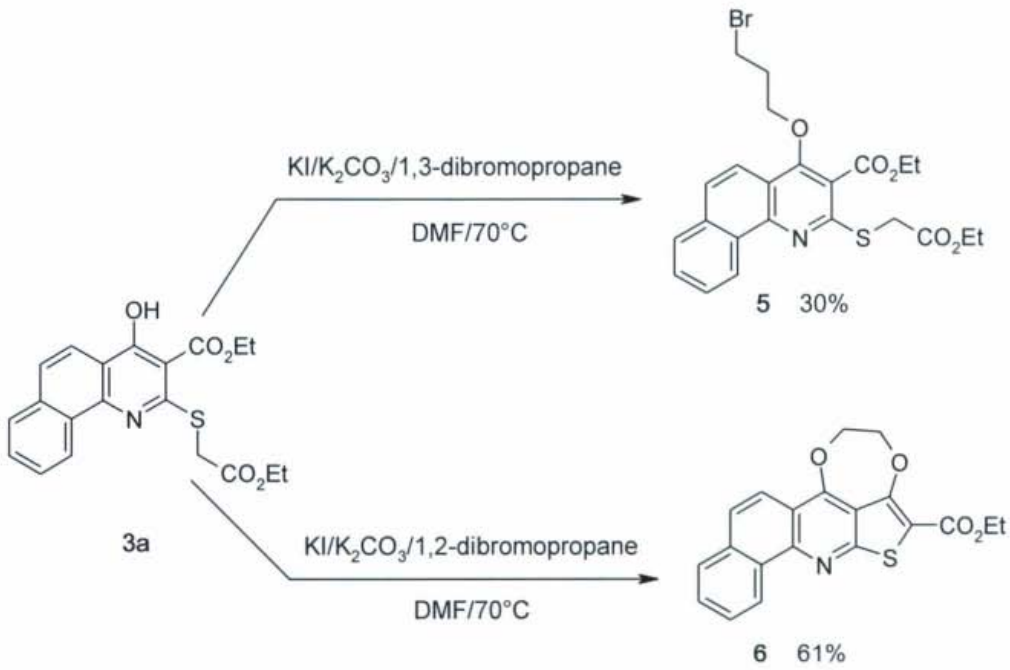

Scheme 4-4: *O*-alkylated products (**5** and **6**).

In order to confirm the involvement of the pseudohalide (iodobromide), formed by the reaction of 1,2-dibromopropane and KI, in the oxidative cyclization of Compound **3a** to **4a**, we attempted the reaction of **3a** with either iodobromide (IBr) or iodine (I_2) in the presence of K_2CO_3. In both attempts, we were able to obtain Compound **4a** in good yields.

The X-ray crystallographic structures of Compound **4a** and its carboxylic acid derivative (**4b**) [17] are shown in **Figure 4-2**.

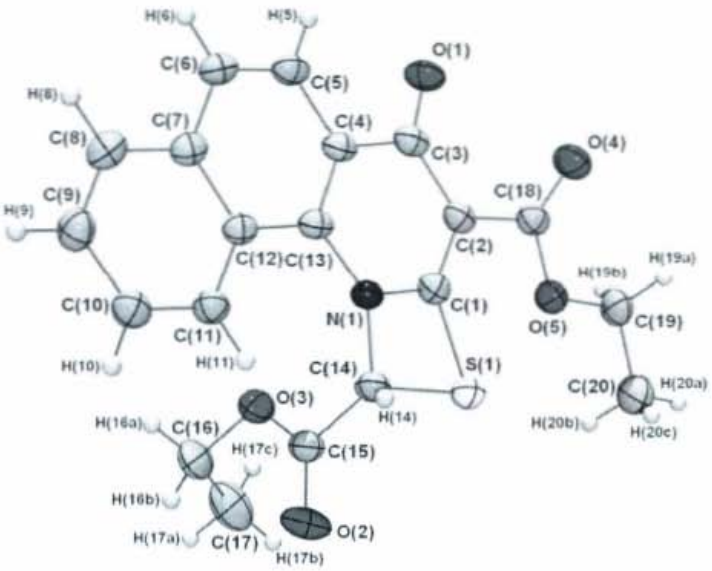

A

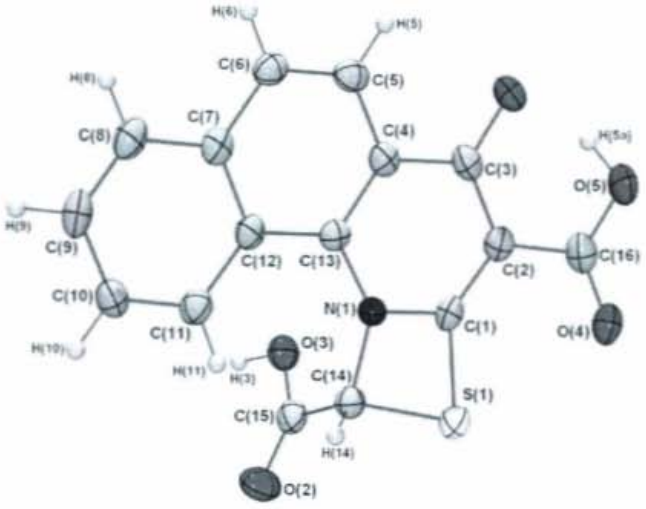

B

Figure 4-4: ORTEP representations of the X-ray structures of thiazetoquinoline derivatives **4a** and **4b**, with 50% probability ellipsoids.

We also attempted the decarboxylation of **4b** using conventional decarboxylation procedures with no success. Unexpectedly, when **4b** was allowed to react with ethylchloroformate followed by hydroxylamine hydrochloride, Compound **4d** was afforded. Formation of **4d** can be explained *via* the reaction of ethyl chloroformate with the carboxylate anions (formed in the presence of Et_3N) to afford a mixed-anhydride intermediate **4b-b**, which upon reaction with hydroxylamine hydrochloride leads to decarboxylation of the conjugated anhydride, while the unconjugated anhydride transforms into a carboxylic acid, as depicted in **Scheme 4-5**.

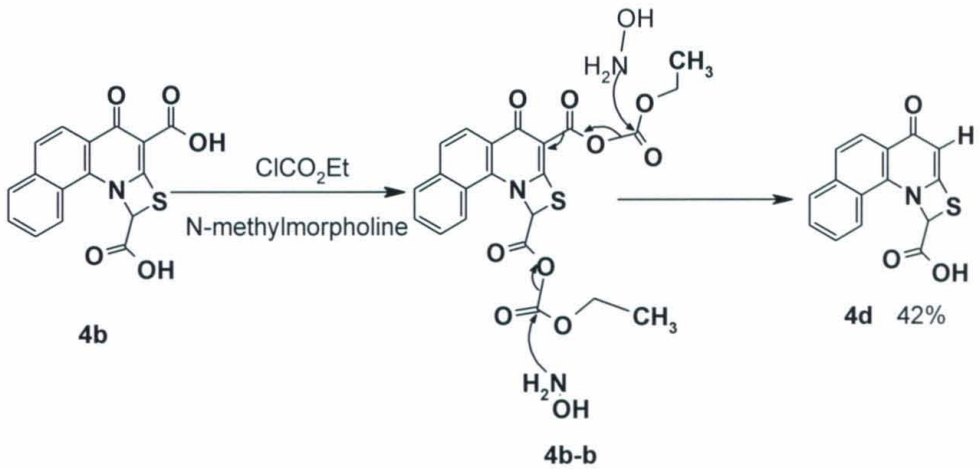

Scheme 4-5: Suggested mechanism for mono decarboxylation of Compound **4b**.

4.3 *In vitro* testing

Compounds **4a-4d** and **6** were tested for cytotoxicity against HeLa cells in comparison with doxorubicin, as a reference compound. The test results revealed the lack of cytotoxicity of the tested compounds against HeLa cells.

Table 4-1: Cytotoxicity results of tested derivatives.

Inhi% at 100ug/ml	Inhi% at 10ug/ml	Inhi% at 1ug/ml	Inhi% at 0.1ug/ml	IC_{50} ug/ml
4a	-2.90	-62.26	-65.23	100
4b	25.18	-11.01	-15.45	90
4c	36.00	-35.26	-43.54	>100
4d	-17.46	-45.83	-55.34	>100
6	15.13	38.64	-46.04	>100
Ref.	23.28	18.04	5.97	76.65

4.4 Molecular modeling

4.4.1 Methods

Docking calculations were carried out according to the DockingServer methodology [18]. The MMFF94 force field [19] was used for energy minimization of the ligand molecule using DockingServer. PM6 semiempirical charges calculated by MOPAC2009 (J. P. Stewart, Computer code MOPAC2009, Stewart Computational Chemistry, 2009) were added to the ligand atoms. Non-polar hydrogen atoms and rotatable bonds were defined.

Docking calculations were carried out on the topoisomerase II structure with the pdb code 1QZR. Essential hydrogen atoms, Kollman united atom type charges, and

solvation parameters were added with the aid of AutoDock tools [20]. Affinity (grid) maps of 25×25×25 Å grid points and 0.375 Å spacing were generated using the Autogrid program. AutoDock parameter set- and distance-dependent dielectric functions were used in the calculation of the van der Waals and the electrostatic terms, respectively.

Docking simulations were performed using the Lamarckian genetic algorithm (LGA) and the Solis & Wets local search method [21]. Initial position, orientation, and torsions of the ligand molecules were set randomly. Each docking experiment was derived from 100 different runs that were set to terminate after a maximum of 2,500,000 energy evaluations. The population size was set to 150. During the search, a translational step of 0.2 Å, and quaternion and torsion steps of 5 were applied.

4.4.2 Human topoisomerase II docking

Topoisomerase II is an ATPase belonging to the GHKL (Gyrase, Hsp90, histidine Kinase, mutL) family. The mechanism of function of human toposiomerase II is to simultaneously cut both strands of the DNA helix using the energy derived from ATP hydrolysis. The inhibition of human topoisomerase II is the target of oncology research. There are more ways to inhibit the enzyme's action [22]:

1-While exerting its function, the enzyme creates a transient covalent DNA-enzyme complex. Topoisomerase II poisons exert their effect by stabilizing this transient complex, thus, causing DNA damage. Since these compounds are very toxic to normal cells, alternative ways of topoisomerase II inhibition are subjects of interest in drug research.

2-An alternative way of inhibition is to block the enzyme before the DNA cleavage step or in the last step of its catalytic cycle. The competition for the ATP binding site as well as stabilization of a transient dimer interface between two ATPase monomers have been described [23]. Nevertheless, these ways of inhibition take place at the ATPase region of the protein. Among the available structures of the human topoisomerase II protein, 1PVG and 1QZR carry the ATPase region. Additionally, 1PVG contains modified methionine residues (MSE), while 1QZR contains phosphoaminophosphonic acid-adenylate ester (ANP) at the ATP binding site and an inhibitor ICRF-187 at the interface of the homodimer. All docking calculations were done using 1QZR.

4.4.3 Docking experiment

First, the blind docking procedure was applied. The docking result showed no cluster possessing significantly higher frequency or lower energy as compared to the other clusters. Thus, blind docking in this case was not able to clearly define the possible binding site. Therefore, biochemical knowledge was used for binding site identification. The cluster possessing the highest interaction surface between the docked ligand and the protein indicating strong binding was located at the ATP binding site. None of the results were found at the inhibitor's (ICRF-187) binding site. Thus, focused docking calculations were carried out at the ATP binding site of the protein.

4.5 Focused docking results

All compounds were calculated to bind at the ATP binding site with reasonable affinity, with **4b** possessing the lowest docking energy. It is noted that in the X-ray

structure Mg^{2+} is coordinated by 3 oxygen atoms coming from ANP. None of the tested derivatives were able to donate non-bonding electrons to Mg^{2+}.

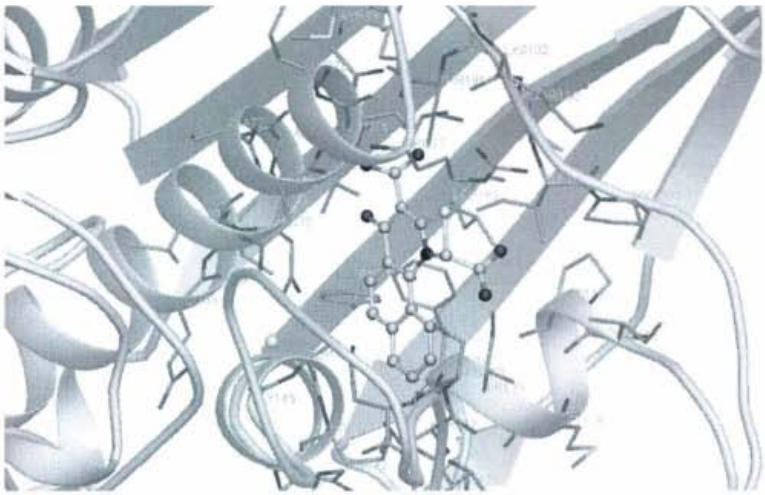

Figure 4-5: Docked structure of Compound **4b** at the ATP binding site of 1QZR.

Table 4-2: Calculated interactions of Compound **4b** at the ATP binding site.

Polar	Hydrophobic	pi-pi
O3 (9) [3.86] – ASN74 (OD1)	C3 (6) [3.31] – ILE104 (CD1)	C15 (22) [3.83] – PHE121 (CE1, CZ)
O4 (10) [3.46] – ASN74 (OD1)	C4 (7) [3.57] – ILE104 (CD1)	C16 (23) [3.21] – PHE121 (CE1, CZ)
O3 (9) [3.53] – ASN99 (OD1)	C11 (18) [3.76] – ILE120 (CB)	C7 (13) [3.47] – PHE121 (CZ)
O1 (1) [3.76] – SER128 (OG)	C12 (19) [3.78] – ILE120 (CB)	
O4 (10) [3.51] – THR195 (OG1)	C9 (16) [3.70] – ILE120 (CD1)	
	C10 (17) [3.47] – ILE120 (CD1)	
	C1 (2) [3.58] – ILE120 (CD1)	
	C6 (11) [3.74] – PHE121 (CZ)	
	C15 (22) [3.54] – ALA146 (CB)	

4.6 *In vitro* testing

HeLa human cervix adenocarcinoma were grown in DMEM (GIBCO) with 15% FBS and antibiotics (penicillin 100 U/ml, streptomycin 100 ug/ml). Cells were maintained at 37℃ in a humidified 5% CO_2 atmosphere.

4.6.1 Cytotoxicity assay

Cells were trypsinized and seeded into 96-well cell culture plates at 180 ul/well (about 5000 cells/well). After 16 h incubation, the cells were treated for 48h by the compound at final concentrations of 100, 10, 1, 0.1 ug/ml. The compounds were prepared in DMSO (stock solution of 10 ug/ml), and further diluted with culture medium to obtain the desired concentration. All tests included controls with equivalent concentrations of media DMSO corresponding to the relevant dilutions of the test compound. The 3-(4,5-Dimethylthiazol-2-yl)-2,5-diphenyl tetrazolium bromide (MTT) was added in the final concentration of 1 mg/ml, and 30 ul/well. After 4h incubation the MTT-formazan product was solubilized using DMSO (150 ul/well) with shaking 10 min. The absorbance measurements were carried out using a microplate reader at 490 nm.

4.7 Computational methods

All mechanistic modeling calculations were performed using Gaussian09 [24] at the HF/6-311G(d) and B3LYP/6-311G(d) levels of theory. As the 6-311G(d) basis set for iodine [25] is not included explicitly in the software package, all basis set information [25-28] was read in, as a general basis set input as obtained from the EMSL Basis Set

Exchange [29,30]. Calculations were performed both in the gas phase and solution phase. Solution phase calculations were performed with *N*,*N*-dimethylformamide as the modeled solvent, using the Polarizable Continuum Model (PCM) [31].

Once transition states were found and confirmed by frequency analysis, intrinsic reaction coordinate (IRC) [32,33] calculations were performed following both directions of the reaction coordinate. The end geometries of these IRC calculations were then used as starting points for geometry optimizations to find the reactant and product complexes associated with the transition state. All energy minimized geometries were also confirmed by frequency analysis.

4.7.1 Computational results

To test the plausibility of the mechanism described in **Scheme 4-3**, three individual steps of the scheme were computationally modeled to see if the energetics of each step were reasonable in terms of both activation energy barriers and overall energy change from reactants to products.

As the reaction to give **4a** from **3a** in the presence of IBr and K_2CO_3 has been observed, the initial modeled step was the formation of the carbanion form of **3a** via proton abstraction by carbonate. Two possible proton abstractions were attempted, one for each proton on the $-CH_2-$ group next to the sulfur atom. These protons can be described as the "ringward" proton on the same side of the molecule as the fused-ring portion of the molecule, and the "chainward" proton (**Figure 4-6a**) on the other side of the molecule. Using the reactant complex of carbonate and **3a** (**Figure 4-6a**) as the

reference point for zero energy, the chainward side transition state (**Figure 4-6b**) structure lies 10 kJ/mol above the reactant complex in the gas phase using B3LYP/6-311G(d), and the product **3a** carbanion/bicarbonate complex (**Figure 4-6c**) lies 192 kJ/mol below the reactant complex. The proton abstraction is highly exothermic, as the formation of the carbanion/bicarbonate complex creates two negatively charged ions that electrostatically repel each other. It should be noted that attempts to model the abstraction of the chainward proton were unsuccessful at this level of theory.

Attempts to model the proton abstraction on the ringward side using B3LYP/6-311G(d) were successful, but gave a transition state barrier of 22 kJ/mol, while the product complex lies below the reactant complex by 195 kJ/mol. However, regardless of the side from which the proton is removed, the resulting carbanion structure is the same.

The transition state barrier for the ringward proton abstraction is 39 kJ/mol in the gas phase using HF/6-311G(d), with the product complex lying 237 kJ/mol below the reactant complex. Attempts at finding the chainward transition state were unsuccessful at this level of theory.

In the solution phase it is interesting to note that at the HF/6-311G(d) level of theory, the proton abstraction occurs on the chainward side with a higher transition state barrier of 50 kJ/mol than is seen in the gas phase. Also, the step is only exothermic by 21 kJ/mol as compared to 195 kJ/mol in the gas phase. For the B3LYP calculations in solution, the barrier on the chainward side is 7 kJ/mol and the overall step is exothermic by 43 kJ/mol. In the solution phase calculations, the two negatively charged ions do not move as spatially distant from each other in the gas phase, as the ions can be stabilized by

the somewhat polar solvent molecules. This will tend to reduce the energy difference between the reactant and product complexes.

Overall, the proton abstraction step has been shown to have a reasonably sized activation energy barrier at the modeled levels of theory, and the step is exothermic overall.

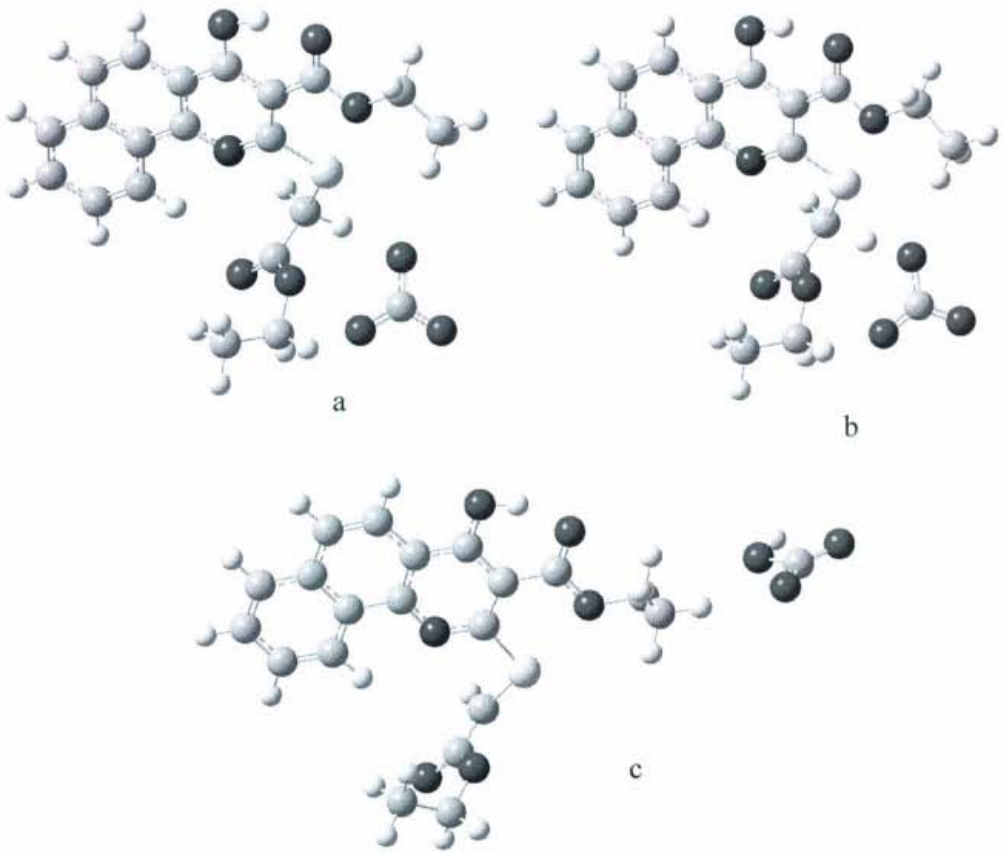

Figure 4-6: Reactant complex (**a**), transition state (b) and product complex (**c**) for the carbanion formation step calculated at the B3LYP/6-311G(d) level of theory.

The next modeled step involves the nucleophilic attack of the **3a** carbanion IBr to form Compound **3a-a**. Initial attempts to find the transition state for this step were unsuccessful, but the product complex of **3a-a** and bromide was found as shown in **Figure 4-7** for the structure calculated at the HF/6-311G(d) level of theory.

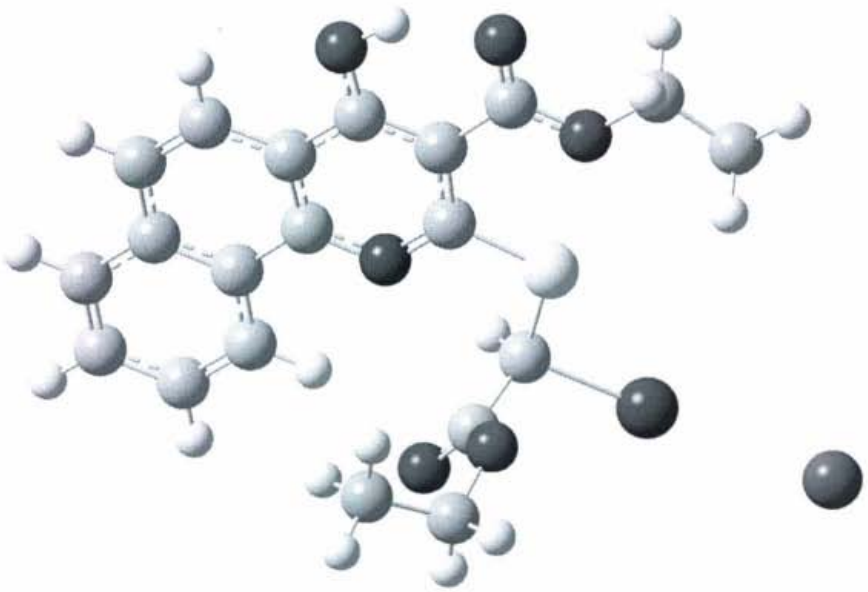

Figure 4-7: The structure of the **3a-a**/bromide product complex at the HF/6-311G(d) level of theory.

In the B3LYP/6-311G(d) product complex the iodine is 2.36 Å from the carbon, while the bromide lies 2.98 Å from the iodine atom, which significantly differs from the equilibrium bond length of IBr, which is calculated at B3LYP/6-311G(d) to be 2.53 Å. These three atoms effectively lie in a straight line, with an angle of 178.5 degrees.

In the next attempt to find the transition state, a fixed coordinate scan was undertaken at HF/6-311G(d) where the C-I bond length was increased by increments of 0.1 Å and the rest of the complex was optimized with the fixed C-I bond length. As the C-I bond length is increased, the energy of the resulting complex increases, indicating that this step appears to have no activation energy barrier, and instead shows an energetic profile very similar to a barrierless bond dissociation. Unfortunately this also means it is very difficult to identify a carbanion/IBr reactant complex for this reaction. However, when the C-I distance is fixed at 5.0 Å the IBr bond length is 2.51 Å, which is not significantly different from the HF/6-311G (d) bond length in IBr of 2.49 Å, and so for energetic comparisons, we choose our "reactant complex" to have a fixed C-I distance of 5.0 Å. We then compare the energy of this complex to that of the product complex to estimate the energy change of the **3a-a**/iodide formation step.

At the HF/6-311G(d) level of theory, the product complex lies 199 kJ/mol below the "reactant complex" in the gas phase, and 254 kJ/mol below in the solution phase. For B3LYP, the product complex lies energetically below the reactants by 150 kJ/ mol and 206 kJ/mol in the gas and solution phases respectively. Overall, this step has no activation barrier and is highly exothermic at all levels of theory examined.

Modeling the abstraction of the phenolic-type proton of intermediate **3a-a** by either carbonate or the solvent *N*,*N*-dimethylformamide was not undertaken, as this step represents acid-base type chemistry. The electron withdrawing ester group next to the phenolic group and the extended aromatic system allow for many resonance structures to be drawn for the phenolate form of **3a-a**, including one which puts the negative charge on

the nitrogen atom of the ring system. Because of this, the phenolate form should be reasonably stable and the abstraction of the proton step of the mechanism should occur with some facility. In fact, comparison of the calculated HF/6-311G(d) Mulliken charges of **3a-a** and the phenolate form do show an increase in the negative charge on the nitrogen atom of the phenolate from -0.61e to -0.68e, increasing its nucleophilicity. This has the potential to affect the energetics of the nucleophilic cyclization step of the mechanism.

The importance of the phenolic proton abstraction prior to the nucleophilic cyclization step was explored by modeling the ring closing of both the phenolic and phenolate forms of **3a-a**. For HF calculations, the ring closing of **3a-a** to give protonated **4a** and iodide has an activation energy barrier of 149 kJ/mol (gas phase) or 110 kJ/mol (solution phase), while the product complex lies energetically above the reactant complex by 87 kJ/mol in the gas phase or 40 kJ/mol below the reactant complex in the solution phase. For the phenolate form of **3a-a**, the ring closing to give **4a** and iodide at HF/6-311G(d) has an energy barrier of only 77 kJ/mol (gas phase TS - **Figure 4-8b**) or 81 kJ/mol (solution phase) while the product complex lies below the reactant complex by 59 kJ/mol in the gas phase and 120 kJ/mol below the reactant complex in the solution phase.

Calculations carried out with B3LYP show similar trends. The ring closing of **3a-a** to protonated **4a** and iodide has an activation energy barrier of 108 kJ/mol (gas phase) or 79 kJ/mol (solution phase), while the product complex lies energetically above the reactant complex by 86 kJ/mol in the gas phase or 1 kJ/mol above the reactant complex in the solution phase. However, for the phenolate form of **3a-a** (**Figure 4-8a**), the ring

closing to give **4a** and iodide (**Figure 4-8c**) at B3LYP/6-311G(d) has an energy barrier of only 44 kJ/mol (gas phase TS - **Figure 4-8b**) or 49 kJ/mol (solution phase) while the product complex lies below the reactant complex by 25 kJ/mol in the gas phase and 70 kJ/mol below the reactant complex in the solution phase.

The large difference in the energetics of the modeled ring closing steps can be attributed to the creation of the positively charged protonated **4a** and the negatively charged iodide. The ring closing of the phenolic form would create separation of opposing charges, which should be energetically prohibitive. However, when the negatively charged **3a-a** phenolate form undergoes ring closing, the single negative charge is carried away by the iodide leaving group. With the removal of the phenolic proton, all model chemistries show a reasonable activation energy barrier and an exothermic step overall.

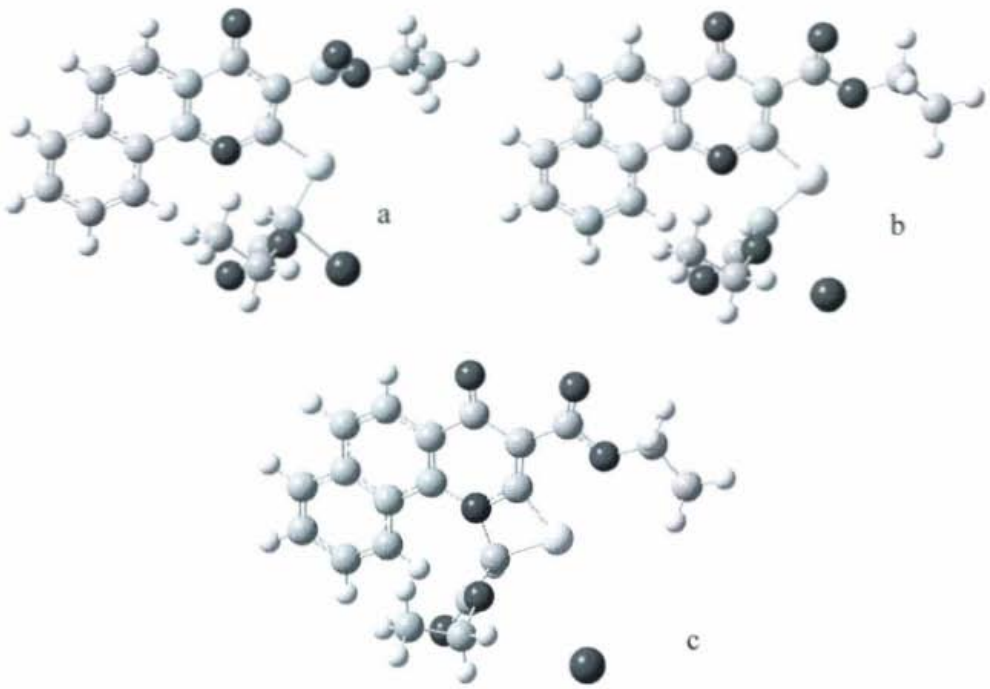

Figure 4-8: Phenolate form of **3a-a** (**a**), ring closing transition state (**b**) and **4a**/iodide product complex (**c**) for the ring closing step at the B3LYP/6-311G(d) level of theory.

Overall, modeling of these three steps of the proposed mechanism show that the first two steps have small to nonexistent activation energy barriers, and are highly exothermic in concert. Even if the abstraction of the phenolic proton were to have a relatively large activation energy barrier in the order of 250 kJ/mol (which is unlikely for such acid-base chemistry) the transition state would still lie energetically below the **3a**/carbonate reactant complex of the first step. Combined with the reasonable transition state barrier of the phenolate form ring closing step, which is itself exothermic, the theoretical calculations support the notion that the proposed mechanism is energetically

favourable. In fact, since the activation energy barriers to reverse any of the mechanistic steps would be prohibitively high, reverse reactions are unlikely to occur, and the proposed mechanism would have to lead to fairly high yields of product **4a** at a reasonable temperature. As the experimental results show yields in the order of 75% for the reaction run for 24 hours at 70 ℃, the modeled energetics of the proposed mechanism support the observed yield as well.

4.8 Conclusion

We have presented herein a novel and effective method for a facile synthesis of the 4-oxo-thiazetoquinoline nucleus *via* a homo- or heterohalide catalyzed oxidative cyclization of 2-((2-ethoxy-2-oxoethyl)thio- or 2-((cyano-methyl)thio)-4-hydroxybenzo[*h*]quinoline-3-carboxylate. The designed structures did not show cytotoxicity as shown in the MTT cytotoxicity bioassay on the HeLa cell line. The synthesized derivatives exihibited a good binding affinity to the ATP binding site of the human topoisomerase but did not show any chelation to the Mg^{2+}.

4.9 Experimental

^{1}H and ^{13}C NMR spectra, HSQC, and COSY spectra were recorded on a Bruker 500 MHz NMR spectrometer using TMS as an internal standard. LC-MS and HR-MS were conducted using a GCT Premier Micromass spectrometer. X-Ray structures were measured on a Rigaku Saturn 70 instrument, equipped with a CCD area detector and a SHINE optic, using Mo Kα radiation. Silicycle Ultrapure silica gel (0-20 μm) G and F-254 was used for the preparative-layer TLC, and Silicycle Silia-P Ultrapure Flash silica

gel (40-63 μm) was used for flash column chromatography. TLC was conducted on Polygram SIL G/UV254 precoated plastic sheets. Solvents were purified using standard conditions before use. The reaction yields are included in the corresponding schemes.

Sodium 3-ethoxy-2-(ethoxycarbonyl)-1-(naphthalen-1-ylamino)-3-oxoprop-1-ene-1-thiolate (1a):

To a suspension of sodium hydride (0.60 g, 25 mmol) in MeCN (50 mL) at 5-10 °C was added dropwise diethyl malonate (4.0 mL, 26.34 mmol) over a period of 15 min. The mixture was stirred at 5-10 °C for additional 30 min., then 1-naphthylisothiocyanate (5.0 g, 26.99 mmol) was added portionwise at the same temperature and stirring was continued for another 30 min. Evaporation of MeCN yielded a yellowish solid which was washed with Et_2O; mp 118-120 °C; ^{1}H-NMR: (500 MHz, DMSO-d_6): δ = 12.33 (s, NH), 8.57 (d, J = 7.1 Hz, 1H), 8.16 (t, J = 7.7 Hz, 1H), 7.91-7.86 (m, 1H), 7.52 (ddd, J = 4.7, 11.1, 8.8 Hz, 3H), 7.46-7.38 (m, 1H), 4.02 (q, J = 7.0 Hz, 4H), 1.16 (t, J = 7.0 Hz, 6H);^{13}C NMR (175 MHz, DMSO-d_6): δ = 181.6, 166.4, 136.1, 132.5, 127.0, 126.6, 124.3, 124.2, 123.9, 121.2, 120.6, 119.4, 116.8, 95.2, 56.8 ($2CH_2$), 13.3 ($2CH_3$); APCI-MS: 368.4 (**M^+**+1, 100).

Ethyl 2-((2-ethoxy-2-oxoethyl)thio)-4-hydroxybenzo[*h*]quinoline-3-carboxylate (3a):

To the above yellow solid (**1a**, 2.0 g, 5.44 mmol) in THF (50 mL) was added $BrCH_2COOCH_2CH_3$ (0.60 mL, 5.44 mmol) dropwise at 0 °C and the mixture was stirred for 1 h at room temperature. The solvent was then evaporated, extracted with $CHCl_3$ and dried over Na_2SO_4. The organic layer was evaporated by rotary evaporator to give a yellow oil (**2a**). The obtained oil was heated at 170-180 °C in an oil bath under vacuum

for 10 min. The resulting oil was solidified, then washed with ether to afford (**3a**) as white needles; mp 136-138 °C; ^{1}H-NMR: (500 MHz, $CDCl_3$): δ = 13.11 (s, 1H, OH), 9.22-9.15 (m, 1H), 8.10 (d, *J* = 8.9 Hz, 1H), 7.89 (dd, *J* = 3.1, 6.0 Hz, 1H), 7.76-7.68 (m, 3H), 4.61 (q, *J* = 7.0, 6.9 Hz, 2H), 4.22 (q, *J* = 7.0, 6.9 Hz, 2H), 4.13 (s, 2H), 1.60 (t, *J* = 7.0 Hz, 3H), 1.29 (t, *J* = 7.0 Hz, 3H); ^{13}C NMR (175 MHz, $CDCl_3$): δ = 170.9, 170.4, 168.2, 158.1, 147.6, 135.8, 130.6, 129.4, 128.1, 127.1, 126.2, 125.9, 119.9, 115.1, 104.0, 63.2, 61.9, 34.6, 14.6, 14.6; HR-MS (TOFEI) calcd for $C_{20}H_{19}NO_5S$: (385.0984); found (385.0991).

Ethyl 2-((ethoxymethyl)thio)-4-hydroxybenzo[*h*]quinoline-3-carboxylate (3b):

This compound was prepared according to the same procedure as that applied for **3a** using chloromethyl ethyl ether; yellow crystals; mp 120-122 °C; ^{1}H-NMR: (500 MHz, $CDCl_3$): δ = 13.11 (s, 1H, OH), 9.26-9.19 (m, 1H), 8.13 (d, *J* = 9.0 Hz, 1H), 7.91 (d, *J* = 3.3 Hz, 1H), 7.75 (d, *J* = 9.0 Hz, 1H), 7.72 (dd, *J* = 3.2, 6.1 Hz, 2H), 5.76 (s, 2H), 4.60 (q, *J* = 7.1 Hz, 2H), 3.76 (q, *J* = 7.0 Hz, 2H), 1.59 (t, *J* = 7.0 Hz, 3H), 1.25 (t, *J* = 7.0 Hz, 3H);^{13}C NMR (175 MHz, $CDCl_3$): δ = 171.1, 168.3, 158.2, 147.4, 135.8, 129.4, 128.2, 127.3, 126.2, 125.7, 120.0, 115.1, 104.3, 71.4, 65.7, 63.1, 31.2, 15.4, 14.6; HR-MS (TOFEI): calcd for $C_{19}H_{19}NO_4S$ (357.1035); found (357.1031).

Ethyl 2-((cyanomethyl)thio)-4-hydroxybenzo[*h*]quinoline-3-carboxylate (3c):

Following a reported procedure [34], to a stirring solution of **4** (0.8 g, 2.67 mmol) in THF (10 mL) and H_2O (40 mL) was added $NaHCO_3$ (1 g, 7.23 mmol), and stirred for 15 min., then bromoacetonitrile (0.5 g, 4.16 mmol) was added to the resulting solution and stirred for 4 h at room temperature. After completion of the reaction, the solution was acidified

by acetic acid, extracted with chloroform, dried over Na_2SO_4, filtered to give **3c** as a white powder; mp 208-210 °C; ^{1}H-NMR: (500 MHz, DMSO-d_6): δ = 12.42 (s, 1H, OH), 9.26-9.21 (m, 1H), 8.12 (d, J = 8.8 Hz, 1H), 8.10-8.07 (m, 1H), 7.97 (d , J = 9.1 Hz, 1H), 7.82 (m, 2H), 4.53 (q, J = 7.09, 7.08 Hz, 2H), 4.43 (s, 2H), 1.45 (t, J = 7.1 Hz, 3H); ^{13}C NMR (175 MHz, DMSO-d_6): δ = 169.9, 168.0, 155.0, 147.2, 135.5, 130.1, 129.4, 127.9, 127.4, 126.6, 125.3, 119.3, 117.4, 115.0, 103.4, 63.1, 17.2, 14.2; HR-MS (TOFEI) calcd. for $C_{18}H_{14}N_2O_3S$ (338.0725); found (338.0722).

Diethyl 4-oxo-1,4-dihydrobenzo[*h*][1,3]thiazeto[3,2-*a*]quinoline-1,3-dicarboxylate (4a):

i) Oxidative Cyclization using KI and 1,2-dibromopropane

To a mixture of **3a** (0.385 g, 1 mmol) and K_2CO_3 (0.386 g, 2.8 mmol) in dry DMF (25 mL) under nitrogen atmosphere was added 1,2-dibromopropane (0.56g, 2.8 mmol) along with KI (0.464 g, 2.8 mmol). The reaction mixture was heated at 70 °C for 24 h, and then poured into ice-H_2O. The resulting thiazetoquinoline derivative was collected by filtration and recrystallized from hexane: $CHCl_3$ (1:3) to afford yellowish crystals; yield = 75%

ii) *Oxidative Cyclization using iodobromide and/or iodine*

To a mixture of **3a** (0.385 g, 1 mmol) and K_2CO_3 (0.386 g, 2.8 mmol) in dry DMF (25 mL) under nitrogen atmosphere was added iodobromide and/or iodine (2.8 mmol).

The reaction mixture in case of iodobromide was stirred at room temperature for 24 h (in case of iodine the reaction mixture was heated at 70 °C for 24 h). After cooling, both reaction mixtures were poured into ice-H_2O. The resulting thiazetoquinoline derivative was collected by filtration and recrystallized from hexane: $CHCl_3$ (1:3) to afford yellowish crystals; yield (IBr) = 40%, yield (I_2) = 49%. mp 223-225 °C; ^{1}H-NMR: (500 MHz, $CDCl_3$): δ = 8.42 (d, *J* = 8.6 Hz, 1H), 7.91 (d, *J* = 8.3 Hz, 1H), 7.82 (d, *J* = 8.5 Hz, 1H), 7.68 (d, *J* = 8.7 Hz, 1H), 7.61 (t, *J* = 7.4 Hz, 1H), 7.56 – 7.52 (m, 1H), 6.67 (s, 1H), 4.38 (q, *J* = 6.7, 6.2 Hz, 2H), 4.23 (q, *J* = 7.2 Hz, 2H), 1.41 (t, *J* = 7.3 Hz, 3H), 1.08 (t, *J* = 7.3 Hz, 3H);^{13}C NMR (175 MHz, $CDCl_3$): δ = 173.2, 165.7, 165.4, 136.1, 135.8, 129.9, 129.0, 127.5, 123.9, 122.4, 122.4, 121.7, 121.6, 106.9, 67.7, 64.1, 61.7, 31.3, 14.7, 14.1; HR-MS (TOFEI) calcd for $C_{20}H_{17}NO_5S$ (383.0827); found (383.0826).

4-Oxo-1,4-dihydrobenzo[*h*][1,3]thiazeto[3,2-*a*]quinoline-1,3-dicarboxylic acid (4b):

Following a reported procedure [35], a mixture of ester (**4a**) (0.385 g, 1 mmol) and sodium hydroxide (0.08g, 2.2 mmol) in water (20 mL) was stirred and heated at 100 °C for 3-4 h. After cooling, the reaction mixture was neutralized with hydrochloric acid (1 mol/L), extracted with CH_2Cl_2, dried over $MgSO_4$, then evaporated. The solid obtained was purified by recrystallization from EtOH to afford Compound **4b** as yellowish white powder; mp 233-235 °C; ^{1}H-NMR: (500 MHz, DMSO-d_6): δ = 8.27 (d, *J* = 8.8 Hz, 1H), 8.25 (d, *J* = 8.4 Hz, 1H), 8.17 (d, *J* = 7.5 Hz, 1H), 8.02 (d, *J* = 8.8 Hz, 1H), 7.83 (dd, *J* = 11.0, 4.0 Hz, 1H), 7.81-7.76 (m,1H), 7.73 (s, 1H); ^{13}C NMR (175 MHz, DMSO-d_6): δ = 175.7, 165.6, 165.2, 164.2, 136.0, 135.2, 129.5, 128.9, 127.5, 126.0, 122.6, 122.3, 121.5,

121.1, 103.6, 70.4; HR-MS (TOFEI) calcd for $C_{15}H_9NO_3S$ (283.0303); found (283.0313) [36] .

Ethyl 1-cyano- 4-oxo-1,4-dihydrobenzo[*h*][1,3]thiazeto[3,2-*a*]quinoline-3-carboxylate (4c).

This compound was prepared using the same procedure as that used for the synthesis of **4a** using KI, K_2CO_3 and 1,2-dibromopropane starting from **3c**; white powder; mp 220-222 °C; ^{1}H-NMR: (500 MHz, $CDCl_3$): δ = 9.35 (dd, *J* = 5.3, 3.1 Hz, 1H), 8.17-8.02 (m,1H), 7.90 (dd, *J* = 5.5, 3.4 Hz, 1H), 7.86-7.81 (m, 1H), 7.79-7.72 (m, 2H), 4.59 (q, *J* = 7.11,7.08 Hz, 2H), 4.17 (1H, s), 1.56 (t, *J* = 7.13 Hz, 3H); ^{13}C NMR (175 MHz, $CDCl_3$): δ= 168.3, 167.9, 149.3, 147.9, 135.5, 130.2, 130.0, 128.0, 127.8, 127.7, 126.1, 118.9, 115.8, 109.3, 103.2, 63.8, 30.9, 14.2; HR-MS (TOFEI) calcd for $C_{18}H_{12}N_2O_3S$ (336.0568); found (336.0561).

Ethyl 4-(3-bromopropoxy)-2-((2-ethoxy-2-oxoethyl)thio)benzo[*h*]quinoline-3-carboxylate (5):

To a mixture of **3a** (0.385 g, 1 mmol) and K_2CO_3 (0.386 g, 2.8 mmol) in dry DMF (25 mL) under nitrogen atmosphere was added 1,3-dibromopropane (0.56 g, 2.8 mmol) along with KI (0.464 g, 2.8 mmol). The reaction mixture was heated at 70 °C for 24 h., and then poured into ice-H_2O. The resulting product was collected by filtration and recrystallized from hexane: $CHCl_3$ (1:3) to yield a white powder; mp 162-164 °C; ^{1}H-NMR: (500 MHz, $CDCl_3$): δ = 9.21-9.14 (m, 1H), 7.95(d, *J* = 8.9 Hz, 1H), 7.91-7.85 (m, 1H), 7.76 (d, *J* = 8.9 Hz, 1H), 7.70 (m, 2H), 4.53 (q, *J* = 7.1Hz, 2H), 4.35 (t, *J* = 5.8 Hz, 2H), 4.22 (q, *J* =

7.1Hz, 2H), 4.15 (s, 2H), 3.70 (t, CH_2Br, J = 6.4 Hz, 2H), 2.42 (q, $CH_2CH_2CH_2$, J = 6.1 Hz, 2H), 1.49 (t, J = 7.1 Hz, 3H), 1.27(t, J = 7.1 Hz, 3H); ^{13}C NMR (175 MHz, $CDCl_3$): δ = 162.1, 160.6, 160.2, 153.7, 148.0, 134.2, 130.2, 129.0, 127.6, 127.0, 125.9, 125.4, 119.9, 115.8, 113.8, 70.9, 70.0, 61.2, 33.8, 29.8, 25.0, 14.4, 14.3; APCI-MS: 506.40 (M^++1, 100).

Ethyl 8,9-dihydro-7,10-dioxa-12-thia-13-azaazuleno [8,1-*ab*]phenanthrene-11-carboxylate (6):

This compound was prepared using the same procedure as that used for the synthesis of **4a** using 1,2-dibromoethane to afford a yellow crystalline product; mp 250-252 °C; ^1H-NMR: (500 MHz, $CDCl_3$): δ = 9.35-9.28 (m, 1H), 8.14 (d, J = 9.1 Hz, 1H), 7.93-7.87 (m, 1H), 7.74 (dt, J = 5.9, 9.7 Hz, 3H), 4.96-4.92 (m, 2H), 4.84-4.79 (m, 2H), 4.42 (q, J = 7.1 Hz, 2H), 1.43 (t, J = 7.1 Hz, 3H); ^{13}C NMR (175 MHz, $CDCl_3$): δ = 162.1, 159.5, 158.2, 152.8, 148.3, 134.3, 130.1, 129.1, 127.6, 127.0, 125.8, 125.4, 119.4, 113.8, 111.4, 104.8, 73.6, 72.2, 61.1, 14.4; HR-MS (TOFEI) calcd for $C_{20}H_{15}NO_4S$ (365.0722); found (365.0727).

4-Oxo-1,4-dihydro benzo[*h*][1,3]thiazeto[3,2-*a*]quinoline-1-carboxylic acid (4d):

Following a reported procedure [37], to a solution of **4b** (2.43 g, 8.6 mmol) and *N*-methylmorpholine (0.960 g, 9.5 mmol) in THF (15 mL) at 0 °C was added ethyl chloroformate (1.03 g, 9.5 mmol) dropwise and the mixture was stirred for 30 min. The solid was filtered off and the filtrate was added to the solution of hydroxylamine hydrochloride (0.896 g, 12.9 mmol) and Et_3N (1.3 g, 12.9 mmol) in DMF (20 mL) for 10 min. The reaction mixture was stirred for 30 min at 25 °C. DMF was evaporated *in vacuo*.

The residue was extracted with EtOAC (80 mL) and washed with water. The solvent was dried over $MgSO_4$ and evaporated to dryness. The crude product was purified by silica gel column chromatography using EtOAC: hexane (1:1); yellow powder; mp 250-252 °C; ^{1}H-NMR: (500 MHz, DMSO-d_6): δ = 8.28 (t, J = 9.1 Hz, 2H), 7.98 (d, J = 7.9 Hz, 1H), 7.68 (m, 2H), 7.55 (t, J = 7.6 Hz, 1H), 6.43 (s, 1H), 5.68 (s, 1H). ^{13}C NMR (175 MHz, DMSO-d_6): δ = 178.9, 173.5, 171.1, 170.5, 141.5, 139.8, 133.5, 133.3, 131.2, 129.5, 128.2, 128.2, 128.1, 116.7, 76.1; HR-MS (TOFEI) calcd for $C_{15}H_9NO_3S$ (283.0303); found (283.0301).

Appendix 4A: Structure Report, 4-Oxo-1,4-Dihydrobenzo[*h*][1,3]thiazeto[3,2-*a*]quinoline-1,3-Dicarboxylic Acid

Louise N. Dawe,[a] Abeer Ahmed[b] and Mohsen Daneshtalab[b]*

Acta Cryst., 2011, E67, o529 (available online).

[a]Department of Chemistry, Memorial University of Newfoundland, St. John's, NL, A1B 3X7, Canada, and [b]School of Pharmacy, Memorial University of Newfoundland, St. John's, NL, A1B 3V6, Canada.

Abstract

The title compound, $C_{16}H_9NO_5S$, (**4a**) was obtained from the reaction of ethyl 2-{[2- ethoxy-2-oxoethyl)thio)-4-hydroxybenzo[h]quinoline-3-carboxylate with 1,2-dibromopropane in the presence of KI (2.8 mmol), followed by Saponification using sodium hydroxide. A combination of intermolecular interactions led to π- stacked molecules that were further organized into O—H···O hydrogen-bonded chains.

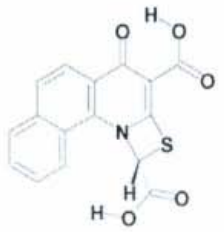

4A.1 Related literature

For background on the biological importance of thiazetoquinoline antibiotics see reference [13b]. For similar work using different procedures see references [15] and [38].

4A.2 Experimental

4A.2.1 Crystal data

$C_{16}H_9NO_5S$ $V = 1341.5$ (7) Å3

$Mr = 327.31$ $Z = 4$

Monoclinic, $P21/c$ Mo $K\alpha$ radiation, $\lambda = 0.71075$ Å

$a = 7.237$ (2) Å $\mu = 0.27$ mm−1

$b = 16.171$ (5) Å $T = 153$ K

c = 11.929 (4) Å 0.18 × 0.04 × 0.04 mm

β = 106.081 (8)°

4A.2.2 Data collection

Rigaku Saturn

Diffractometer 2769 independent reflections

Absorption correction: Numerical

[46] 2614 reflections with $I > 2\sigma(I)$

Tmin = 0.974, Tmax = 0.996 Rint = 0.074

17300 measured reflections

4A.2.3 Refinement

$R[F2 > 2\sigma(F2)]$ = 0.088 2 restraints

$wR(F2)$ = 0.164 H atoms treated by a mixture of independent and constrained refinement

S = 1.30 Δρmax = 0.31 e Å−3

2769 reflections Δρmin = −0.31 e Å−3

214 parameters

Data collection: *CrystalClear* [38]; cell refinement: *CrystalClear*; data reduction: *CrystalClear*; program(s) used to solve structure: *SHELXL97* [39]; program(s) used to refine structure: *SHELXL97*; molecular graphics: Mercury [40]; software used to prepare material for publication: publCIF [41].

Table 4-3: Hydrogen-bond geometry (Å, °).

D-H. . *A*	*D*-H	H. . *A*	*D*. . *A*	*D*-H. . *A*
O5-H5*A*. . .O1	0.96 (4)	1.57 (4)	2.504 (4)	161 (4)
O3-H3. . .O4^{i}	0.97 (3)	1.62 (3)	2.569 (4)	166 (3)

Symmetry code: (i) *x-1, -y+1/2, z-1/2.*

Table 4-4: Π..... Π interactions (Å, °)

Angle of elevation defined as the angle of the *Cg*(*I*)→*Cg*(*J*) vector and the normal to plane *J*. *Cg*1, *Cg*2 and *Cg*3 are the centroids of the C7-C12, N1/C1-C4/C13 and C4-C7/C12/C13 rings, respectively.

Π ..... Π	**Distance**	**Angle of Elevation**
*Cg*1. . .*Cg*2^{i}	3.560 (2)	19.56
*Cg*3. . .*Cg*2^{i}	3.644 (2)	22.75
*Cg*3. . .*Cg*3^{i}	3.688 (2)	24.39

Symmetry code: (i) -*x* + 1, -*y*, -*z*.

4A.3 Comment

Compound **1** crystallized in P21/c, with one entire molecule contained in the asymmetric unit. Multiple short π contacts between aromatic ring centroids (**Figure 4-7**) result from the close association of molecules in π-stacks (**Figure 4-8**). Centroid-centroid distances range from 3.57 to 3.69 Å with angles of elevation between 65.6 and 69.1° (**Table 4-4**), while the inter-planar distance, as defined by adjacent 14-atom (N1, C1—C13) ring systems is 3.34 Å. Further, (**1**) exhibits intra- (O5—H5a···O1) and

intermolecular (O3—H3···O4i) hydrogen bonding, leading to a chain-like arrangement of molecules which run perpendicular to the π stacks.

4A.4 Refinement

H_3 and H_5a were located from different Fourier maps, and were refined positionally with restrained distances (shelxl DFIX 0.96) and fixed Uiso values (1.2Ueq of the attached atom). All other H atoms were introduced in idealized positions with constrained distances and with Uiso(H) values set to either 1.2Ueq or 1.5Ueq of the attached atom. They were refined on a riding model. All non-hydrogen atoms were refined anisotropically.

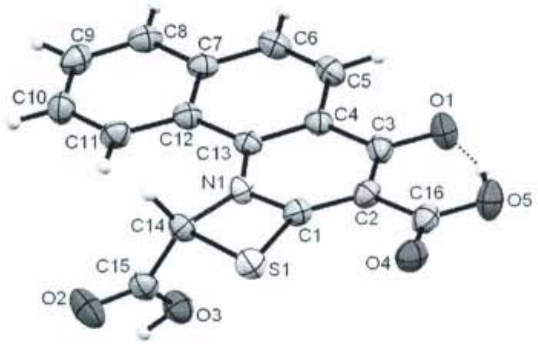

Figure 4-9: A view of the molecular structure of the title molecule, with displacement ellipsoids drawn at the 50% probability level.

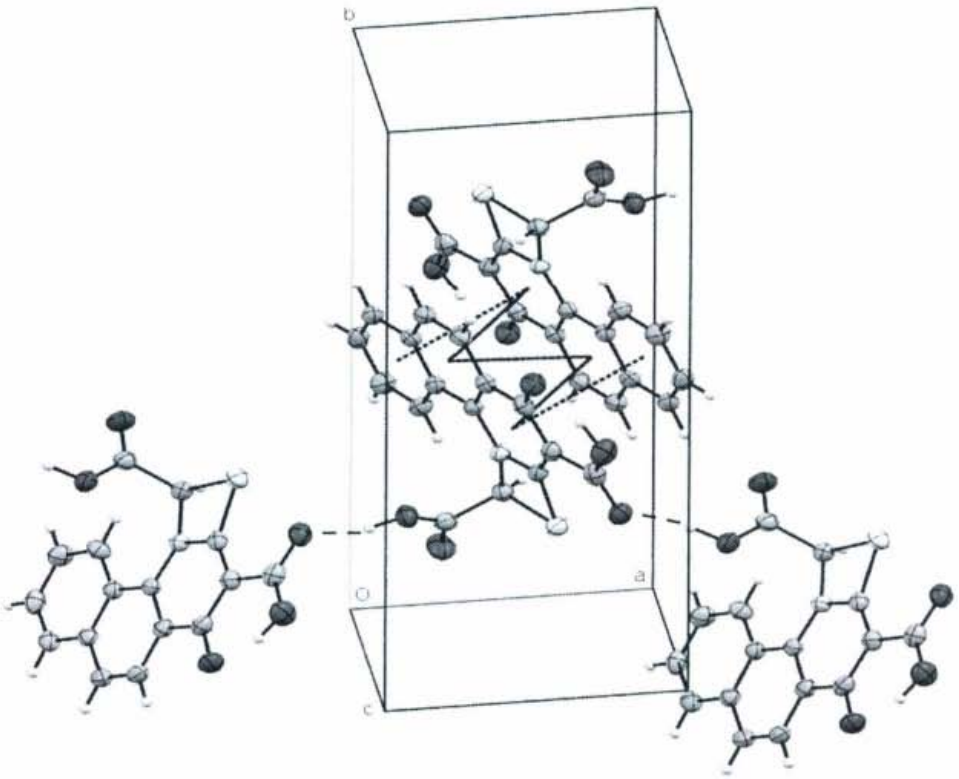

Figure 4-10: A partial view of the crystal packing of the title compound.

Both the hydrogen bonding [symmetry codes: (i) x-1, y, z; (ii) x, -y+1/2, z+1/2; (iii) x+1, y, z+1] and $\pi\cdots\pi$ interactions [symmetry codes: (ii) x, -y+1/2, z+1/2; (iv) -x+1, y+1/2, -z+1/2] are shown as dashed lines; ring centroids are marked by small spheres.

References

1. Hooper, D. (2000). *Quinolones. in: Mandell, Douglas, and Bennett's principles and practice of infectious diseases* (5th ed.). Churchill Livingstone: Philadelphia., 404.
2. Hooper, D. C., & Wolfson, J. S. (Eds.). (1993). Quinolone antimicrobial agents (2nd ed.) Washington, DC : American Society for Microbiology, 53.
3. Hooper, D. C. (1999). Mode of action of fluoroquinolones. Drugs, 58, 6-10.
4. Hosomi, J., Asahina, Y., & Suzue, S. (1989). PCT Int. Appl. WO 89 12055. Preparation of thiazoloquinolonecarboxylic acid derivatives and their pharmaceutical compositions as antitumor agents (Chem.. Abstr. 1990, 113, 6328m).
5. Dinakaran, M., Senthilkumar, P., Yogeeswari, P., China, A., Nagaraja, V., & Sriram, D. (2008). Synthesis, antimycobacterial activities and phototoxic evaluation of 5H-thiazolo[3,2-a]quinoline-4-carboxylic acid derivatives. Med. Chem., 4 (5), 482-491.
6. Segawa, J., Kitano, M., Kazuno, K., Tsuda, M., Shirahase, I., Ozaki, M., et al. (1992). Studies on pyridonecarboxylic acids .2. synthesis and antibacterial activity of 8-substituted-7-fluoro-5-oxo-5H-thiazolo[3,2-a]quinoline-4-carboxylic acids. J. Heterocycl. Chem., 29 (5), 1117-1123.
7. Enomoto, H., Kise, M., Ozaki, M., Kitano, M., & Morita, I. (1987). Preparation and formulation of quinolonecarboxylic acid derivatives as antibacterials US 4659734.
8. Matsumura, S., Kise, M., Ozaki, M., Tada, S., Kazuno, K., Watanabe, H., Kunimoto, K., Tsuda, M., & Enomoto, H. (1982). Substituted carboxylic acid derivatives. EP 58392.

9. Jinbo, Y., Kondo, H., Inoue, Y., Taguchi, M., Tsujishita, H., Kotera, Y., et al. (1993). Synthesis and antibacterial activity of a new series of tetracyclic pyridone carboxylic acids. J. Med. Chem., 36 (18), 2621-6.
10. a) Fritsche, T. R., Biedenbach, D. J., & Jones, R. N. (2009). Antimicrobial activity of prulifloxacin tested against a worldwide collection of gastroenteritis-producing pathogens, including those causing traveler's diarrhea. Antimicrob.Agents Chemother., 53 (3), 1221-1224; (b) Rafailidis, P. I., Polyzos, K. A., Sgouros, K., & Falagas, M. E. (2011). Prulifloxacin: A review focusing on its use beyond respiratory and urinary tract infections. Int. J. Antimicrob. Agents, 37 (4), 283-290.
11. Giannarini, G., Tascini, C., & Selli, C. (2009). Prulifloxacin: Clinical studies of a broad-spectrum quinolone agent. Future Microbiology, 4 (1), 13-24.
12. Kise, M.; Kitano, M.; Ozaki, M.; Kazuno, K.; Matsuda, M.; Shirahase, I., & Segawa, J. (1989). Quinolinecarboxylic Acid Derivative, JP patent 1294680.
13. a) Ozaki, M., Matsuda, M., Tomii, Y., Kimura, K., Segawa, J., Kitano, M., et al. (1991). In vivo evaluation of NM441, a new thiazeto-quinoline derivative. Antimicrob. Agents Chemother., 35 (12), 2496-9; b) Keam, S. J., & Perry, C. M. (2004). Prulifloxacin. Drugs, 64 (19), 2221-34; c) Ozaki, M., Matsuda, M., Tomii, Y., Kimura, K., Kazuno, K., Kitano, M., et al. (1991). In vitro antibacterial activity of a new quinolone, NM394. Antimicrob. Agents Chemother., 35 (12), 2490-5.
14. Prats, G., Rossi, V., Salvatori, E., & Mirelis, B. (2006). Prulifloxacin: A new antibacterial fluoroquinolone. Expert. Rev. Anti Infect. Ther., 4 (1), 27-41.

15. Ito, Y.; Kato, H.; Yasuda, S.; Yoshida, T. & Yamamoto, Y. (1992). Preparation of 4-oxo-1H,4H-[1,3]thiazeto[3,2-a]quinoline-3-carboxylic acid derivs. as antibacterial, antitumor, and anti-AIDS agents. Jpn. Kokai TokkyoKoho. JP 04356491 A 19921210.

16. a) Matsuoka, M., Segawa, J., Amimoto, I., Masui, Y., Tomii, Y., Kitano, M., et al. (1999). Synthesis and antibacterial activity of novel 7-substituted-6-fluoro-1-fluoromethyl-4-oxo-4H-[1,3]thiazeto[3,2-a]quinoline-3-carboxylic acid derivatives. Chem. Pharm. Bull., 47 (12), 1765-73; b) Segawa, J ., Kitano, M ., Kazuno, K ., Matsuoka, M., Shirahase, I., Ozaki, M., et al. (1992). Studies on pyridonecarboxylic acids. 1. Synthesis and antibacterial evaluation of 7-substituted-6-halo-4-oxo-4H-[1,3]thiazeto[3,2-a]quinoline-3- carboxylic acids. J. Med. Chem., 35 (25), 4727-38.

17. Dawe, L. N., Ahmed, A., & Daneshtalab, M. (2011). 4-oxo-1,4-dihydrobenzo[h] [1,3]thiazeto[3,2-a]quinoline-1,3-dicarboxylic acid. Acta Cryst. E., E67 (o529).

18. Bikadi, Z., & Hazai, E. (2009). Application of the PM6 semi-empirical method to modeling proteins enhances docking accuracy of AutoDock. J. Chem. Inf., 1 (1), 15.

19. Halgren, T. A. (1996). Merck molecular force field basis, form, scope, parameterization, and performance of MMFF94. J. Comput. Chem., 17 (5/6), 490-519.

20. Morris, G. M., Goodsell, D. S., Halliday, R. S., Huey, R., Hart, W. E., Belew, R. K., et al. (1998). Automated docking using a Lamarckian genetic algorithm and an empirical binding free energy function. Ibid., 19 (14), 1639-1662.

21. Solis, F. J., & Wets, R. J. (1981). Minimization by random search techniques. Math. Oper. Res., 6 (1), 19-30.

22. Furet, P., Schoepfer, J., Radimerski, T., & Chene, P. (2009). Discovery of a new class of catalytic topoisomerase II inhibitors targeting the ATP-binding site by structure based design. part I. Bioorg.Med.Chem.Lett., 19 (15), 4014-4017.

23. Classen, S., Olland, S., & Berger, J. M. (2003). Structure of the topoisomerase II ATPase region and its mechanism of inhibition by the chemotherapeutic agent ICRF-187. Proc. Nat. Acad. Sci. USA., 100 (19), 10629.

24. Gaussian 09, Revision A.02, Frisch, M. J., Trucks, G. W., Schlegel, H. B., Scuseria, G. E., Robb, M. A., Cheeseman, J. R., Scalman, G., Barone, V., Mennucci, B., Petersson, G. A., Nakatsuji, H., Caricato, M., Li, X., Hratchian, H. P., Izmaylov, A. F., Bloino, J., Zheng, G., Sonnenberg, J. L., Hada, M., Eha ra, M., Toyota, K., Fukuda, R., Hasegawa, J., Ishida, M., Nakajima, T., Honda, Y., Kitao, O., Nakai, H., Vreven, T., Montgomery, J. A., Jr., Peralta, J. E., Ogliaro, F., Bearpark, M., Heyd, J. J., Brothers, E., Kudin, K. N., Staroverov, V. N., Kobayashi, R., Normand, J., Raghavachari, K., Rendell, A., Burant, J. C., Iyengar, S. S., Tomasi, J., Cossi, M., Rega, N., Millam, J. M., Klene, M., Knox, J. E., Cross, J. B., Bakken, V., Adamo, C., Jaramillo, J., Gomperts, R., Stratmann, R. E., Yazyev, O., Austin, A. J., Cammi, R., Pomelli, C., Ochterski, J. W., Martin, R. L., Morokuma, K., Zakrzewski, V. G., Voth, G. A., Salvador, P., Dannenberg, J. J., Dapprich, S., Daniels, A. D., Farkas, O., Foresman, J. B., Ortiz, J. V., Cioslowski, J., and Fox, D. J., Gaussian, Inc., Wallingford CT, 2009.

25. Glukhovtsev, M. N., Pross, A., McGrath, M. P., & Radom, L. (1995). Extension of gaussian-2 (G2) theory to bromine- and iodine-containing molecules: Use of effective core potentials. J. Chem. Phys., 103 (5), 1878.

26. Krishnan, R., Binkley, J. S., Seeger, R., Pople, J. A., & Department of Chemistry, Carnegie-Mellon University, Pittsburgh, Pennsylvania 15213. (1980). Self-consistent molecular orbital methods. XX. A basis set for correlated wave functions. ibid., 72:1, 650-654.

27. Curtiss, L. A., McGrath, M. P., Blaudeau, J., Davis, N. E., Binning Jr, R. C., & Radom, L. (1995). Extension of gaussian-2 theory to molecules containing third-row atoms ga-kr. ibid., 103 (14), 6104.

28. Blaudeau, J., McGrath, M. P., Curtiss, L. A., & Radom, L. (1997). Extension of gaussian-2 (G2) theory to molecules containing third-row atoms K and ca. ibid., 107 (13), 5016-5021.

29. Feller, D. (1996). The role of databases in support of computational chemistry calculations. J. Comput. Chem., 17 (13), 1571-86.

30. Schuchardt, K. L., Didier, B. T., Elsethagen, T., Sun, L., Gurumoorthi, V., Chase, J., et al. (2007). Basis set exchange: A community database for computational sciences. J. Chem. Inf. Model., 47 (3), 1045-52.

31. Tomasi, J., Mennucci, B., & Cammi, R. (2005). Quantum mechanical continuum solvation models. Chem. Rev., 105 (8), 2999-3094.

32. Fukui, K. (1981). The path of chemical reactions - the IRC approach. Acc. Chem. Res. 14 (12), 363-368.

33. Hratchian, H. P., & Schlegel, H. B. (2005). Using hessian updating to increase the efficiency of a hessian based predictor-corrector reaction path following method. J. Chem. Theory Comput., 1 (1), 61-69.

34. Kakehi, A., Ito, S., Fujii, T., Morimoto, Y., Matsumoto, S., & Shiohara, M. (1989). Preparation of new nitrogen-bridged heterocycles: smooth synthesis of thieno[3,2-a]- and thieno[2,3-b]indolizine derivatives. Bull. Chem. Soc. Jpn., 62 (1), 119-127.

35. Howarth, N., Wakelin, L., & Walker, D. (2003). Synthesis of the four diastereoisomers of 3-thymine-1-(t-butoxycarbonyl)aminocyclopentane-1-carboxylic acid. Tetrahedron Lett., 44 (4), 695-698.

36. While X-ray,1H- and 13C-NMR data confirmed the dicarboxylic acid structure for 4b, the HR-MS displayed a molecular peak that matched the mono-carboxylic acid product.

37. Rho, H. S., Baek, H. S., Ahn, S. M., Yoo, J. W., Kim, D. H., & Kim, H. G. (2009). Hydroxamic acid derivatives as anti-melanogenic agents: The importance of a basic skeleton and hydroxamic acid moiety. Bull. Korean Chem. Soc., 30 (2), 475-478.

38. Rigaku Corporation, Molecular Structure Corporation,. (1999). In Pflugrath J. W. (Ed.), CrystalClear software user's guide.

39. Sheldrick, G. M. (2008). A short history of SHELX. Acta Crystallogr A found Crystallogr., 64 (1), 112-122.

40. Edgington, P. R., McCabe, P., Macrae, C. F., Pidcock, E., Shields, G. P., Taylor, R., et al. (2006). Mercury: Visualization and analysis of crystal structures. J. Appl. Crystallog., 39 (3), 453-457.

41. Westrip, S. P. (2010). PublCIF: Software for editing, validating and formatting crystallographic information files. J. Appl. Crystallog., 43 (4), 920-925.

CHAPTER 5

Development of Anti-Viral Angular Furobenzo[*h*][2,3-*b*]Quinoline Agents Using Molecular Modeling and Virtual Screening Techniques

Abeer Ahmed[a] and Mohsen Daneshtalab[a]*

[a]School of Pharmacy, Memorial University of Newfoundland, St. John's, Newfoundland and Labrador, Canada A1B 3V6. Fax: +1(709)-777-7044; E-mail: mohsen@mun.ca

Preface

This chapter describes the synthesis and biological evaluation of furoquinolines as isosteres of the thienoquinolines that were previously discussed in Chapter 3. The previously described thienoquinolines did not show *in vitro* cytotoxicity on cancer cell lines, although the docking study showed binding affinity for the ATP binding site in topoisomerase II (1QZR). The synthesized furo derivatives showed no cytoxicity, as well, either in the Brine Shrimp Lethality assay or the MTT assay. The structural similarity and the angular configuration of this class of compounds to the previously reported furocoumarins encouraged us to test and explore their antiviral properties.

Abstract

Recently, thienoquinoline derivatives have attracted the attention of medicinal chemists due to the demonstration of diverse biological activities, including memory enhancing, anti-allergic, antiinflammatory, immunoregulator, analgetic and antipyretic, antibacterial and anaphylactic activities. Previously, the biological activities of the thienoquinoline derivatives were designed, synthesized and evaluated. In this chapter preparation of a series of angular benzo[*h*]furo[2,3-*b*]quinolines as bioisosteres of the previously synthesized angular benzo[*h*]thieno[2,3-*b*]quinolines is described. Much literature has shown that the furoquinolines have a wide range of pharmacological activities, but few papers have addressed the activities of the benzo[*h*]furo[2,3-*b*]quinolines.

Keywords: Furo[2,3-*b*]quinolines, dowtherm, Vilsmeier –Haack , Chloroacetyl chloride.

5.1 Introduction

Two forms of furano-coumarin condensation occur in nature. The first form comprise linear molecules, that are constructed by linking the 3',2' furan bond to the 6,7 coumarin bond. The 3',2' bond may also link to the 7,8 coumarin bond to produce angular furocoumarins (Angelicin). Linear furocoumarins (Psoralen de rivatives), as structural representatives of furoquinolines, are a well-known family of natural and synthetic photosensitizing compounds which exihibit interesting photobiological and phototherapeutical activities [1,2].

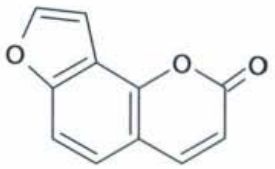

Angelicin

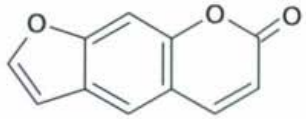

Psoralen

Some of these compounds are used in PUVA photochemotherapy (psoralen plus UV-A) to treat a variety of skin diseases. They are also employed in extracorpored photochemotherapy (photopheresis) to treat cutaneous T-cell lymphomas; Psoralen plus UV-A is also used as a selective immunosuppressive agent for the cure of various autoimmune diseases and to prevent rejection in organ transplants [1,2].

Moreover, psoralen derivatives are also used as tools in biophysical studies on nucleic acids and are now recognized as effective antiviral agents, especially against enveloped viruses such as the *Herpes simplex* virus or HIV-1 [3,4].

The preferred derivative is 8-methoxypsoralen (8-MOP) but also 5-methoxypsoralen (5-MOP) and 4, 5`, 8-trimethylpsoralen (TMP) are used. They exhibit a

good antiproliferative effect due to their capability of photodamaging DNA, leading to monofunctional and two different kinds of bifunctional adducts, interstrand cross-links (ISC) [5] and DNA-protein cross-links (DPC), connecting a DNA base and a protein A.A together [6-8].

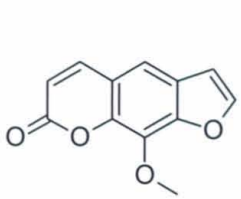

8-MOP

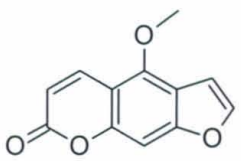

5-MOP

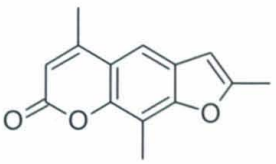

TMP

The bifunctional damage, especially the induction of ISC, was shown as the main cause responsible for the furocoumarin toxicity i.e. skin erythemas, genotoxicity with induction of point mutations in bacteria [1,9-12].

Recently, the formation of chromosomal aberrations was mainly attributed to DPC [13]; therefore, to obtain less toxic compounds, various authors planned to study new compounds that are characterized by a prevalent ability of forming monofunctional damage. The main research line dealt with Angelicin preventing the formation of ISC, which was due to its geometrical properties [14,15].

Furoquinoline alkaloids are characterised as secondary metabolites of the *Rutacea* family, in which they occur with the chemically-related furocoumarins [16,17]. Some of these plants are used in phytotherapy, e.g. *Ruta graveolens* and *Dictamnus albus.* Others are known as sources for the isolation of antineoplastic agents like acronycine from *Acronychia baueri* and *Fagara zanthoxyloides* [18,19].

Furo[2,3-*b*]quinoline constitutes an important group of bioactive natural products such as dictamine, acrophylline, confusameline, skimmianine, kokusaginine, and haplopine [20-23].

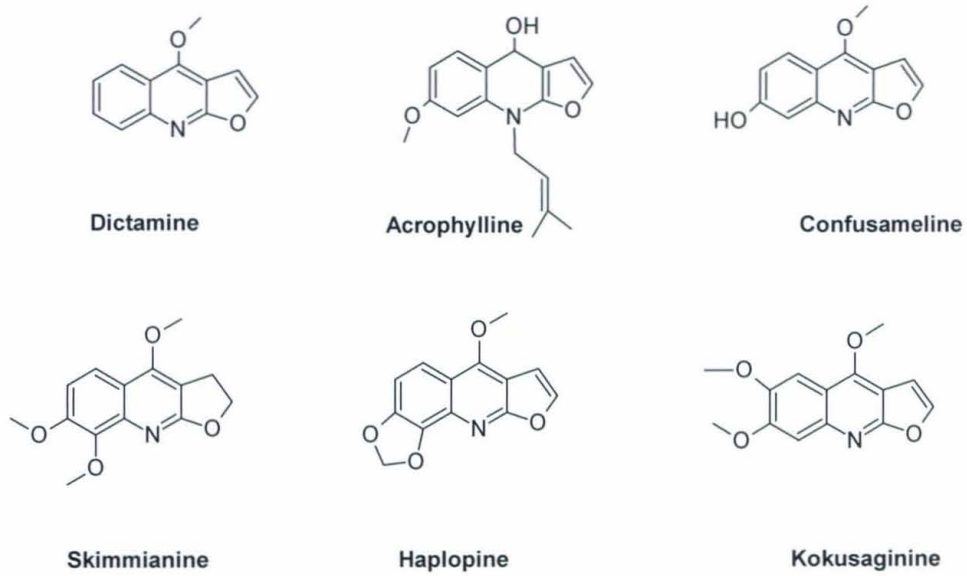

Figure 5-1: Structurally-related furoquinolines natural products.

The furoquinoline alkaloids were found to have a wide range of biological activities [24] including anti-allergic [20], cytotoxic [21], antiplatlet aggregation [13, 23] and voltage-gated potassium channel blocking [24].

The development of efficient syntheses of furoquinolines has been the focus of much research for many decades and continues to be an active and rich research area [25,26].

Most procedures used for the synthesis of furoquinolines suffer from the limited availability of substrates or require multistep procedures to construct the furan ring

individually. In the last decade, many new procedures for the synthesis of furoquinolines have been published [27-38].

DNA-intercalators containing a linear or angular planar chromophore with a polyaromatic ring can influence the structures and physiological functions of DNA [39].

Some intercalators such as furocoumarines, acridines, anthraquinones, naphthalimides, and phenanthridines are used in cancer treatment [40-43]. Angelicin, an angular furocoumarin, has been used to treat pain in the loins and knees [44], and skin diseases in phototherapy [45]. Guiotto *et al.* have synthesized a series of furoquinolinones [46-51], in which the oxygen atom of furocoumarin has been substituted by NH, and some of them showed strong antiproliferative activity against tumor cell lines upon UVA (Ultraviolet-A) irradiation. However, these furoquinolinones also demonstrated skin phototoxicity and marked clastogenic activity due to the formation of covalent monoadducts (MA) with DNA base and covalent DNA–protein cross-links (DPC) upon UVA activation. In the dark, these furoquinolinones exhibited weak antiproliferative activity with a mechanism of action related to topoisomerase II inhibition. In contrast to normal cells, many tumor cells show high expression levels of topoisomerase II, making this enzyme an ideal drug target [52-54].

For understanding the biological importance of furoquinolines, much of the literature has addressed the synthesis and biological activities of several substituted furo[2,3-*b*]quinoline derivatives [55-57].

Yeh-Long Chen *et al.* [56] had reported the synthesis of certain linear 4-anilinofuro[2,3-*b*]quinoline and angular 4-anilinofuro[3,2-*c*]quinoline derivatives and

their *in vitro* anticancer activity against the full panel of NCI's 60 cancer cell lines. Among the linear 4-anilinofuro[2,3-*b*]quinoline derivatives, 1-[4-(furo[2,3-*b*]quinolin-4-ylamino)phenyl]ethanone **I** is the most cytotoxic with a mean GI_{50} value of 0.025 μM. Among the angular 4-anilinofuro[3,2-*c*]quinoline derivatives, (*E*)-1-[3-(furo[3,2-*c*]quinolin-4-ylamino)phenyl]ethanone oxime **II** exhibited potent inhibitory activities on UO-31, UACC-257, and UACC-62 cells, with GI_{50} values of 0.03, < 0.01, and < 0.01 μM respectively.

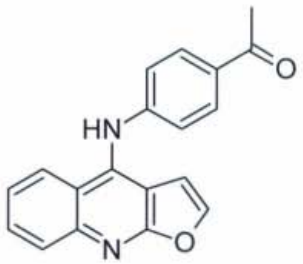

I

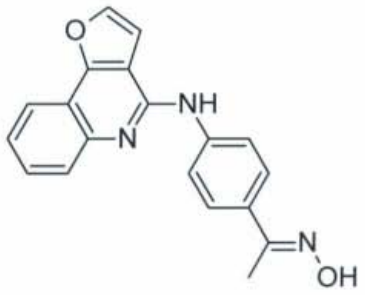

II

Based on the latest data obtained on furoquinolines [58] explaining the importance of furoquinolines as inhibitors of multiple targets in the PI3K/Akt-mTOR Pathway, we became interested in the design and synthesis of the angular benzo[*h*]furo[2,3-*b*] quinolines as potential cytotoxic agents. The synthesis part has been done in an attempt to prepare a bifunctional compound in which furo[2,3-*b*]quinoline moiety acts as an intercalator while the lactone ring plays the role of an alkylating unit.

Synthesis of the title Compounds **3a** and **3b** was accomplished by adding the activated diethylmalonate solution to chloroacetylchloride in THF followed by triethylamine and 1-naphthylamine. This procedure resulted in the formation of the

uncyclized intermediate after overnight stirring at room temperature. Thermal cyclization of this mixture in dowtherm under vacuum affords the cyclized furo[2,3-*b*]quinolines as depicted in **Scheme 5-1**.

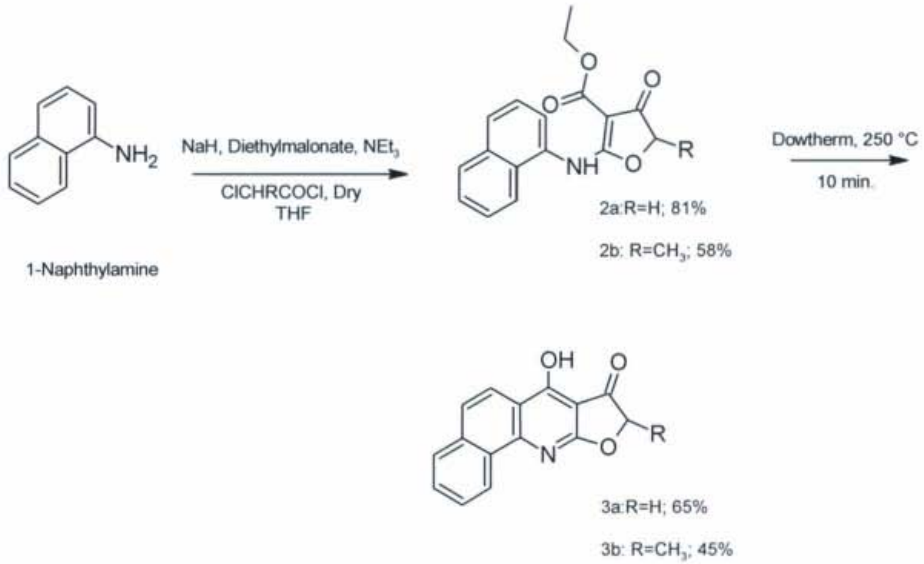

Scheme 5-1: Synthesis of cyclized Furo[2,3-*b*]quinolines.

Further reactions of **3a** to afford several substituted analogues are depicted in **Scheme 5 -2**. Namely, the reaction of **3a** with phen yltrimethylammonium tribromide (PTAB) in THF afforded **3c** in a reasonable yield.

Also, croton condensation took place upon reacting **3a** with *p*-fluorobenzaldehyde in acetic acid in the presence of HCl to afford Compound **3e**.

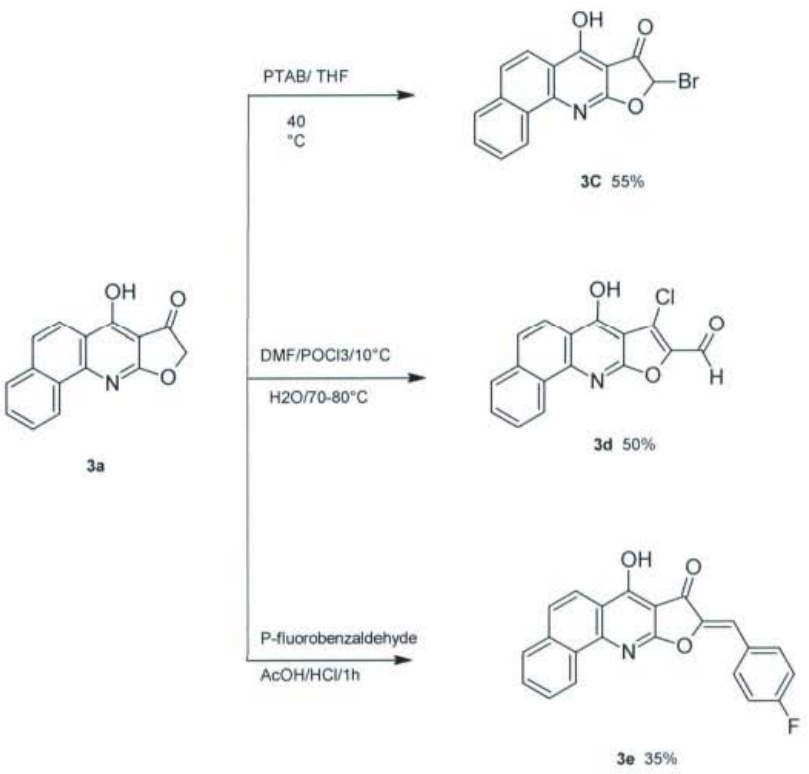

Scheme 5-2: Synthesis of Furo[2,3-*b*]quinolines derivatives.

In our attempt to improve the hydrophobic-hydrophilic balance in these molecules, Compounds **3a** and **3b** were allowed to react with hydrazine hydrate and acetone to afford Compounds **3f** and **3g** in reasonable yields, as depicted in **Scheme 5-3**.

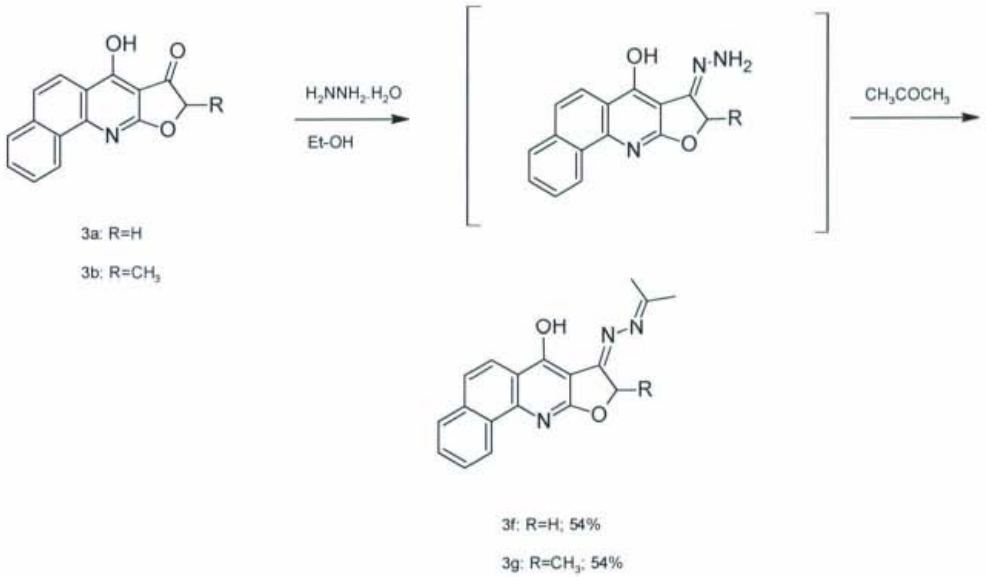

Scheme 5-3: Synthesis of the hydrazone derivatives **3f** and **3g**.

In a trial to develop a bioisostere to the previously synthesized derivative (**6a**) (Chapter 3), Compound **3i** was synthesized as shown in **Scheme 5-4**. Compound **3a** was allowed to react with carbon disulfide and 30% sodium hydroxide in dimethylsulfoxide to obtain Compound **3h**, further reaction of which with sodium hydroxide in methanol afforded Compound **3i**.

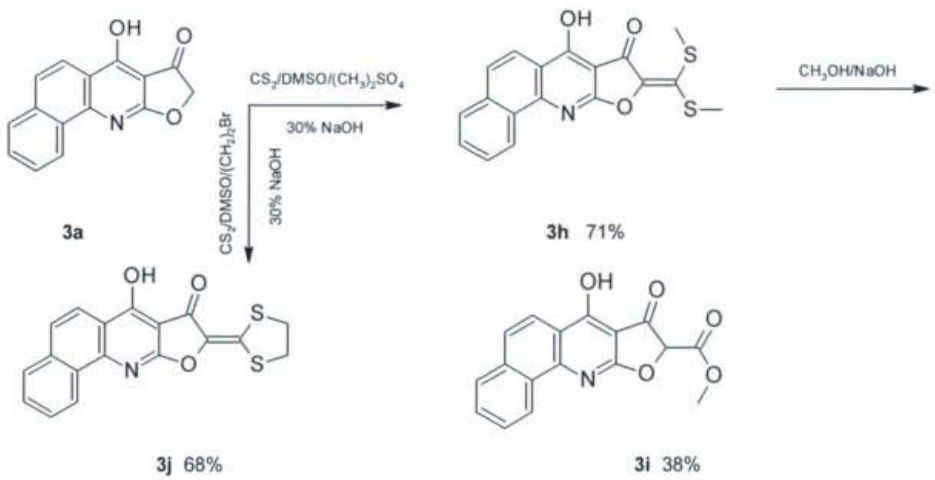

Scheme 5-4: Synthesis of the furo bioisostere.

Since our cytotoxic screening failed to generate potential leads to initiate a drug discovery effort, we embarked on a molecular docking approach to explore other possible biological activity profiles of this class of compounds.

5.2 Molecular modeling

5.2.1 Methods

Docking calculations were carried out according to the DockingServer methodology [60]. The MMFF94 force field [61] was used for energy minimization of ligand molecule (RHODAMINE B) using DockingServer. PM6 semiempirical charges calculated by MOPAC2009 (J. P. Stewart, Computer code MOPAC2009, Stewart Computational Chemistry, 2009) were added to the ligand atoms. Non-polar hydrogen atoms were merged, and rotatable bonds were defined.

Docking calculations were carried out on HCV helicase structure with the pdb code 3KQN. Essential hydrogen atoms, Kollman united atom type charges, and solvation

parameters were added with the aid of AutoDock tools [62]. Affinity (grid) maps of 25×25×25 Å grid points and 0.375 Å spacing were generated using the Autogrid program. AutoDock parameter set- and distance-dependent dielectric functions were used in the calculation of the van der Waals and the electrostatic terms, respectively.

Docking simulations were performed using the Lamarckian genetic algorithm (LGA) and the Solis & Wets local search method [63]. Initial position, orientation, and torsions of the ligand molecules were set randomly. Each docking experiment was derived from 100 different runs that were set to terminate after a maximum of 2,500,000 energy evaluations. The population size was set to 150. During the search, a translational step of 0.2 Å, and quaternion and torsion steps of 5 were applied.

5.2.2 Results

Novel Benzo[*h*]furoquinoline derivatives have been synthesized and now are being experimentally tested for their antiviral properties. In the present study *in-silico* investigation of HCV inhibitor properties of the novel compounds is carried out. As there are many X-Ray structures for the Hepatitis C virus helicase available in the Protein Data Bank, inhibition of HCV helicase has been widely studied. According to the recent publications there are different classes of inhibitors: ATP binding inhibitors, HCV replication activity inhibitors, and allosteric inhibitors which influence conformational change of the protein. Thus, the protein for docking calculation should contain ATP as well as bound DNA that enables us to explore all possible binding sites and modes of the ligands. X-Ray structures 3KQL, 3KQN and 3KQU meet these criteria, with 3KQN

possessing the most accurate X-Ray determination (lowest resolution). Therefore, 3KQN was chosen for docking calculations.

5.2.3 Blind docking results

First, docking calculations of Compounds **3a** were carried out on the whole protein (blind docking method) in order to explore the possible binding sites of the ligands. Blind docking methodology calculates the energy of ligand binding at different sites of the protein. The site where the ligand is bound with the lowest energy is then further subjected to focused docking calculation. All docking calculations revealed that the compounds under study are most likely to bind to the ATP binding site of the protein. **Figure 5-1** shows the first rank result of blind docking calculation of Compound **3c**.

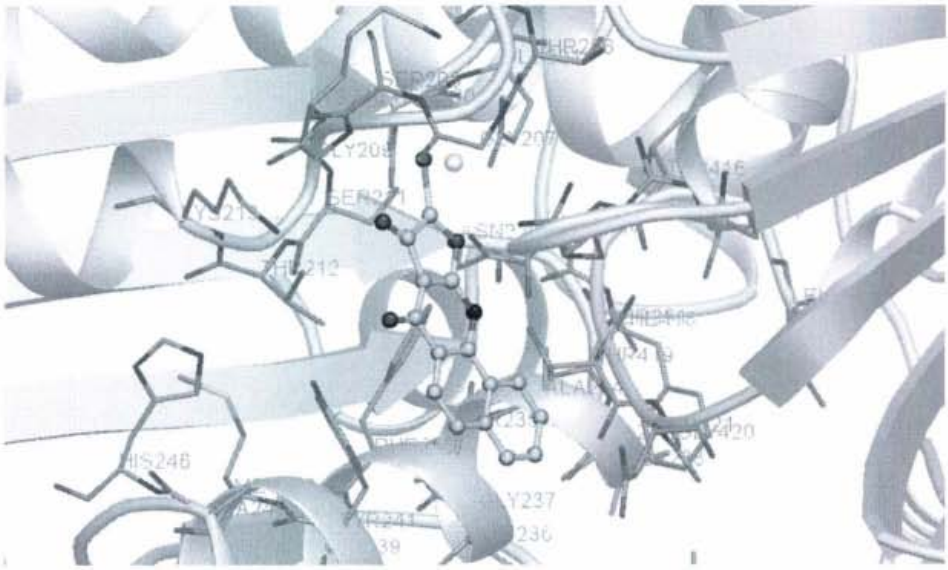

Figure 5-1: Compound **3c** docked to HCV helicase ATP binding site.

5.2.4 Focused docking results

Based on the results of blind docking calculation, all of the investigated compounds were docked into the ATP binding site of 3KQN.

Table 5-1: Docking energies of the investigated compounds at the ATP binding site.

Compound	Docking energy (kcal/mol)
3c	-8.77
3g	-8.66
3e	-8.56
3f	-8.38
3j	-8.27
3i	-8.21
3d	-8.04
3h	-7.93
3b	-7.79
3a	-7.41

Table 5.1 shows the calculated interaction energies at the ATP binding site. Among the investigated Compounds **3c** was calculated to bind to the protein with the highest affinity. Next the interactions of the compounds with the best affinities were analyzed.

Table 5-2: Interactions of Compound **3c** with HCV helicase at the ATP binding site.

Hydrogen bonds			Polar			Hydrophobic			pi-pi			Metal-ligand			Halogen-bond		
O1 [3.40]	–	THR212 (OG2, OG1)	O3 [3.77]	–	SER211 (OG)	C13 [3.83]	–	ALA234 (CB)	C6 [3.41]	–	PHE238 (CD1, CE1)	C4 [3.16]	–	Mn 3 (Mn)	Br1 [3.34]	–	SER211 (OG)
O2 [3.07]	–	THR212 (OG1)	O3 [3.01]	–	ARG467 (NH2)	C14 [3.81]	–	ALA234 (CB)	C5 [3.25]	–	PHE238 (CE1)	Br1 [2.37]	–	Mn 3 (Mn)			
N1 [2.79]	–	GLY417 (O)	N1 [3.78]	–	ARG467 (NH2)				C8 [3.50]	–	TYR241 (CB, CD1, CG)	O3 [3.14]	–	Mn 3 (Mn)			
N1 [3.20]	–	THR419 (OG1)							C9 [3.52]	–	TYR241 (CB, CG)						
									C12 [3.85]	–	PHE418 (CD1, CE1)						
									C13 [3.37]	–	PHE418 (CD1, CE1)						

Compound **3c** is mainly stabilized by hydrogen bonds and pi-pi interactions. It forms five hydrogen bonds with both side chain (SER211, THR212, THR419) and main chain (GLY207, GLY417) of 3KQN. The planar aromatic moiety of the ligand fits in the hydrophobic cavity formed by PHE238, TYR241 and PHE418. An additional halogen bond is observed with the side chain of SER211. Mn^{2+} is in interacting distance of the ring oxygen and bromo group.

5.3 Conclusion

This Chapter describes the design and synthesis of the novel furoquinoline derivatives. These compounds were found to demonstrate weak or no cytotoxicity to cancer cell lines. Moreover, docking of the compounds in the ATP active site of HCV helicase may suggest that the synthesized compounds possibly act as HCV inhibitors and this may contribute in part to their antiviral properties.

5.4 Experimental

^{1}H and ^{13}C NMR spectra, HSQC, and COSY spectra were recorded on a Bruker 500 MHz NMR spectrometer using TMS as an internal standard. LC-MS and HRMS were conducted using a GCT Premier Micromass spectrometer. X-ray structures were measured with the Rigaku Saturn 70 instrument, equipped with a CCD area detector and a SHINE optic, using Mo Kα radiation. Silicycle Ultrapure silica gel (0-20 μm) G and F-254 were used for the preparative TLC, and Silicycle Silia-P Ultrapure Flash silica gel (40-63 μm) was used for flash column chromatography. TLC was conducted on Polygram SIL G/UV254 precoated plastic sheets. Solvents were purified using standard conditions before use. The reaction yields are included in the corresponding schemes.

Ethyl (2*E*)-2-(naphthalen-1-ylimino)-4-oxotetrahydrofuran-3-carboxylate *(2a):*

Sodium hydride (3.35 g, 139.67 mmol) washed with dry n-hexane was suspended in dry tetrahydrofuran (250 mL) and a solution of diethyl malonate (21.20 mL, 139.67 mmol) in tetrahydrofuran was added dropwise. The clear salt was transferred to dropping funnel, and added dropwise to a solution of chloroacetylchloride (5.93 mL, 74.48 mmol) in tetrahydrofuran (6 mL) over a period of 1 h. The reaction mixture was stirred for 2 h. Triethyl amine (25.95 mL, 186.21 mmol) was added to the reaction mixture and it was stirred for 2 h. 1-naphthylamine (10 g, 69.83 mmol) in tetrahydrofuran (100 mL) was then added dropwise over a period of 1 h. The reaction mixture was stirred overnight; THF was evaporated *in vacuo*, followed by the addition of water and extraction with chloroform. The organic layer was washed with water, and dried over sodium sulfate. Chloroform was evaporated under vacuum and the residue was triturated with ether,

filtered and washed with additional ether to yield yellowish brown crystals. Mp 148-150°C. ^{1}H-NMR: (500 MHz, $CDCl_3$): δ = 10.72 (1H, s, OH), 8.01 (1H, d, *J* = 8.3 Hz), 7.93 (1H, d, *J* = 8.0 Hz), 7.82 (1H, d, *J* = 8.2 Hz), 7.69 (1H, d, *J* = 7.4 Hz), 7.66-7.61(1H, m,), 7.58 (1H, t, *J* =7.5 Hz), 7.51(1H, t, *J* = 7.8 Hz), 7.26 (1H, s), 4.66 (2H, s), 4.48-4.42 (2H, q, *J* = 7.2, 9.0 Hz, $O\underline{CH_2}CH_3$), 1.45 (3H, t, *J* = 7.1 Hz, $OCH_2\underline{CH_3}$). ^{13}C NMR (175 MHz, $CDCl_3$): δ = 188.5, 178.6, 165.9, 134.1, 129.9, 128.7, 127.4, 127.4, 127.2, 126.8, 125.3, 120.9, 87.9, 75.4, 60.7, 30.9, 14.6. APCI-MS 296.30 **(M^+-1, 100).**

Synthesis of 7-hydroxybenzo[*h*]furo[2,3-*b*]quinolin-8(9*H*)-one*(3a):*

Compound **2a** (2.0 g, 6.74 mmol), as a fine powder, was added with stirring in one lot to Dowtherm (50 mL) maintained at 240 °C. The temperature was then raised to 255 °C and maintained for 10 min. The mixture was then cooled to room temperature and diluted with a large volume of hexane to precipitate a brown solid that was collected and washed with hot hexane. Mp>300 °C. ^{1}H-NMR: (500 MHz, DMSO-d6): δ = 8.82 (1H, d, *J* =7.5 Hz), 8.15 (1H, d, *J* =7.7 Hz), 8.07-8.11 (1H, m), 7.85 (1H, d, *J* = 7.5 Hz), 7.75-7.80 (2H, m), 4.90 (2H, s). ^{13}C NMR (175 MHz, DMSO-d6): δ = 193.2, 178.2, 173.5, 148.3, 134.8, 130.6, 127.1, 126.9, 125.0, 124.6, 122.7, 122.3, 119.5, 99.5, 71.7. HR-MS (TOFEI) calcd for $C_{15}H_9NO_3$ (251.0582); found (251.0581).

Synthesis of (4*Z*,5*E*)-4-(ethoxymethylidene)-2-methyl-5-(naphthalen-1-ylimino)dihydrofuran-3(2*H*)-one *(2b):*

Sodium hydride (3.35 g, 139.67 mmol) washed with dry n-hexane, was suspended in dry tetrahydrofuran (250 mL) and a solution of diethyl malonate (21.20 mL, 139.67

mmol) in tetrahydrofuran was added dropwise. The clear salt was transferred to dropping funnel, and added dropwise to a solution of 2-chloropropionyl chloride (7.22 mL, 74.48 mmol) in tetrahydrofuran (6 mL) over a period of 1 h. The reaction mixture was stirred for 2 h. Triethyl amine (25.95 mL, 186.21 mmol) was added to the reaction mixture and it was stirred for 2 h. 1-Naphthylamine (10 g, 69.83 mmol) in tetrahydrofuran (100 mL) was then added dropwise over a period of 1 h. The reaction mixture was stirred overnight; THF was evaporated *in vacuo*, followed by the addition of water and extraction with chloroform. The organic layer was washed with water and dried over sodium sulfate. Chloroform was evaporated under vacuum and the residue was triturated with ether, filtered and washed with additional ether to yield reddish brown powder. Mp 140-142°C. ^{1}H-NMR: (500 MHz, $CDCl_3$): δ = 10.75 (1H, s, OH), 8.00 (1H, d, J = 8.2 Hz), 7.91 (1H, d, J = 7.6 Hz), 7.80 (1H, d, J = 8.2 Hz), 7.69 (1H, d, J = 7.4 Hz), 7.67-7.46 (3H, m, J = 4.5, 15.7, 27.3 Hz), 7.28 (1H, d, J = 5.1 Hz), 4.75 (1H, q, J = 6.9 Hz), 4.43 (2H, q, J = 7.1 Hz), 1.54 (3H, d, J = 7.0 Hz), 1.44 (3H, t, 7.1 Hz). ^{13}C NMR (175 MHz, $CDCl_3$): δ = 191.4, 177.1, 166.2, 134.1, 130.1, 128.7, 127.3, 127.3, 127.1, 126.7, 125.3, 120.9, 120.7, 86.7, 84.1, 60.6, 16.9, 14.5. APCI-MS: 310.33 **(M^+-1, 100).**

Synthesis of 7-hydroxy-9-methylbenzo[*h*]furo[2,3-*b*]quinolin-8(9H)-one *(3b):*

Compound **2b** (2.0 g, 6.42 mmol), as a fine powder, was added with stirring in one lot to Dowtherm (50 mL) maintained at 240° C. The temperature was then raised to 255 °C and maintained for 10 min. The mixture was then cooled to room temperature and diluted with a large volume of hexane to precipitate a pale yellow solid that was collected and washed with hot hexane. Mp > 300 °C. ^{1}H-NMR: (500 MHz, DMSO-d6): δ = 8.82

(1H, d, J =7.7 Hz), 8.14 (1H, d, J = 8.7 Hz), 8.10-8.02 (1H, m), 7.83 (1H, d, J = 8.5 Hz), 7.79-7.71 (2H, m), 5.11-5.02 (1H, q, J = 7.0, 7.0 Hz), 1.53 (3H, d, J = 7.0 Hz). HR-MS (TOFEI) calcd for $C_{16}H_{11}NO_3$ (265.0739); found (265.0735).

Synthesis of 9-bromo-7-hydroxybenzo[*h*]furo[2,3-*b*]quinolin-8(9H)-one *(3c):*

A mixture of furoquinoline **3a** (0.5 0 g, 2.0 mmol) and 175 mL of anhydrous tetrahydrofuran was heated to 40 °C. A solution of (0.75 g , 2.0 mmol) phenyltrimethyl ammonium tribromide (PTAB) in 65 mL of dry THF was added dropwise over 30 min and the mixture was stirred for an additional 75 min at 40 °C and kept at room temperature for 20 min. The insoluble material was removed by suction filtration and the filtrate was evaporated. The residue was recrystallized from toluene and the precipitate was dissolved in acetone. After addition of 150 mg of charcoal, the mixture was stirred at room temperature for 30 min. and filtered. The filtrate was evaporated to dryness to obtain a light brown solid. Mp> 310 °C. ^{1}H-NMR: (500 MHz, DMSO-d6): δ = 12.08 (1H, s), 9.98 (1H, d, J = 8.3), 8.13 (1H, d, J = 7.8), 7.91-7.85 (2H, m), 7.82 (2H, t, J = 6.0 Hz), 5.95 (1H, s). ^{13}C NMR (175 MHz, DMSO-d6): δ = 192.9, 180.5, 157.4, 142.0, 136.2, 130.2, 128.9, 128.8, 128.2, 127.3, 123.5, 123.0, 121.3, 118.2, 100.8. HR-MS (TOFEI) calcd for $C_{15}H_8BrNO_3$ (328.9688); found (328.9698).

Synthesis of 7-hydroxy-8-chloro-8,9-dihydrobenzo[*h*]furo[2,3-*b*]quinoline-9-carbaldehyde *(3d):*

Phosphorus oxychloride (2.3 mL) was added dropwise to DMF (2 mL) at 10 °C. A solution of Compound **3a** (2.25 g, 9 mmol) in 25 mL of DMF and 75 mL dioxane was

then added to the $POCl_3$-DMF mixture. The reaction mixture was then heated for 2 h in a water bath. The precipitate was filtered off, washed by water and hot acetone (3 times). The reaction mixture was poured into water (700 mL) and then heated for 5-7 min at 80-90 °C. The solution was left overnight; the formed red precipitate was then filtered off and recrystallized from acetone. Mp 230-232 °C. ^{1}H-NMR: (500 MHz, DMSO-d6): δ = 10.17 (1H,s), 9.25-9.20 (1H, m), 8.32 (1H, d, *J* = 9.2), 8.24-8.18 (2H, m), 8.00-7.90 (2H, m). ^{13}C NMR (175 MHz, DMSO-d6): δ = 178.7, 157.2, 154.9, 146.5, 146.2, 133.7, 130.2, 129.5, 128.6, 128.3, 128.1, 124.8, 122.3, 119.9, 90.0, 79.7. TOF-MS EI: 316.13 **(M^++1, 100).**

Synthesis of (9*Z*)-9-(4-fluorobenzylidene)-7-hydroxybenzo[*h*]furo[2,3-*b*]quinolin-8(9*H*)-one *(3e). (croton condensation):*

A mixture of Compound **3a** (0.575 g , 2.3mmol), glacial acetic acid (12 mL), conc.HCl (6 mL) and *p*-flurobenzaldehyde (2 mL, 19 mmol) was heated for 1 h under reflux. The precipitate was filtered off and recrystallized from DMSO to give rise to a dark brown powder. Mp >300 °C. ^{1}H-NMR: (500 MHz, DMSO-d6): δ = 9.02-8.93 (1H, m), 8.21 (1H, d, *J* = 8.8 Hz), 8.09 (3H, dt, *J* = 5.5, 10.6 Hz), 7.87 (1H, d, *J* = 8.8 Hz), 7.79 (2H, dd, *J* = 3.5, 5.7 Hz), 7.42 (2H, t, *J* = 8.8 Hz), 6.92 (1H, s). ^{13}C NMR (175 MHz, DMSO-d6): δ =169.5, 164.2, 135.0, 133.3, 133.2, 129.1, 128.6, 128.2, 126.9 (8 aromatic carbons), 124.5, 121.1, 116.3, 116.0, 108.8, 99.8. HR-MS (TOFEI) calcd for $C_{22}H_{11}NO_3F$ (356.0723); found (356.0721).

Synthesis of (8*Z*)-8-(propan-2-ylidenehydrazinylidene)-8,9-dihydrobenzo[*h*] furo[2,3-b]quinolin-7-ol *(3f) :*

A solution of **3a** (0.55 g, 2.2 mmol), 10 mL of 80% aquoes hydrazine hydrate and 30 mL of ethyl alcohol was heated at reflux for 2 h, the alcohol was removed *in vacuo* and the resulting oil was allowed to stand for several days at room temperature; crystals were separated out, collected and washed with a small amount of ethyl alcohol. An equimolar quantity of acetone was added and the mixture was refluxed in alcohol for 4 h in the presence of a few drops of glacial acetic acid. The solvent was evaporated and the product was poured onto cold water, filtered and dried. The crude solid was recrystallised from ethanol to give the product **3f**. Mp>300 °C. ^{1}H-NMR: (500 MHz, DMSO-d6): δ = 8.97 (1H, d, *J* = 7.8), 8.19 (1H, s), 8.06 (1H, d, *J* = 8.9), 7.93 (1H, d, *J* = 7.4), 7.74-7.60 (3H, m), 5.24 (2H, s), 2.30 (6H, d, *J* = 11.6). ^{13}C NMR: (175 MHz, DMSO-d6): δ = 171.2, 170.5, 166.4, 162.8, 149.3, 134.9, 129.7, 128.6, 127.5, 126.1, 124.9, 123.1, 120.6, 114.5, 98.1, 70.7, 24.0, 18.5. HR-MS (TOFEI) calcd for $C_{18}H_{15}N_3O_2$ (305.1164); found (305.1171).

Synthesis of (8*Z*)-9-methyl-8-(propan-2-ylidenehydrazinylidene)-8,9-dihydrobenzo [*h*]furo[2,3-*b*]quinolin-7-ol *(3g):*

This compound was prepared using the same procedure as that for the Compound **3f**. Mp 270-272°C. ^{1}H-NMR: (500 MHz, DMSO-d6): δ = 15.33 (1H, s), 7.88 (1H, dd, *J* = 7.7, 9.0 Hz), 6.85 (1H, d, *J* = 8.5 Hz), 6.59 (1H, dd, *J* = 7.1, 8.7 Hz), 6.38 (3H, m), 4.05 (1H, q, *J* = 6.4, 3.5 Hz), 1.00 (6H, d, *J* =3.3 Hz), 0.43 (3H, t, *J* = 3.0).^{13}C NMR: (175 MHz, DMSO-d6): δ = 169.9, 169.8, 169.5, 163.2, 150.1, 135.2, 130.1, 128.6, 127.4,

126.0, 125.2, 123.3, 120.7, 114.8, 97.6, 78.6, 24.4, 19.9, 18.6. APCI-MS: 318.10 (M^+-1,100).

Synthesis of 9-[bis(methylsulfanyl)methylidene]-7-hydroxybenzo[*h*]furo[2,3-b]quinolin-8(9*H*)-one *(3h):*

Carbon disulfide (0.176 g, 2.2 mmol) was added dropwise to a stirred solution of **3a** (0.55 g, 2.2 mmol) in dimethyl sulfoxide (5 mL) and 30% aqueous sodium hydroxide (0.7 mL) at 5°C, and stirring was continued at the same temperature for 0.5 h. Dimethyl sulfate (0.77g, 6.1 mmol) was added dropwise to the mixture at 5 °C, and stirring was continued at the same temperature for 1.5 h. Ice-water was added, and the mixture was extracted with ethyl acetate (2 x 100 mL). The combined extract was washed with brine and dried over magnesium sulfate and then filtered. The solvent was removed and the crude product was purified by recrystallization from ethylacetate-hexane to afford **3h** as yellow crystals. Mp > 300°C. ^{1}H-NMR: (500 MHz, DMSO-d6): δ = 8.95-8.79 (1H, m), 8.10 (1H, d, J = 8.6 Hz), 7.97-7.83 (1H, m), 7.76-7.44 (3H, m), 2.54 (3H, s), 2.46 (3H, s). ^{13}C NMR: (175 MHz, DMSO-d6): δ = 161.3, 160.8, 159.0, 157.9, 151.5, 135.4, 134.9, 130.3, 128.8, 127.2, 122.8, 120.8, 119.3, 118.4, 114.3, 100.9, 25.2, 20.2, APCI-MS: 354.43 (M^+-1, 100).

Synthesis of methyl 7-hydroxy-8-oxo-8,9-dihydrobenzo[*h*]furo[2,3-*b*]quinoline-9-carboxylate *(3i):*

A solution of sodium hydroxide (3.5 g, 60 mmol) in methanol (35 mL) was added to a stirred solution of **3h** (2.13 g, 6 mmol) in THF (45 mL), and the mixture was heated

at 50 °C for 1.5 h. After addition of 10% hydrochloric acid (20 mL), the mixture was extracted with ethylacetate (2 x 300 mL). The combined extracts were washed with brine (3x50 mL) and dried over magnesium sulfate. After removal of the solvent, the crude product was purified by column chromatography on silica gel using ethylacetat–hexane (1:4) as an eluent, followed by recrystallization from ethylacetate-hexane to afford **3i** as pale yellow crystals. Mp 211-213 °C. ^{1}H-NMR: (500 MHz, DMSO-d6): δ = 9.02-8.75 (1H, m), 8.15 (1H, d, *J* = 8.7), 8.13-8.05 (1H, m), 7.89 (1H, d, *J* = 8.8 Hz), 7.77 (2H, dd, *J* = 5.2, 9.1 Hz), 5.83 (1H, s), 3.83 (3H, s). ^{13}C NMR: (175 MHz, DMSO-d6): δ = 170.3, 160.8, 159.0, 157.9, 151.5, 135.4, 134.9, 130.3, 128.8, 127.2, 122.8, 120.8, 119.3, 118.4, 114.3, 95.3, 40.2, HR-MS (TOFEI) calcd for $C_{17}H_{11}NO_5$ (309.2729); found (309.2722).

Synthesis of 9-(1,3-dithiolan-2-ylidene)-7-hydroxybenzo[*h*]furo[2,3-*b*]quinolin-8(9*H*)-one *(3j):*

This compound was prepared using the same procedure as that for Compound **3h,** using 1,2-dibromoethane. Mp 256-258 °C. ^{1}H-NMR: (500 MHz, DMSO-d6): δ = 8.87 (1H, d, *J* = 7.8 Hz), 8.09 (1H, d, *J* = 8.7 Hz), 7.88 (1H, d, *J* = 7.5 Hz), 7.64-7.53 (3H, m), 3.60-3.56 (2H, m), 3.55-3.49 (2H, m). ^{13}C NMR: (175 MHz, DMSO-d6): δ = 178.0, 175.6, 172.9, 169.0, 156.9, 137.3, 134.8, 127.7, 127.5, 125.6, 124.6, 122.0, 121.4, 101.5, 66.2, 64.7, 38.9, 38.6, HR-MS (TOFEI) calcd for $C_{18}H_{11}NO_3S_2$ (353.0180); found (353.0188).

References

1. Parrish, J. A., Stern, R. S., Pathak, M. A., Fitzpatrick, T. B. In The Science of Photomedicine; Regan, J. D., Parrish, J. A., Eds.; Plenum: New York, 1982; p. 595.
2. Gasparro, F. P. (1994). Extracorporeal photochemotherapy : Clinical aspects and the molecular basis for efficacy. Landes Press, Georgetown, TX.
3. Cimino, G. D., Gamper, H. B., Isaacs, S. T., & Hearst, J. E. (1985). Psoralens as photoactive probes of nucleic acid structure and function: Organic chemistry, photochemistry, and biochemistry. Annual Rev. Biochem., 54, 1151-93.
4. North, J., Neyndorff, H., & Levy, J. G. (1993). New trends in photobiology. Photosensitizers as virucidal agents. J. Photochem. Photobiol. B: Biol., 17(2), 99-108.
5. Ben-Hur, E. and Song, P. S. The photochemistry and photobiology of furocoumarins (psoralens). Adv. Radiat. Biol., 1984, 11, 131.
6. Bordin, F., Carlassare, F., Busulini, L., & Baccichetti, F. (1993). Furocoumarin sensitization induces DNA- protein cross links. Photochem. Photobiol., 58 (1), 133-136.
7. Bordin, F., Baccichetti, F., Marzano, C., Carlassare, F., Miolo, G., Chilin, A., et al. (2000). DNA damage induced by 4,6,8,9-tetramethyl-2H-furo[2,3-h]quinolin-2-one, a new furocoumarin analog: Photochemical mechanisms. Ibid., 71 (3), 254.
8. Marzano, C., Baccichetti, F., Carlassare, F., Chilin, A., Lora, S., & Bordin, F. (2000). DNA damage induced by 4,6,8,9-tetramethyl-2H-furo[2,3-h]quinolin-2-one, a new furocoumarin analog: Biological consequences. Ibid., 71 (3), 263.

9. Kirkland, D. J., Creed, K. L., & Mannisto, P. (1983). Comparative bacterial mutagenicity studies with 8-methoxypsoralen and 4,5',8-trimethylpsoralen in the presence of near-ultraviolet light and in the dark. Mutation Res., 116 (2), 73-82.
10. Venturini, S., Tamaro, M., Monti-Bragadin, C., & Carlassare, F. (1981). Mutagenicity in salmonella typhimurium of some angelicin derivatives proposed as new monofunctional agents for the photochemotherapy of psoriasis. Ibid., 88 (1), 17-22.
11. Hook, G. J., Heddle, J. A., & Marshall, R. R. (1983). On the types of chromosomal aberrations induced by 8-methoxypsoralen. Cytogenet. Cell. Genet., 35 (2), 100-103.
12. Stern, R. S., & Lange, R. (1988). Members of the Photochemotherapy Follow-up Study. Non-melanoma skin cancer occurring in patients treated with PUVA five to ten years after first treatment. J. Invest. Dermatol., 91(2), 120-124.
13. Chen, K., Chang, Y., Teng, C., Chen, C., & Wu, Y. (2000). Letters - furoquinolines with antiplatelet aggregation activity from leaves of melicope confusa. Planta Medica., 66 (1), 80.
14. Guiotto, A., Rodighiero, P., Manzini, P., Pastorini, G., Bordin, F., Baccichetti, F., Carlassare, F., Vedaldi, D., Dall'Acqua, F., Tamaro, M., Recchia, G. and Cristofolini. M. (1984). 6-methylangelicins: A new series of potential photochemotherapeutic agents for the treatment of psoriasis. J. Med. Chem., 27, 959.
15. a) Grundon, M. F. and McCorkindale, N. J. The synthesis of dictamine and γ-fagarrine. J. Chem. Soc., 1957, 2177.; b) Tuppy, H., & Bohm, F. (1956). Synthesis

of dictamnin. Monatsh. Chem., 87(6), 720-724.; c) Narasimhan, N. S., & Mali, R. S. (1974). Synthetic application of lithiation reactions—VI New synthesis of linear furoquinoline alkaloids. Tetrahedron, 30(23-24), 4153-4157.; d) Pirrung, M. C., & Blume, F. (1999). Rhodium-mediated dipolar cycloaddition of diazoquinolinediones. J. Org. Chem., 64 (10), 3642-3649.;

16. a) Michael, J. P. (2002). Quinoline, quinazoline and acridone alkaloids. Nat. Prod. Rep. 19 (6), 742-760.; b) Michael, J. P. (2004). Quinoline, quinazoline and acridone alkaloids. Nat. Prod. Rep.21 (5), 650.
17. Mester, J. (1983) Structural diversity and distribution of alkaloids in the Rutales. In Waterman.P.G. and Grundon.M.F. (eds), Chemistry and Chemical Taxonomy of the Rutales, Annual Proceedings of the Phytochemical Society of Europe, no. 22. Academic Press, London, 31-95.
18. Svoboda, G. H., Poore, G. A., Simpson, P. J., & Boder, G. B. (1966). Alkaloids of Acronychia baueri schott I: Isolation of the alkaloids and a study of the antitumor and other biological properties of acronycine. J. Pharm. Sci., 55 (8), 758-768.
19. Messmer, W. M., Tin-wa, M., Fong, H. H. S., Bevelle, C., Farnsworth, N. R., Abraham, D. J., et al. (1972). Fagaronine, a new tumor inhibitor isolated from Fagara zanthoxyloides lam. (rutaceae). J. Pharm. Sci., 61(11), 1858-1859.
20. Huang, A., Lin, T., Kuo, S., & Wang, J. (1995). The antiallergic activities of synthetic acrophylline and acrophyllidine. J. Nat. Prod., 58 (1), 117-120.

21. Setzer, W. N., Setzer, M. C., Schmidt, J. M., Moriarity, D. M., Vogler, B., Reeb, S., et al. (2000). Cytotoxic components from the bark of stauranthus perforatus from Monteverde, Costa Rica. Planta Medica, 66 (5), 493-4.

22. Chen, I., Chen, H., Cheng, M., Chang, Y., Teng, C., Tsutomu, I., et al. (2001). Quinoline alkaloids and other constituents of Melicopesemecarpifolia with antiplatelet aggregation activity. J. Nat. Prod., 64 (9), 1143-1147.

23. Butenschön, I., Möller, K., & Hänsel, W. (2001). Angular methoxy-substituted furo- and pyranoquinolinones as blockers of the voltage-gated potassium channel Kv1.3. J. Med. Chem., 44 (8), 1249-56.

24. a) Chen, Y. L., Chen, I. L., Lu, C. M., Tzeng, C. C., Tsao, L. T., & Wang, J. P. (2004). Synthesis and anti-inflammatory evaluation of 4-anilinofuro[2,3-b]quinoline and 4-phenoxyfuro[2,3-b]quinoline derivatives. part 3. Bioorg. Med. Chem., 12 (2), 387-92.; b) Chen, Y. L., Chen, I. L., Lu, C. M., Tzeng, C. C., Tsao, L. T., & Wang, J. P. (2003). Synthesis and anti-inflammatory evaluation of 9-phenoxyacridine and 4-phenoxyfuro[2,3-b]quinoline derivatives. Part 2. Ibid., 11 (18), 3921-7. ;

25. a) Baston, E., Palusczak, A., & Hartmann, R. W. (2000). 6-substituted 1H-quinolin-2-ones and 2-methoxy-quinolines: Synthesis and evaluation as inhibitors of steroid 5alpha reductases types 1 and 2. Eur. J. Med. Chem., 35 (10), 931-40.; b) Ashrof, M. A., & Raman, P. S. (1994). Studies on cyclisation of allylacetoacetanilides and spectral characterisation of the products. J. Ind. Chem. Soc.,71 (12), 733.

26. Zhang, Z., Zhang, Q., Sun, S., Xiong, T., & Liu, Q. (2007). Domino ring-Opening/Recyclization reactions of doubly activated cyclopropanes as a strategy for

the synthesis of furoquinoline derivatives. Angew. Chem. Int. Ed.46 (10), 1726-1729.

27. Fayol, A., & Zhu, J. (2002). Synthesis of Furoquinolines by a Multicomponent Domino Process. Angew. Chem., 114 (19), 3785-3787.; Angew.Chem. Int. Ed., 2002, 41, 3633.
28. Du, W., & Curran, D. P. (2003). Synthesis of carbocyclic and heterocyclic fused quinolines by cascade radical annulations of Unsaturated N-aryl thiocarbamates, thioamides, and thioureas. Org. Lett., 5 (10), 1765-1768.
29. Aillaud, I., Bossharth, E., Conreaux, D., Desbordes, P., Monteiro, N., & Balme, G. (2006). A synthetic entry to furo[2,3-b]pyridin-4(1H)-ones and related furoquinolinones via iodocyclization. Ibid., 8 (6), 1113-6.
30. Bhoga, U., Mali, R. S., & Adapa, S. R. (2004). New synthesis of linear furoquinoline alkaloids. Tetrahedron Lett., 45 (51), 9483-9485.
31. Godet, T., Bosson, J., & Belmont, P. (2005). Efficient base-catalyzed 5-exo-dig cyclization of carbonyl groups on unactivated alkynyl-quinolines: An entry to versatile oxygenated heterocycles related to the furoquinoline alkaloids family. Synlett, (18), 2786-2790.
32. Diment, J., Ritchie, E., & Taylor, W. (1969). The conversion of platydesmine into dictamnine. Aust. J. Chem., 22 (8), 1797-1801.
33. Collins, J. F., Donnelly, W. J., Grundon, M. F., Harrison, D. M., & Spyropoulos, C. G. (1972). Aromatic hydroxylation in quinoline alkaloids. the biosynthesis of

skimmianine from dictamnine, and a convenient synthesis of furanoquinoline alkaloids. J. Chem. Soc., Chem. Commun., (18), 1029.

34. Sekiba, T. (1973). New syntheses of maculosidine and pteleine. Bull. Chem. Soc. Jpn., 46 (2), 577-580.
35. Cooke, R., & Haynes, H. (1958). The synthesis of furoquinoline alkaloids: Dictamnine and evolitrine. Aust. J. Chem., 11 (2), 221.
36. Sato, T., & Ohta, M. (1958). Synthesis of evolitrine, an alkaloid of evodia littoralis. Bull. Chem. Soc. Jpn., 31 (2), 161-162.
37. Narasimhan, N. S., Paradkar, M. V., & Alurkar, R. H. (1971). Synthetic application of lithiation reactions—IV: Novel synthesis of linear furoquinoline alkaloids and a synthesis of edulitine. Tetrahedron, 27 (6), 1351-1356.
38. Kuwayama, Y., Ota, T., Mikata, T., & Kanda, H. (1968). Studies on making use of gamma-butyrolactone. XIV. synthesis of furoquinoline alkaloid "pteleine". Yakugaku Zasshi, 88 (8), 1050-3.
39. Xie, L., Qian, X., Cui, J., Xiao, Y., Wang, K., Wu, P., et al. (2008). Novel angular furoquinolinones bearing flexible chain as antitumor agent: Design, synthesis, cytotoxic evaluation, and DNA-binding studies. Bioorg. Med. Chem., 16 (18), 8713-8718.
40. Braña, M. F., & Ramos, A. (2001). Naphthalimides as anti-cancer agents: Synthesis and biological activity. Curr. Med. Chem..Anti-Cancer Agents, 1 (3), 237-55.

41. Martinez, R., & Chacon-Garcia, L. (2005). The search of DNA-intercalators as antitumoral drugs: What worked and what did not work. Curr. Med. Chem., 12 (2), 127-152.

42. Wheate, N. J., Brodie, C. R., Collins, J. G., Kemp, S., & Aldrich-Wright, J. R. (2007). DNA intercalators in cancer therapy: Organic and inorganic drugs and their spectroscopic tools of analysis. Mini Rev. Med. Chem., 7 (6), 627-48.

43. Dalla, V. L., & Marciani, M. S. (2001). Photochemotherapy in the treatment of cancer. Curr. Med. Chem., 8 (12), 1405-18.

44. Wang, X., Wang, Y., Yuan, J., Sun, Q., Liu, J., & Zheng, C. (2004). An efficient new method for extraction, separation and purification of psoralen and isopsoralen from fructus psoraleae by super critical fluid extraction and high speed counter current chromatography. J. Chromatogr. A, 1055 (1-2), 135-40.

45. Gambari, R., Lampronti, I., Bianchi, N., Zuccato, C., Viola, G., Vedaldi, D., & Dall'Acqua, F. (2007). Structure and biological activity of furocoumarins. Top. Heterocycl. Chem., 9, 265-76.

46. Rodighiero, P., Guiotto, A., Chilin, A., Bordin, F., Baccichetti, F., Carlassare, F., et al. (1996). Angular furoquinolinones, psoralen analogs: Novel antiproliferative agents for skin diseases. synthesis, biological activity, mechanism of action, and computer-aided studies. J. Med. Chem., 39 (6), 1293-302.

47. Marzano, C., Chilin, A., Guiotto, A., Baccichetti, F., Carlassare, F., & Bordin, F. (2000). Photobiological properties of 1-(3'-hydroxypropyl)-4,6,8-trimethylfuro(2,3-h)quinolin-2(1H)-one, a new furocoumarin analogue. Il Farmaco, 55 (9), 650-58.

48. Chilin, A., Marzano, C., Guiotto, A., Baccichetti, F., Carlassare, F., & Bordin, F. (2002). Synthesis and biological evaluation of a new furo[2,3-h]quinolin-2(1H)-one. J. Med. Chem., 45 (5), 1146-1149.

49. Marzano, C., Chilin, A., Bordin, F., Baccichetti, F., & Guiotto, A. (2002). DNA damage and biological effects induced by photosensitization with new N(1)-unsubstituted furo[2,3-h]quinolin-2(1H)-ones. Bioorg. Med. Chem., 10 (9), 2835-44.

50. Chilin, A., Marzano, C., Baccichetti, F., Simonato, M., & Guiotto, A. (2003). 4-hydroxymethyl- and 4-methoxymethylfuro[2,3-h]quinolin-2(1H)-ones: Synthesis and biological properties. Ibid., 11 (7), 1311-8.

51. Marzano, C., Chilin, A., Baccichetti, F., Bettio, F., Guiotto, A., Miolo, G., et al. (2004). 1,4,8-trimethylfuro[2,3-h]quinolin-2(1H)-one, a new furocoumarin bioisoster. Eur. J. Med. Chem., 39 (5), 411-419.

52. Jahnz, M., Medina, M. A., & Schwille, P. (2005). A novel homogenous assay for topoisomerase II action and inhibition. Chembiochem : A Eur. J. Chem. Biology, 6 (5), 920-6.

53. Holden, J. A. (2001). DNA topoisomerases as anticancer drug targets: From the laboratory to the clinic. Curr. Med. Chem. Anti-Cancer Agents, 1 (1), 1-25.

54. Denny, W. A., & Baguley, B. C. (2003). Dual topoisomerase I/II inhibitors in cancer therapy. Curr. Top. Med. Chem., 3 (3), 339-53.

55. Chen, I., Chen, Y., Tzeng, C., & Chen, I. (2002). Synthesis and cytotoxic evaluation of some 4-anilinofuro(2,3-b)quinoline derivatives. Helvetica Chimica Acta., 85 (7), 2214-2212.

56. Chen, Y. L., Chen, I. L., Wang, T. C., Han, C. H., & Tzeng, C. C. (2005). Synthesis and anticancer evaluation of certain 4-anilinofuro[2,3-b]quinoline and 4-anilinofuro[3,2-c]quinoline derivatives. Eur. J. Med. Chem., 40 (9), 928-34.

57. Zhao, Y. L., Chen, Y. L., Tzeng, C. C., Chen, I. L., Wang, T. C., & Han, C. H. (2005). Synthesis and cytotoxic evaluation of certain 4-(phenylamino)furo[2,3-b]quinoline and 2-(furan-2-yl)-4-(phenylamino)quinoline derivatives. Chem. Biodivers., 2 (2), 205-14.

58. Lohar, M.V., Mundada, R., Deore, V., Yewalkar, N., Vishwakarma, R. A., Kumar S., et al. (2008). Design and synthesis of novel furoquinoline based inhibitors of multiple targets in the PI3K/Akt-mTOR pathway. Bioorg. Med. Chem. Lett. 18 (12), 3603-3606.

59. Pasquini, S., Mugnaini, C., Tintori, C., Botta, M., Corelli, F., Trejos, A., et al. (2008). Investigations on the 4-quinolone-3-carboxylic acid motif. 1. synthesis and structure-activity relationship of a class of human immunodeficiency virus type 1 integrase inhibitors. J. Med. Chem., 51 (16), 5125-5129

60. Bikadi, Z., & Hazai, E. (2009). Application of the PM6 semi-empirical method to modeling proteins enhances docking accuracy of AutoDock. J Chem. Inf., 1 (1), 15.

61. Halgren, T. A. (1996). Merck molecular force field. I. basis, form, scope, parameterization, and performance of MMFF94. J. Comput. Chem., 17 (5/6), 490-519.

62. Morris, G. M., Goodsell, D. S., Halliday, R. S., Huey, R., Hart, W. E., Belew, R. K., et al. (1998). Automated docking using a Lamarckian g enetic algorithm and an empirical binding free energy function. Ibid., 19 (14), 1639-1662.

63. Solis, F. J., & Wets, R. J. (1981). Minimization by random search techniques. Math. Oper. Res. 6 (1), 19-30.

CHAPTER 6

Conclusion and Future Research

6.1 Conclusion and future research

Quinolones are among the widely prescribed antibacterial agents for the treatment of a wide variety of infections in humans. Apart from the founding members of this drug class, which had little clinical impact, successive generations include the most active and broad spectrum oral antibacterials that are currently in use. Quinolones have a very distinctive mechanism of action as they do not only kill bacteria by inhibiting a critical cellular process but also they corrupt the activities of two essential enzymes, DNA gyrase and topoisomerase IV, resulting in generating high levels of double-stranded DNA breaks and bacterial death. The important characteristic of quinolones is their differential ability to target these two enzymes in different bacteria. Either DNA gyrase or topoisomerase IV serves as the primary cytotoxic target of drug action. This unusual feature of quinolones opened new aspects for the clinical use of this drug class. In addition to the antibacterial quinolones, specific members of this drug family display high activity against eukaryotic type II topoisomerases, as well as cultured mammalian cells and *in vivo* cancer cell lines. These antineoplastic quinolones represent a potentially important source of new anticancer agents and provide an opportunity to examine drug mechanisms across diverse species.

Antibacterial fluoroquinolones were shown to be effective against the *vaccinia* virus and *popavavirus*. These preliminary results prompted the synthesis of new quinolone derivatives to optimize the antiviral action and improve their selectivity index. The introduction of an aryl group at the piperazine moiety of the fluoroquinolone shifted the activity from antibacterial to antiviral, with a specific action against HIV. The

antiviral activity seemed to be related to an inhibitory effect at the transcriptional level, and further evidence suggested a mechanism of action mediated by inhibition of Tat functions.

The mechanism of action of antiviral quinolones remains unclear. Most of the tested drugs were proved to be effective against HIV-1 but, when assayed against a variety of different viruses, quinolones were shown to possess nonspecific activity. These data indicate that the drugs' targets are likely to be structures common to a wide range of viruses.

In this dissertation, a literature review (Chapter 2) focuses on the different biological activities of the quinolines scaffold. More than 10,000 derivatives have been patented or published, which explains the enormous progress that has been made in understanding the molecular mechanisms of action behind the different pharmacological actions of this privileged molecule.

Quinolones as a class of antibacterial agents have been known for over 40 years. Although considerable results in the research of new antibacterial quinolones have been already achieved, they are still a matter of study because of the continuous demand for novel compounds active against resistant strains of bacteria. Research efforts are mainly focused on obtaining new compounds active against very resistant bacterial strains or acting on the mechanisms of resistance.

Currently, fluoroquinolones are approved as second-line drugs by the WHO to treat TB but their use in MDR-TB is increasing due to the fact that they have a broad and potent spectrum of activity and can be administered orally. Moreover, they have

favourable pharmacokinetic profiles and good absorption, including proficient penetration into host macrophages.

Quinolones are not new in the antiviral field. Their previously reported data on binding with bacterial chromosome has strengthened the hypothesis that these drugs could also bind to the viral nucleic acid and has prompted the investigation of their antiviral activity.

Many structures containing the basic quinolone carboxylic acid template and different lipophilic substituents were patented as antiviral agents: most of them were tested against human immunodeficiency virus-1 (HIV-1) and were claimed to be effective in the treatment or prophylaxis of Acquired Immune Deficiency Syndrome (AIDS). Also, quinoline/one derivatives used as anti HCV agents have been discussed focusing on the structural requirements to act as anti HCV agents.

In Chapter 3 we tried to complete our search for novel small molecule heterocycles with potential antineoplastic activity, which the Daneshtalab group started years ago. The idea started when a joint patent published by Japanese pharmaceutical companies, Kyorin/Kyowa-Hakko, in which thiazoloquinolone carboxylic acids, including Compound **A**, were claimed as novel compounds with an impressive anticancer profile. The clinical candidate compound had exhibited favourable drug-like properties in different animal models in preclinical studies.

Compound A, like other quinolone carboxylic acid derivatives, was presumed to interact with topoisomerase II via its β-keto acid functional group and chelation with the Mg^{2+} ion to inhibit the enzyme. Considering this mode of action, we hypothesized that a

quinolone with a β-diketo functionality may be able to mimic the action of β-keto acid functionality, thus potentially providing the same level of complexity with the Mg^{2+} ion at the active site of the topoisomerase II. Also, due to the absence of a free carboxylic acid, the target quinolone may cause less gastric damage when used via oral administration.

The target compounds were designed using the Hyperchem-3^{TM} molecular modeling program. By applying Molecular Mechanics Optimization (MMO) and Molecular Dynamic Option methods we were able to identify linear tricyclic quinolones with β-diketo components that matched the angular feature of Compound A. In this respect, Compound B, 9-benzyl-7-fluoro-3-hydroxythieno [4,5-*b*]quinoline-4(9*H*)-one, at its optimized steric/energetic configuration, was found to have the best match, with a perfect 3-point overlay with Compound A.

Compound B and its derivatives were synthesized in our group using the Gould-Jacob method. This series of compounds displayed promising cytotoxic activity against several cancer cell lines. Furthermore, we succeded in annelating a thieno ring to the benzo[*h*]quinoline nucleus in an angular pattern. In this context, we attempted the syntheses of benzo[*h*]thieno[2,3-*b*]quinoline derivatives. The weak cytotoxicity on HeLa and KB cell lines by most cytotoxic derivatives in the Brine Shrimp Lethality Bioassay prompted us to explore, theoretically, the possibility of these derivatives to act as topoisomerase inhibitors.

The *In silico* study revealed the possibility of the synthesized derivatives to bind to the ATP binding site in human topoisomerase II while not being able to make appropriate chelation with Mg^{2+}, a characteristic that is required for inhibition of topoisomerase II.

On the other hand, another successful strategy has been applied in order to synthesize a quinoline-fused isothiazolone moiety. This was designed in accordance with what was in the literature: the isothiazole moiety was able to replace the C_3-carboxylic acid group with retained (or enhanced) antibacterial activity either in fused or isolated forms. In this context we synthesized isothiazolobenzo[*h*]quinoline through the interaction of the thiol intermediate **4** with hydroxylamine-*O*-sulphonic acid to yield the corresponding thioamino derivative. The synthesized derivative did not show cytotoxicity either.

In an attempt to lower the log *p* of the synthesized derivatives, Compound **6a** was allowed to react with hydrazine hydrate to yield the pentacyclic pyrazoloquinoline **9**. Pyrazoloquinolines are considered as a very attractive scaffold for medicinal chemists. The structure of Compound **9** was confirmed by spectral analysis and X-ray crystallography.

Most of the synthesized derivatives are within the limits of the Lipinski rule of 5. Much work is needed to decrease the log *p* to be in the most optimum range to effect 100% absorption of the synthesized derivatives and this can be done by phosphorylation of the free hydroxyl group in Compound **6b** followed by reduction using H_2,Pd/C and then sodium salt formation as outlined in **Scheme 6-1**. This will improve the solubility and dephosphorylation will be effected by phosphatases inside the body.

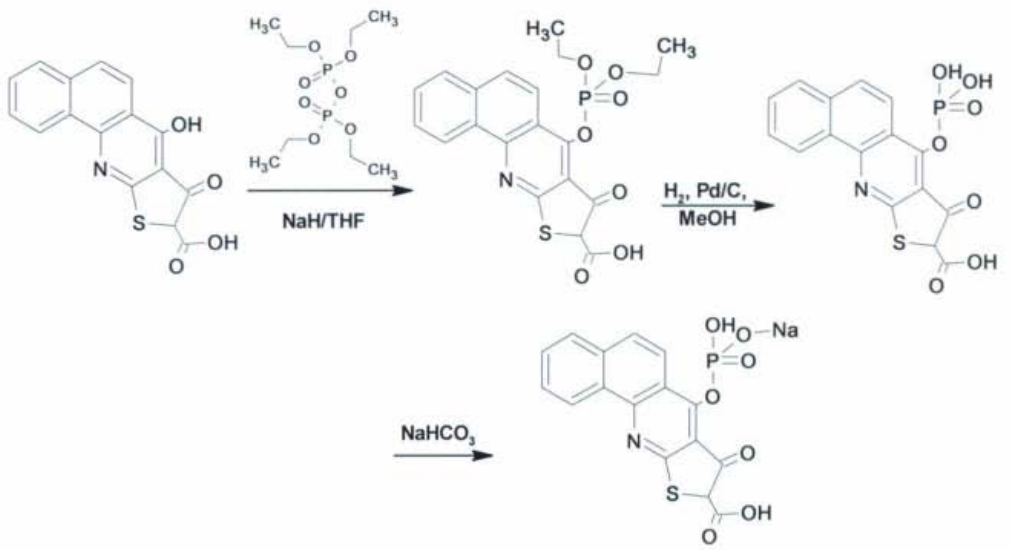

Scheme 6-1: Phosphorylation of quinoline derivatives.

Furthermore, the synthesized derivatives had been docked into the HCV-Helicase (data not shown) showing good binding affinities to the ATP binding region. Screening of these derivatives on MOLT-4 cells will be the aim in the near future.

In Chapter 4, in continuation of the Daneshtalab's ongoing research towards the discovery of novel polycyclic quinoline-based antineoplastic agents using conventional synthetic procedures, it was possible to isolate and identify, unexpectedly, a 4-oxo-benzo[*h*]thiazetoquinoline derivative (**4a**). The structure of this novel molecule was elucidated by ^{1}H-NMR, ^{13}C-NMR, HR-MS, and X-ray crystallography. Despite the availability of several papers on the syntheses and bioactivity of angular 4-oxo-thiazolo[3,2-*a*]quinoline-3-carboxylic acid derivatives, there are limited reports on the synthesis of 4-oxo-thiazeto[3,2-*a*]quinolines and there is no reported synthesis of 4-oxo-benzo[*h*]thiazeto[3,2-*a*]quinoline derivatives. In the synthesis described herein, the 4-

oxo-thiazetoquinoline nucleus is formed *via* reaction of the carbanion at the alkylsulfide group of the C-2 position of the quinoline ring with a pseudohalogen (IBr), formed *via* reaction of the iodide anion with the *vic*-dihaloalkane, or a halogen (I_2), followed by nucleophilic attack of the N-1 on halogenated carbon and the departure of halogen. The role of the vicinal dihaloalkane in this process is the provision of a pseudohalogen (such as IBr) without direct interaction with the quinoline system. This synthetic procedure provides us with diverse 4-oxo-thiazetoquinoline-3-carboxylic acid derivatives possessing electron-withdrawing groups at the C-1 position.

To test the plausibility of the mechanism described in **Scheme 4-3**, three individual steps of the scheme were computationally modeled to see if the energetics of each step were reasonable in terms of both activation energy barriers and overall energy change from reactants to products.

Overall, modeling of these three steps of the proposed mechanism shows that the first two steps have small- to -nonexistent activation energy barriers, and are highly exothermic in concert. Even if the abstraction of the phenolic proton was to have a relatively large activation energy barrier on the order of 250 kJ/mol (which is unlikely for such an acid-base chemistry) the transition state would still lie energetically below the **3a**/carbonate reactant complex of the first step. Combined with the reasonable transition state barrier of the phenolate form ring closing step, which is itself exothermic, the theoretical calculations support the notion that the proposed mechanism is energetically favourable. In fact, since the activation energy barriers to reverse any of the mechanistic steps would be prohibitively high, reverse reactions are unlikely to occur, and the

proposed mechanism would have to lead to fairly high yields of product **4a** at a reasonable temperature. As the experimental results show yields on the order of 75% for the reaction run for 24 h at 70℃, the modeled energetics of the proposed mechanism support the observed yield as well.

Generally, synthesis of novel system (benzo[*h*]thiazetoquinolone) derivatives has been achieved using *in situ* halogenations and alkylation methodologies. The mechanism by which the cyclization occurs is confirmed using computational calculations.

Compound **28** has also been prepared during this study. This derivative showed a better log *p* in comparison with the tested derivatives. Also, this compound did not show any cytotoxic properties against cancer cell lines in MTT assay.

Compound **28** is structurally different from the other compounds synthesized in this series, in which the main requirement of the 4-quinolones component is missing.

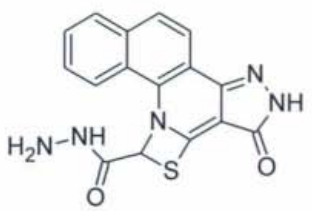

28

Starting from this derivative, much work must be done in order to get a new series capable of demostrating the potential to act as antimycobacterial agents.

In Chapter 5, isosteric replacements of sulfur in thienoquinolines by oxygen revealed a new series of furoquinolines. The synthesized derivatives did not show a cytotoxic pattern on cancer cell lines. Since our screening failed to generate potential

leads to initiate a drug discovery effort, we embarked on a structure-based design approach. The diketo acid class of compounds has been most aggressively developed because of its marked antiretroviral activities. Also, it was proven that 4-quinolone-3-carboxylic acid is a good alternative to the diketo acid structure for potent strand transfer inhibition. All the investigated compounds were docked into the ATP binding site of 3KQN. The protein for docking calculation should contain ATP as well as bound DNA that enables us to explore all possible binding sites and modes of the ligands. X-Ray structures 3KQL, 3KQN and 3KQU meet these criteria, with 3KQN possessing the most accurate X-ray determination (lowest resolution). Therefore, 3KQN was chosen for docking calculations.

All the synthesized furo derivatives showed good binding affinities to the ATP portion of the protein. In conclusion the synthesized furoquinolines did not exhibit cytotoxicity against cancer cell lines; meanwhile they showed good binding affinities to the HCV-helicase.

6.2 Originality of the thesis

With the continuous progress in protein crystallography and NMR, structure-based drug design is acquiring increasing importance in the search for new drugs. Modeling usually starts from the 3-D structure of the target protein in order to construct molecules which are complementary to a binding site, in their chemistry and geometry as well as in their physicochemical properties. The main contribution of this thesis is firstly the design and synthesis of different fused quinoline derivatives (ligands) using structure-based drug design starting with the synthesis of the novel angular benzo[*h*]thienoquinolines. The

synthesis of a novel series of thienoquinolines focusing on some criteria of the new system is described in chapter 3; for example, the constant production of the *O*-alkylated derivatives upon alkylation with different alkylating agents. Also, the synthesis of a novel pentacyclic derivative applies a new method which was based on reacting the starting material with ethylacetoacetate. The reaction with hydrazine hydrate also was designed to add a hydrophilic moiety to the designed molecule which unexpectedly produced a new pyrazoloquinoline derivative.

As there are not many reports on thiazeto-quinolone derivatives, the synthesis of the novel thiazetobenzo[*h*]quinolones via a novel oxidative cyclization process was successfully achieved. Also, to come up with a reasonable structure activity relationship, the novel furobenzo[*h*]quinolines which are considered as structural isosteres of the newly synthesized thienoquinolines were designed and synthesized.

None of the synthesized derivatives exhibited cytotoxic properties at the nanomolar levels against normal or cancer cell lines. The only risk which faced us with lead structure optimization by structure-based design was the neglect of other important biological properties, such as bioavailability and metabolic stability, which will be the focus of future research.

Secondly, in order to come up with a possible explanation for the lack of cytotoxicity of these derivatives, the *in-silico* study was initiated which highlighted the possibility of these synthesized derivatives to bind to the ATP binding site of the human topoisomerase with no chelation to Mg^{2+}.

The inability to chelate Mg^{2+} explains in part the weak cytotoxicity of the prepared derivatives. Another possible explanation may also be due to the difficulty for the drug to enter the cell and this can be explained on the basis of the pharmacokinetic parameters of the drug or the efflux pump mechanisms.

Synthesis of quinoline derivatives with different fusion rings; for example, thieno, thiazolo, thiazeto and furobenzo[*h*]quinolines, have introduced a new library of quinoline derivatives with weak or no cytotoxic properties on cancer cell lines. All the synthesized derivatives showed a binding affinity towards the ATP binding site in the topoisomerase-II with no chelation to Mg^{2+}.